Exploring Microbial Dynamics: Cercozoan Algivory in Polar Biocrusts

Inaugural – Dissertation

zur

Erlangung des Doktorgrades
der Mathematisch-Naturwissenschaftlichen Fakultät
der Universität zu Köln

vorgelegt von

Ana Cristina Martínez Rendón

aus Guatemala Stadt, Guatemala

Köln, 2025

Berichterstatter:

PD Dr. Kenneth Dumack

Prof. Dr. Burkhard Becker

Vorsitz der Prüfung:

Prof. Dr. Christine Heim

Tag der mündlichen Prüfung: **25. April 2025**

Soil is more than dirt. It is the source and sink of nutrients, wastes, pharmaceuticals, and energy required to make Earth supportive of life—***it is Earth's most vital organ*****.**

Schloss & Handelsman (2006)

Table of Contents

Summary

Biological soil crusts (hereafter biocrusts) dominate polar landscapes, where cyanobacteria and microalgae drive primary production in the absence of higher plants. However, the structure and functioning of biocrust food webs remain poorly understood, particularly regarding microbial predators that regulate algal populations and influence nutrient cycling. This study investigated the role of cercozoans as algivorous predators in polar biocrusts, combining network analyses, trait-based approaches, and experimental validation to assess their trophic interactions.

Using FlashWeave and HMSC, I inferred microbial interaction networks, revealing consistent predator-prey associations between cercozoans and microalgae across distinct polar regions. While FlashWeave enabled high-throughput detection of putative interactions, HMSC incorporated environmental covariates and hierarchical dependencies, refining our understanding of species co-occurrence and co-abundance patterns. FlashWeave and the trait-based approach revealed that only 4.7 to 9.3% of these correlations linked cercozoans to suitable algal prey. HMSC yielded similar numbers, with 7.5% found with co-occurrence and 4.8% with co-abundance networks**.** These network-based predictions were experimentally tested through co-culture feeding assays, which confirmed predation in 82% of tested interactions. Collectively, these results highlight the value of network analyses for inferring predator-prey interactions while underscoring the need for cautious interpretation of microbial association patterns. They also reinforce the importance of integrating trait-based approaches to enhance the accuracy and reliability of predicted biological interactions.

Beyond direct predation, cercozoans likely contribute to nutrient cycling, facilitating carbon and nitrogen fluxes through microbial food webs. However, their predatory roles might be shaped by prey defenses, resource availability, and competitive interactions with other microbial grazers, underscoring the complexity of biocrust trophic networks. While our findings establish cercozoans as key microalgal consumers, further research is needed to quantify their *in situ* ecological impact and interactions with other biotic and abiotic factors.

This study provides critical insights into microbial predator-prey dynamics in polar soils, laying the foundation for future research on microbial food webs in extreme environments. By integrating network ecology, trait-based functional classification, and experimental approaches, I contribute to a broader understanding of microbial community structuring and the ecological significance of protistan predation in terrestrial ecosystems.

1. Introduction

1.1. Overview

Life thrives even in Earth's harshest environments, where adaptations to extreme conditions evidence the resilience and inventiveness of nature. Polar biocrusts are living mosaics of microbial life that exist at the interface of the soil and the atmosphere in some of the coldest and driest regions of the planet. These ecosystems, composed of microorganisms such as cyanobacteria, microalgae, fungi, and protists, are not merely survivors but engineers of soil stability, nutrient cycling, and carbon storage.

A complex web of microbial interactions supports the dynamics within biocrusts, and protists, still often overlooked, increasingly appear as key players in these ecosystems. As predators, grazers, and nutrient recyclers, they bridge trophic levels and participate in the microbial networks that define soil functionality. Yet, the full extent of their ecological roles is still not fully uncovered, particularly in polar regions where biocrusts dominate barren landscapes.

This study explores the world of protists within polar biocrusts, surveying some of their multiple interactions and contributions to microbial food webs. Polar biocrusts, characterized by their moderately complex yet resilient communities, offer a unique lens to study the complexities of microbial life. Understanding their dynamics is essential in light of the rapidly changing climate, as polar ecosystems experience profound changes that can have a global impact. By studying the interactions within these microbial ecosystems, I seek to uncover some of the fundamental principles governing life in these extreme environments. In doing so, this study sheds light on hidden connections that sustain one of Earth's most resilient ecosystems, offering insights into a world increasingly shaped by environmental change.

This dissertation incorporates material from the article published in *Microbiome* (doi: 10.1186/s40168-025-02035-8) "Enhancing Microbial Predator-Prey Detection with Network and Trait-Based Analyses," authored by me, Christina Braun, Maria Kappelsberger, Jens Boy, Angélica Casanova-Katny, Karin Glaser, and Kenneth Dumack. The text, figures, and methods have been adapted with proper acknowledgment where necessary.

1.2. Protists: Diversity and functions

Phylogeny

Protists form a diverse, polyphyletic, and highly artificial grouping that gathers completely unrelated microbial eukaryotes distinct from animals, plants, and fungi (Bonkowski et al., 2019). Protists are mostly unicellular, but some can form colonies or filaments of at most a couple of distinct cell types (O'Malley et al., 2013). The group has been traditionally classified based on their morphology and movement, if present, as flagellates, ciliates, and amoebae (Simpson et al., 2017), and on their functional characteristics. These biologically observable traits formed the foundation of classification for protists—and indeed, for all eukaryotes—until the advent of molecular phylogenetics.

Eukaryotic phylogenies have divided the domain into four to eight major supra-kingdom-level groupings, or "supergroups", which are collections of taxa with reasonable evidence of forming a monophyletic group (S. M. Adl et al., 2012, 2019; Burki et al., 2007, 2020; Keeling et al., 2005; Simpson & Roger, 2002). In the last two decades, however, advancements in molecular biology have dramatically reshaped our understanding of eukaryotic relationships. As eukaryotic DNA sequences became increasingly available, phylogenies for the domain were less reliant on biological characters or single gene markers like 18S RNA (Simpson et al., 2017). Now, phylogenies are increasingly based on molecular inferences based on dozens to hundreds of genes, known as phylogenomics (Bonkowski et al., 2019; Burki et al., 2020). This shift to a phylogenomic approach has led to a significant reorganization of the eukaryotic tree, resulting in the replacement or redefinition of many original supergroups that better reflect evolutionary relationships (Figure 1; Burki et al., 2020).

Understanding the evolutionary relationships between the main protist lineages is crucial for resolving the eukaryotic phylogeny, and in particular, the location of its root (Pawlowski, 2014). Novel discoveries of free-living heterotrophic protists have been crucial in uncovering new lineages and informing the modern tree of life, enhancing our understanding of eukaryotic diversity and evolution (Burki et al., 2020). Protists, being primarily unicellular and thus reflecting the ancestral condition of all eukaryotes, offer unique insights into their evolutionary transition, where animals, plants, and fungi represent exceptional yet successful branches of this broader evolutionary tree (O'Malley et al., 2013). Answering how eukaryotes first emerged—a question that remains one of biology's greatest puzzles (Martin et al., 2017)—may well lie in the genomes and metabolic pathways of basal protists.

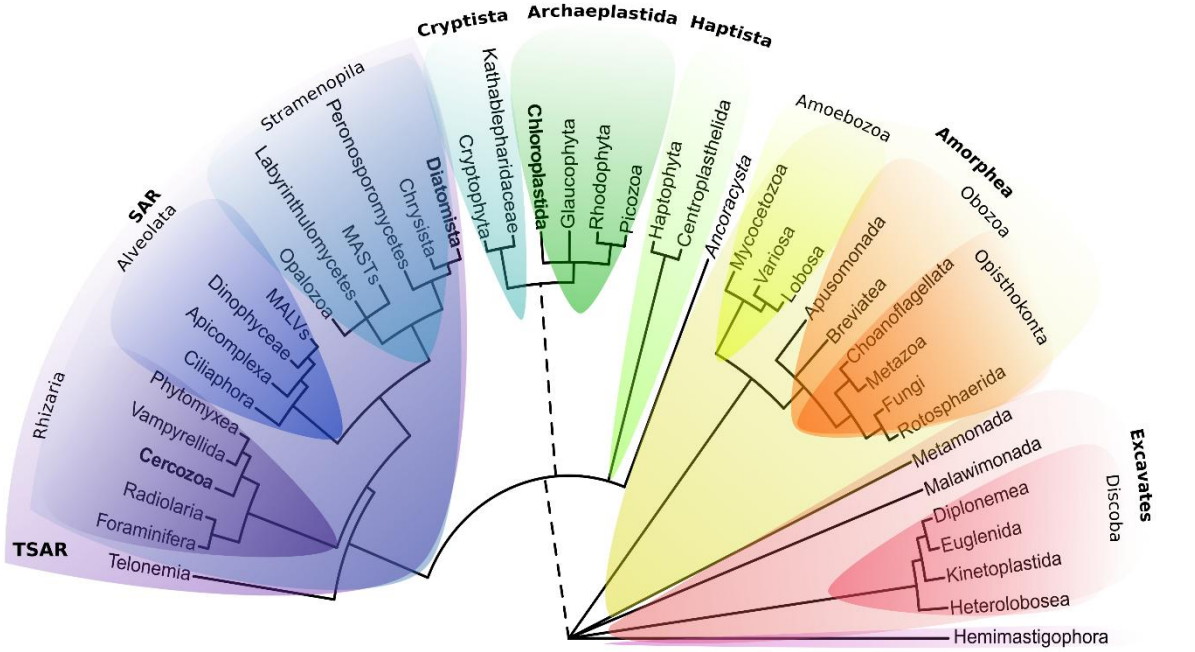

Figure 1. Eukaryotic tree of life based on the modern consensus phylogeny (Burki et al., 2020, 2021). Here, the phylogeny reflects the structure proposed in Burki et al. (2021) with taxonomic resolution extending beyond the "supergroup" level presented in Burki et al. (2020). The CRuMs clade, considered a sister group to Amorphea (Brown et al., 2018), is absent from this figure. According to the authors, the summary is derived from recent phylogenomic studies and represents the current consensus. The colored groupings correspond to the current 'supergroups', except for "Excavates", which remains contentious and is not recognized as a supergroup by all phylogenies. Unresolved branching orders among lineages are shown as multifurcations, and broken lines reflect areas of lower uncertainty concerning the monophyly of particular groups while branching lengths are not informative. Picozoa is represented within Archaeplastida, as the 2021 version of the authors' phylogeny.

Global diversity

Next Generation Sequencing (NGS) of molecular markers from environmental samples—or metabarcoding—has significantly expanded our knowledge of both culturable and unculturable microbes in natural communities, transforming our understanding of protist taxonomic diversity, abundance, and ecological roles (Burki et al., 2021; Caron & Hu, 2019). Metabarcoding data indicate that protists represent the largest share of global eukaryotic biomass, estimated at 4 gigatons (double that of all animals), and account for the majority of eukaryotic diversity on Earth (Bar-On et al., 2018; O'Malley et al., 2013). Although estimates suggest that over one million protist species exist, some researchers posit that the true number could be substantially higher (Pawlowski et al., 2012). Yet, as metabarcoding advances, it may already be capturing intraspecies diversity, raising questions about how best to interpret sequence-based diversity (Caron & Hu, 2019). In any case, diversity surveys are essential for understanding the biogeography, ecology, and community dynamics of protists, as well as for predicting how these communities may respond to climate change (Burki et al., 2021).

Protists also exhibit a remarkable diversity in both form and function (Caron & Hu, 2019). They exist as autotrophs, heterotrophs, mixotrophs, saprotrophs, and eukaryvores, allowing them to serve in roles from primary producers to parasites and predators in natural aquatic and terrestrial environments, including within the complex microbiomes of individual plants, animals, and fungi (Bonkowski et al., 2019; Pawlowski et al., 2012). Their feeding strategies are diverse, involving extracellular digestion, particle ingestion, or cytoplasmic penetration, and their diets span bacteria, microalgae, other protists, and even multicellular organisms as is the case of giant amoebae and dinoflagellates (S. M. Adl et al., 2019; Geisen, 2016). Thus, the characterization of the trophic and ecological function assignment of protists has become integral for interpreting microbial communities, instead of only determining diversity in environmental surveys**.**

Thus, protists' great diversity in size, morphology, taxonomy, nutritional strategies, and behavior, along with their frequent abundance and rapid metabolic rates, make them key players across multiple trophic levels in food webs, often driving complex ecological functions and interactions (Burki et al., 2021). Protist's functions have been thoroughly studied in marine systems, where they form the base of food chains responsible for at least half of the global carbon fixation (Falkowski, 2012). In terrestrial environments, heterotrophic protist consumers are essential for the decomposition and remineralization of nutrient elements, while protist phototrophy is increasingly recognized for its potential ecological relevance (Bonkowski, 2004; Seppey et al., 2017; Singer et al., 2021).

1.2.1. Soil protists and their ecological roles

Over half of all species diversity on Earth is found in soil habitats, where microbial biomass—mainly bacteria, fungi, and protists to a lesser extent—dominates (Anthony et al., 2023; Oliverio et al., 2020; Wang et al., 2024). Soil microbial communities carry out fundamental processes, where protists serve as key regulators within food webs. Protist diversity and community in the soil microbiome vary within and among habitats, and across time, reflecting environmental conditions and the unique functions they perform, often assessed through trait-based approaches (Fierer, 2017; Geisen et al., 2018).

As opposed to Becking's hypothesis that "*everything is everywhere, but the environment selects*", and while environmental factors indeed shape protist diversity to some extent, these alone are not responsible for the structuring of protist communities in the soil at local scales (Becking, 1934; Burki et al., 2021). Among those mechanisms are the biotic interactions established between protists and other microorganisms and plants, abiotic factors (e.g., soil properties like temperature, pH, soil moisture availability; in turn, the soil microbiome modulates some of these factors with its activities), the introduction of new species, disturbance, and stochastic factors (Bonkowski, 2004; Fierer, 2017; Geisen et al., 2014, 2018; Philippot et al., 2024). Nevertheless, no single biotic or abiotic factor has

been consistently identified as the most influential in shaping the soil microbiome's composition (Fierer, 2017).

The diverse functional groups of protists—phototrophs, heterotrophs, and parasites—play a role in shaping their biotic interactions and ecological contributions in soils. Phototrophic protists (microalgae) are most abundant in the sunlit uppermost soil layers, especially in ecosystems lacking extensive plant cover, such as biocrusts (Belnap & Lange, 2013). Although less abundant in other soils, microalgae contribute significantly to soil organic carbon, for example in temperate soils, with a fast turnover that is accelerated by predation (Seppey et al., 2017). Heterotrophic protists (formerly protozoa) dominate protist diversity in soils, with Cercozoa and Ciliophora identified as the most abundant lineages globally (Oliverio et al., 2020). As primary consumers, they control soil nutrient fluxes and enhance plant nutrient uptake by stimulating the mineralization of carbon, nitrogen, phosphorus, and silica (M. S. Adl & Gupta, 2006; Thompson, 2021). A wide range of protists are bacterivorous, exerting top-down control on a wide variety of bacterial prey populations (Y. Jiang et al., 2023; Saleem et al., 2013), a role especially important in the rhizosphere—the root-adjacent soil enriched in plant-derived carbon. Here, the availability of nitrogen is driven by protists and other microfauna through the 'microbial loop' (Bonkowski et al., 2000). Beyond bacterivores, protists occupy various other functional groups, grazing on or preying on archaea, fungi, and microalgae (M. S. Adl & Gupta, 2006; Geisen et al., 2018; Giachello, 2023). Finally, parasitic protists can control populations of much larger organisms such as plants and animals (Burki et al., 2021), while saprotrophic protists contribute to the decomposition of organic matter (S. M. Adl et al., 2019).

Soil microbiomes lack a 'typical' structure due to their small-scale variability and heterogeneous physical configuration, where diverse microhabitats and a mosaic of ecological niches are supported, leading to shifts in abiotic conditions, microbial abundance and activity, and community composition (Burki et al., 2021; Fierer, 2017). Dispersal limitation further influences microbial structure. Most soil protists, whether as active cells, cysts (a dormant stage that enables survival during resource-scarce periods), or spores, lack specific morphological adaptations for active or long-distance dispersal, suggesting that such mechanisms have not played an evolutionary role for these organisms, and they likely dispersed passively by wind or animals (Foissner, 2008; Geisen et al., 2018). The limited dispersal contributes to the 'rare biosphere', characteristic of microbial assemblages: an unexpectedly large number of rare species that remain regional and at low abundances and are detected in only a fraction of the samples in diversity surveys (Guseva et al., 2022; Logares et al., 2014).

The diversity and roles of soil protists within the soil microbiome collectively underpin crucial aspects of soil health, from nutrient cycling and organic matter decomposition to disease suppression,

enhancing soil resilience to environmental disturbances. This local stability contributes to broader ecosystem processes that support global ecological functions.

1.2.2. Soil protists in global ecosystems

Becking's hypothesis has been extensively revisited by protistologists, with evidence suggesting limited cosmopolitanism among some species (Foissner, 2006). A moderate endemicity distribution was proposed by Foissner (2006) for free-living protists, estimating that at least 30% of species are endemic to specific regions, despite suitable habitats existing elsewhere. However, this estimate remains approximate, as endemism and ubiquity vary widely across ecosystems, influenced by local environmental factors (e.g., Ryšánek et al., 2015; Venter et al., 2017). Worldwide, most soils are dominated by protist consumers, making up at least 75% of species; parasites and phototrophs follow and can be particularly abundant in tropical and arid ecosystems, respectively (Oliverio et al., 2020). Furthermore, while tropical and temperate regions often host higher protist diversity, colder climates show reduced species richness due to temperature constraints. However, although soil protists show latitudinal diversity gradients from pole to pole, they are less pronounced compared to other organisms (Burki et al., 2021; Ji et al., 2022; Oliverio et al., 2020).

Globally, soils are estimated to store around 2,000 gigatons of carbon, surpassing the amount found in the atmosphere and vegetation combined (Cavicchioli et al., 2019; Singh et al., 2010). Protists contribute to this storage by driving microbial processes that regulate carbon cycling. In forest ecosystems, heterotrophic protists control the activity and population of fungi and bacteria responsible for decomposing organic material, promoting the formation of stable organic carbon compounds and aggregates that can persist in soils for up to centuries (Geisen et al., 2021; Philippot et al., 2024). Tropical forests, which contain some of the most carbon-rich soils and 25% of the total global carbon stocks, rely partly on protists to mediate rapid organic matter turnover (M. S. Adl & Gupta, 2006; Carvalhais et al., 2014). In agricultural soils, which cover nearly 40% of global soils, protists enhance rhizosphere nutrient cycling efficiency, indirectly contributing to carbon sequestration and optimizing plant growth through the microbial loop (Bonkowski, 2004; Cavicchioli et al., 2019). In addition to carbon, protists regulate nitrogen and phosphorus cycles across ecosystems. Protists release ammonia and orthophosphate through microbial predation—both bioavailable forms essential for plant growth (Bonkowski et al., 2000).

Protists' adaptability to diverse climates highlights their importance in maintaining global ecosystem stability. Nevertheless, as climate warming intensifies, the release of carbon from terrestrial environments increases, and a major concern is the feedback loop introduced by the release of greenhouse gases from carbon-rich environments (Cavicchioli et al., 2019). For instance, permafrost

holds an estimated 1,700 gigatons of carbon, and microbial decomposition in these regions releases CO_2 and CH_4, with 5–15% of this carbon potentially mobilized in the coming decades (Miner et al., 2022; Schuur et al., 2015). Similarly, in peatlands, warming alters microbial activity and plant dynamics, often shifting these ecosystems from carbon sinks to carbon sources (Cavicchioli et al., 2019). The carbon balance of ecosystems such as grasslands, boreal forests, and agricultural soils, heavily depends on climate conditions and land management practices (Jansson & Hofmockel, 2020).

Polar regions are especially vulnerable to climate-induced transformations, where rising temperatures and glacier retreat drastically reshape ecosystems (Bintanja, 2018; Reed et al., 2016; Simoes et al., 2015). Biocrusts, a dominant form of vegetation in polar, alpine, and dryland environments, are particularly sensitive to these changes (Rodriguez-Caballero et al., 2018). As vital microbial habitats, biocrusts dominate the biogeochemical cycling in these regions (Ji et al., 2022) and harbor diverse protist communities, crucial for carbon sequestration and ecosystem stability (Naylor et al., 2020), as they do in other soils worldwide. Understanding the resilience and adaptive capacities of biocrusts in the face of global climate change requires an understanding of protist biodiversity and function within biocrusts, given the intensified stressors affecting these regions.

1.3. Protists in polar biocrusts

Biocrusts are superficial micro-ecosystems composed of soil particles bound to various proportions of eukaryotic and prokaryotic photoautotrophs, heterotrophs, and saprotrophs (Rippin, 2018; Weber et al., 2022). Their photoautotrophic components—cyanobacteria, microalgae, lichens, and bryophytes—form the foundation of the ecosystem, supporting diverse heterotrophic communities including protists, fungi, bacteria, archaea, and microfauna (Weber et al., 2016, 2022).

Protist diversity and abundance can be significant in polar biocrusts, and their contributions vary across developmental stages (Boy et al., 2016). As glaciers retreat, temporal successional gradients across the landscape are led by colonist microorganisms that rapidly initiate biocrust formation (Belnap & Lange, 2001; Bernasconi, 2008; Breen & Lévesque, 2008). Primary succession is dominated by cyanobacteria, which establish nitrogen stocks that facilitate the settlement of terrestrial phototrophic protists; as carbon content increases, bryophytes and lichens arrive, enabling broader microbial networks (Boy et al., 2016). Here, heterotrophic protists participate in regulating microbial prey populations and influencing nutrient turnover as in other environments, although the microbial food web interactions in the polar regions are yet to be fully characterized (Thompson, 2021). Additionally, structures from filamentous phototrophs and bryophyte roots, and organisms' metabolic

products, enhance soil aggregation, stabilization, and moisture retention, resulting in a living crust covering the soil surface as a coherent layer (Breen & Lévesque, 2008; Weber et al., 2016).

Protists in polar biocrusts exhibit remarkable adaptations to survive in these extreme and rapidly changing environments. Many extremotolerant taxa withstand drying–wetting events, prolonged desiccation, or freezing conditions by forming cysts (M. S. Adl & Gupta, 2006; Foissner, 2006; Weber et al., 2022). Some have physiological traits that confer tolerance to repeated freeze-thaw cycles through physiological mechanisms that prevent cellular damage without encysting (Anderson, 2016; Souffreau et al., 2013).

Biocrusts occur globally, covering approximately 12% of Earth's land surface, predominantly in water-limited ecosystems with low plant cover (Rodriguez-Caballero et al., 2018). Climate change and land-use intensification are predicted to cause a decrease in the world's total biocrust cover by around 25-40% within 60 years in drylands in non-polar regions prone to desertification (Rodriguez-Caballero et al., 2018), but more research is needed to understand the biological responses of polar biocrusts to global change (Colesie et al., 2023). As the polar regions experience warming, shifts in precipitation patterns, water availability, wind, snow, and ice cover may cause complex and taxon-specific responses on established biotic dynamics and accelerate nutrient cycling rates, potentially impacting carbon balance (Colesie et al., 2023; Power et al., 2024). For instance, the vegetation in maritime Antarctica is thought to show increases in productivity, abundance, and cover, while the outlook for Continental Antarctica points toward even drier and harsher conditions for survival (Colesie et al., 2023). Moreover, the colonization of deglaciated terrains is expected to accelerate under climate warming in Arctic regions (Klimešová et al., 2012). Climatic and physical disturbances have experimentally shown to drive shifts in biocrust communities, favoring early successional states with reduced moss cover, increased cyanobacteria, and altered hydrological properties such as reduced dew capture and enhanced infiltration and evaporation (Ferrenberg et al., 2015; Li et al., 2018).

Understanding the microbial food webs that sustain biocrusts, particularly the interactions between and within protists, bacteria, and fungi, is essential to predicting their responses to rapid environmental changes.

1.4. Unraveling polar biocrusts' microbial food webs

Over the past two decades, sequencing efforts have significantly expanded our understanding of microbial diversity and community composition within polar biocrusts, building on the foundational discoveries made through microscopy and other earlier methods. These datasets continue to unveil a great hidden soil microbial diversity across both poles (Mugnai et al., 2024; Pushkareva et al., 2024;

Rippin, Lange, et al., 2018) and provide a foundation for exploring trophic and non-trophic interactions among microbial taxa. Despite these advances, food-web functional relationships—such as predator-prey interactions, competition, and nutrient cycling—are yet to be fully elucidated.

While several microbial food webs in polar aquatic ecosystems (e.g., Almela et al., 2019; Kellogg et al., 2019; Velázquez et al., 2017) and their terrestrial counterparts (e.g., Bamforth et al., 2005; Cary et al., 2010; Hodkinson et al., 2003) have been explored to some extent, significant knowledge gaps persist, particularly regarding polar biocrusts. Recent efforts to elucidate polar food webs through network analyses (e.g., Pushkareva et al., 2024; Rippin, Lange, et al., 2018), show promising progress. Notably, Mugnai et al. (2024) provide a valuable contribution by examining inter- and intra-kingdom dynamics among bacterial, fungal, protistan, and metazoan communities across biocrust successional stages in Svalbard. Insights from food web models developed for biocrusts in other global regions and terrestrial polar analog systems can further inform hypotheses about the structure and function of microbial networks in biocrusts on both poles.

Incorporating trait-based approaches, which emphasize functional attributes such as morphology and feeding or resilience strategies, offers a promising framework for interpreting microbial interactions and elucidating food web dynamics. Traits, defined as measurable attributes of an organism that influence its fitness (Cadotte et al., 2011) enable researchers to link individual-level properties to broader ecological processes. When coupled with ecological and molecular data, trait-based approaches can help identify the processes that govern biogeochemical cycles, community stability, and ecosystem resilience in polar biocrusts. Investigating these dynamics is particularly pressing as polar regions face accelerating environmental changes that threaten to reshape microbial community structures and disrupt their ecological functions.

1.4.1. Diversity and functional traits of microbial taxa in polar biocrusts

Polar biocrusts harbor diverse microbial communities, revealing complex bacterial, fungal, and microalgal compositions. In the Arctic, community composition varies with water availability, elevation, and successional stage (Borchhardt et al., 2019; Pushkareva et al., 2022; Steven et al., 2013). In Antarctica, richness and composition are largely driven by water availability, successional stage, pH, aridity, and soil organic matter (Colesie, Gommeaux, et al., 2014; Pushkareva et al., 2024; E. Zhang et al., 2020).

In Arctic biocrusts, dominant bacteria typically include Acidobacteria, Chloroflexi, and Actinobacteria, cyanobacteria often represented by filamentous forms of Nostocales, Synechococcales, and Oscillatoriales (Pushkareva et al., 2021; Rippin, Borchhardt, et al., 2018; Steven et al., 2013). Among eukaryotes, photoautotrophs from Chloroplastida are predominant, with Trebouxiophyceae,

Chlorophyceae, Klebsormidiophyceae, Zygnematophyceae, and Xanthophyceae being especially prevalent (Borchhardt, Baum, et al., 2017; Pushkareva et al., 2022). Eukaryotic heterotrophs are typically dominated by Rhizaria, especially Thecofilosea and Glissomonadida, followed by Stramenopiles (Pushkareva et al., 2022). Interestingly, the chrysophyte *Spumella* (a stramenopile) is ubiquitous in biocrusts from both poles (Rippin, Lange, et al., 2018). Fungi are primarily composed of Ascomycota, Basidiomycota, and Chytridiomycota, while metazoans are represented by nematodes (Borchhardt et al., 2019; Pushkareva et al., 2021).

In Antarctic biocrusts, typical bacterial diversity is dominated by Chloroflexi, Cyanobacteria, and Firmicutes among prokaryotes, with the particular presence of Oscillatoriales, Nostocales, Synechococcales, Chroococcales, and Pseudanabaenales (Pushkareva et al., 2024; Rippin, Borchhardt, et al., 2018; Severgnini et al., 2021). Among eukaryotes, Chloroplastida (Trebouxiophyceae, Ulvophyceae, Xantophyceae, and Zygnematophyceae), Alveolata (Ciliaphora), Rhizaria (Cercozoa), and Metazoa (Nematoda, Rotifera, and Tardigrada) are prevalent (Pushkareva et al., 2024; Rippin, Borchhardt, et al., 2018; Thompson et al., 2020). Fungi belong typically to Ascomycota, followed by Basidiomycota (Canini et al., 2020).

Several functional traits are known for biocrust microbial taxa, and a few that can be relevant in polar biocrusts are mentioned here. Microalgae and cyanobacteria are keystone primary producers, acting as nitrogen fixers and producing extracellular polysaccharides that stabilize the soil (Mugnai et al., 2020). Rhizaria exhibit traits like bacterivory (e.g., Glissomonadida) and eukaryvory or omnivory (e.g., some Thecofilosea as *Fisculla* and *Rhogostoma*; Dumack et al., 2020; Seppey et al., 2017). Ciliates are mostly bacterivores, but some exhibit mixotrophy, osmotrophy, and eukaryvory; as heterotrophs, they contribute to nutrient cycling turnover (Lynn, 2008). Ascomycota participates in organic matter decomposition, nitrogen cycling, and lichen symbiosis, while Basidiomycota facilitates carbon cycling and forms ectomycorrhizal associations to enhance nutrient exchange (Treseder & Lennon, 2015). Metazoans, including nematodes, rotifers, and tardigrades, regulate microbial populations and facilitate organic matter decomposition (A. M. Potapov et al., 2022). However, nematodes are scarce or absent in Antarctic soils (Freckman & Virginia, 1997).

1.4.2. Food web biotic interactions: Insights from polar soils and global biocrusts

Microbiomes are dynamic systems in which microorganisms engage in trophic and non-trophic interactions, which can be positive, negative, or neutral, and may shift between cooperation, competition, antagonism, and exploitation based on environmental conditions (Berry & Widder, 2014; Gupta et al., 2021; Pacheco & Segrè, 2019). Understanding microbial interactions in polar biocrusts is necessary to define the fundamental dynamics influencing community structure, assembly, and

function from the effects of the environment on the structuring of microbial communities (Chu et al., 2020).

Trophic interactions within biocrust food webs, exemplified by those in Moab, Utah (Fig. 2) are structured around cyanobacteria and algae, alongside fungi, which support diverse consumers, including bacterivorous and fungivorous nematodes, protists, and microarthropods like mites and collembolans. Predatory protists, nematodes, and microfauna regulate the lower trophic levels, while energy flows are dominated by microbial interactions. These food webs are distinguished by a greater reliance on microbial interactions and enhanced nitrogen cycling through microbial communities compared to conventional terrestrial ecosystems (Darby & Neher, 2016).

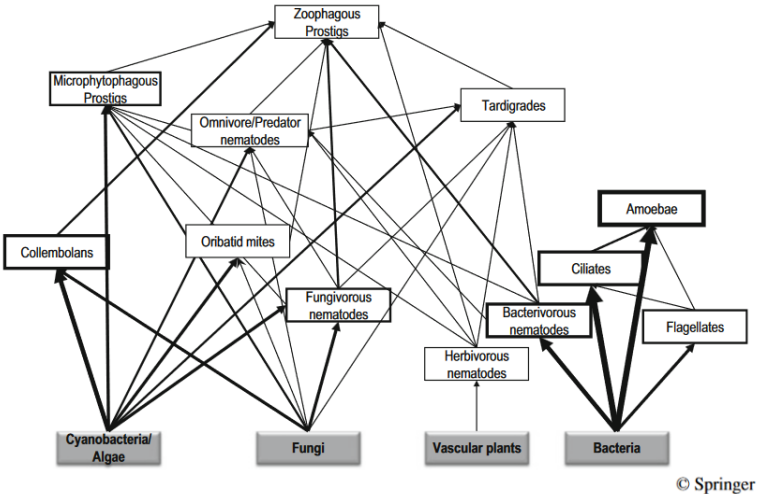

Figure 2. Biocrust food web from a system in Moab, Utah. The web depicts trophic interactions among primary producers (cyanobacteria, algae), consumers, including nematodes, protists, and microarthropods, and fungi. Arrow widths represent the biomass nitrogen flow between trophic levels, and box borders indicate inorganic nitrogen release by consumers. (Extracted from Darby & Neher, 2016).

In contrast, Antarctic terrestrial ecosystems exhibit relatively simplified food webs due to extreme environmental constraints. Primary producers form the base, providing organic matter that supports microbial communities of bacteria and fungi (Fig. 3). These microbes, in turn, are consumed by protists and limited metazoan consumers, such as nematodes, tardigrades, mites, and rotifers, which are represented by fewer than five genera per phylum and exhibit high levels of endemism (Cary et al., 2010). Higher trophic levels, such as predators or omnivores, are largely absent, and

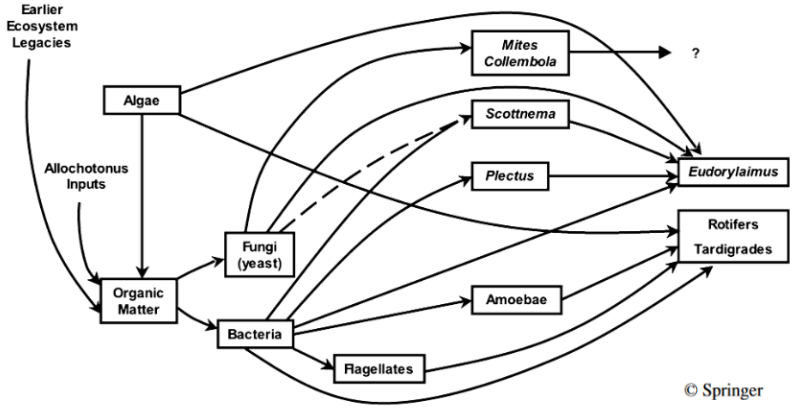

Figure 3. Conceptual soil fauna food web in the McMurdo Dry Valleys modified from (Freckman & Virginia, 1998). Key trophic relationships involve three nematodes: *Scottnema* and *Plectus* feed on bacteria and fungi, while *Eudorylaimus* acts as an omnivore and nematode predator. Tardigrades and rotifers consume algae, while mites and Collembola feed on fungi. The web reflects the trophic relative simplicity of the system, with limited interactions. (Extracted from Bamforth et al., 2005).

communities rarely exceed three trophic levels. Although springtails (Collembola) and mites (Acari) are conspicuous in Antarctic soils, nematodes are typically present in low diversity or entirely absent, while rotifers and tardigrades exhibit patchy distributions or may also be absent altogether (Adams et al., 2006; Bamforth et al., 2005; Freckman & Virginia, 1997). On the other hand, protist abundance can be several orders of magnitude greater than that of the nematodes, and the species diversity much greater, while their ubiquitous distribution suggests their importance in antarctic soil food webs (Bamforth et al., 2005). The extreme climate, limited water availability, and low energy input from primary producers restrict both biodiversity and the complexity of the food web, resulting in a system dominated by microbial interactions and consumer-resource dynamics (Cary et al., 2010).

A key knowledge gap emerges in understanding who feeds on algae when nematodes and other common soil grazers are largely absent in polar soils. Protists, particularly flagellates, and amoebae, are likely candidates for filling this ecological role, but their specific contributions to algal grazing in soil ecosystems remain poorly understood. Investigating the roles of protists in these moderately complex food webs could reveal critical insights into the energy flow and nutrient dynamics in polar biocrusts.

1.5. Network analysis: A window into microbial interactions in polar biocrusts

Association network analysis is a powerful tool for exploring and predicting microbial relationships, offering a window into the dynamic interactions that underpin microbial ecosystems (Guseva et al., 2022). Frequently applied to diverse microbial communities, this approach relies on datasets obtained through high-throughput sequencing to identify statistical associations between taxa based on their co-occurrences or co-abundances, which are then represented as networks (Faust & Raes, 2012).

Networks capture the joint spatial or temporal distributions of microbial taxa and their shared responses to environmental conditions. However, co-occurrence or co-abundance alone does not imply direct ecological interactions, as taxa may co-occur simply due to shared environmental drivers (Blanchet et al., 2020). Advanced methods such as FlashWeave and Hierarchical Modeling of Species Communities (HMSC) address these limitations by integrating environmental covariates, enhancing precision, and reducing spurious associations (Ovaskainen & Abrego, 2020; Tackmann et al., 2019). FlashWeave, a probabilistic graphical modeling tool, typically generates network visualizations where nodes represent microbial taxa and edges indicate positive or negative associations (Deutschmann et al., 2021). In contrast, HMSC, a Bayesian multivariate form of the Joint Species Distribution Modeling (JSDM), constructs association matrices from residual correlations, disentangling environmental effects from potential biotic interactions (Tikhonov et al., 2020; Warton, 2022).

Despite their utility, these networks remain hypothesis-generating tools for understanding community structure and should not be mistaken for ecological food webs, as inferred associations often reflect statistical correlations rather than direct trophic or ecological interactions (Deutschmann et al., 2021). Robust network inference methods and careful interpretation are critical for deriving meaningful biological insights. Furthermore, the limited availability of comprehensive datasets documenting known microbial interactions complicates the refinement of network analyses. Consequently, experimental validation—such as co-culture studies—remains essential for confirming the ecological relevance of predicted associations (Faust & Raes, 2012; Matchado et al., 2021). Nevertheless, most network constructions are rarely followed by experimental confirmation (Faust, 2021).

1.5.1. Where to begin testing microbial interactions?

Even in low-complexity systems, microbial network analyses can yield hundreds or thousands of putative correlations, raising the critical question: Where should experimental validation begin? Simplifying networks is one strategy, achieved by reducing network density through stricter corrected p-value thresholds for inferred edges or by increasing cut-offs for association strength, prevalence, or abundance filtering (Röttjers et al., 2021; Weiss et al., 2016). However, overly stringent criteria risk excluding potentially meaningful interactions, resulting in an incomplete network representation (Röttjers et al., 2021).

An alternative approach involves simplifying microbial communities themselves. For example, serial dilutions have been used to reduce community complexity, enabling the construction of *in silico* networks and subsequent validation of microbial pairs (M.-Z. Jiang et al., 2022, 2024). While effective in isolating specific interactions, this method may overlook high-order interactions that are mediated by other species in natural conditions (M.-Z. Jiang et al., 2022).

Another promising strategy is to aggregate taxa into taxonomic or functional groups to focus on broader patterns rather than individual pairwise interactions (Deutschmann et al., 2021). For instance, Lima-Mendez et al. (Lima-Mendez et al., 2015) adopted a trait-based approach, grouping taxa into functional sets, and validated network-derived hypotheses through microscopy. This approach confirmed symbiotic relationships using a curated collection of 574 known symbiotic interactions in marine eukaryotic plankton. Building on this concept, integrating ecological trait-based approaches—incorporating organism-specific traits into network evaluations—can improve the identification and validation of meaningful interactions. Trait-based ecology links species diversity and traits with the underlying mechanisms driving community structure and ecosystem functioning (Violle et al., 2007). Applying this framework to microbial networks offers a pathway to bridge computational predictions and empirical testing, ensuring that key interactions are neither overlooked nor underestimated.

1.6. Polar biocrusts as model systems for network validation

Soil microbial network analysis is inherently challenging, owing to the heterogeneity of the soil matrix and variability in datasets, with different construction methods affecting network structure and subsequent ecological interpretations (Guseva et al., 2022). Additionally, soil microbial networks often display complex system properties such as scale-free topology (few highly connected nodes or hubs dominate the network), small-world properties (short path lengths between nodes, allowing efficient communication), and modularity (clusters of highly interconnected nodes that perform distinct ecological roles). These properties are thought to enhance the stability and resilience of microbial communities, enabling them to withstand disturbances (Wan et al., 2020).

Among terrestrial ecosystems, biocrusts provide suitable model systems for addressing these challenges in understanding ecosystem functioning (Maestre et al., 2016). Their relatively simple community composition, dominated by microbial primary producers and grazers, allows researchers to focus on core ecological processes without the confounding factors of high biodiversity. From a practical perspective, biocrusts are well-suited for experimental research (Maestre et al., 2016). Biocrust taxa are often amenable to cultivation and manipulation; their small size allows for the creation of compact experimental units that are resource-efficient and easy to manipulate, enabling the exploration of biodiversity-ecosystem functioning relationships, community responses to environmental stressors, and the validation of ecological theories (Bowker et al., 2014; Maestre et al., 2016). Furthermore, biocrusts facilitate hypothesis testing for network analyses. Their relatively simple food-web structures—dominated by primary producers, decomposers, and grazers—are ideal for validating associations inferred from statistical models. Incorporating trait-based approaches could further enhance the interpretation of microbial interactions, linking functional traits to ecological processes within these networks.

Polar biocrusts, in particular, exhibit a considerably lower complexity than other biocrust communities due to the extreme physical conditions that drastically reduce biodiversity. They predominantly feature microbial primary producers and consumers with short life cycles, thus offering exceptional potential to study the drivers and functioning of microbial communities (Pushkareva et al., 2016; Thompson, 2021; Thompson et al., 2020). Thus, polar biocrusts provide a relatively simple food-web structure, making them an appropriate system for validating network hypotheses.

1.7. Cercozoa, a potential key trophic link in polar biocrusts

Cercozoa, a major group of globally dominant soil protists, play critical roles in driving ecosystem functions (Burki et al., 2021; Oliverio et al., 2020). Known as widespread bacterivores, certain taxa

within Cercozoa also include omnivorous or strictly eukaryvorous lineages, such as algivores, that interact directly with primary producers (Dumack et al., 2020; Hess & Melkonian, 2014; Seppey et al., 2017). These functional variations make Cercozoa essential in understanding microbial food web dynamics, particularly in polar biocrusts where they are abundant and ecologically significant (Khanipour Roshan et al., 2021; Pushkareva et al., 2022).

Targeted metabarcoding techniques developed for the taxon have improved the detection of cercozoan diversity in environmental samples, revealing their widespread presence in various climatic regions (Fiore-Donno et al., 2018). For example, co-occurrence analyses in grasslands revealed unexpected positive correlations between terrestrial algae and *Rhogostoma*, a cercozoan genus previously thought to be exclusively bacterivorous (Seppey et al., 2017). Food choice experiments have confirmed its facultative algivory, illustrating the importance of combining high-throughput sequencing with experimental validation to uncover cryptic ecological roles (Dumack et al., 2018). Similarly, in Antarctic glacier forefields, algivorous Vampyrellidae were discovered to be dominating predators in early successional stages, highlighting overlooked roles of cercozoan predators during early primary succession stages (Vimercati et al., 2022).

As both bacterivores and algivores, Cercozoa might serve as a vital trophic link within polar ecosystems, mediating energy transfer between primary producers and higher trophic levels. Their dual roles exemplify the complexity of microbial food webs and underscore the importance of integrating trait-based and molecular approaches to elucidate their ecological significance.

1.8. Aims of the study

This study aims to advance our understanding of microbial interactions in polar biocrusts by focusing on the predator-prey dynamics of Cercozoa and their algal prey. To achieve this, I developed taxon-specific DNA-based amplicon sequencing methods, enabling the generation of comprehensive datasets for Cercozoa and their putative prey. These datasets formed the foundation for cross-kingdom network analyses to identify potential trophic relationships.

Building on these data, and with the assistance of Bachelor students, I established a culture collection of biocrust protists and conducted feeding range experiments to validate the putative interactions identified through network analyses. By integrating systematic testing with a trait-based approach, informed by a curated collection of cercozoan functional traits (Dumack et al., 2020) this research provides direct evidence of algivory and predatory behavior in Cercozoa.

Furthermore, this study applied advanced cross-kingdom network inference to polar biocrusts, predicting interactions between Cercozoa (Rhizaria) and their primary prey: green algae (Archaeplastida) and ochrophytes (Heterokontophyta), two dominant groups in polar biocrusts that play significant roles in nutrient cycling and food-web dynamics (Obbels et al., 2016; Pushkareva et al., 2024; Rippin, Lange, et al., 2018). By combining network analysis with functional traits and experimental validation, this research establishes a robust framework for understanding microbial predator-prey dynamics in polar ecosystems, setting an ecological baseline to assess the impacts of climate change on biocrust functionality.

2. Material and methods

2.1. Study areas

This study encompasses the analysis of biocrusts in three polar regions. One region was included in the Arctic—Svalbard in the Arctic Ocean (Fig. 4a). Two regions were studied in Antarctica: King George Island in the South Shetland archipelago of Maritime Antarctica (Fig. 4b) and the Thala Hills oasis in Enderby Land, East Antarctica (Fig. 4c).

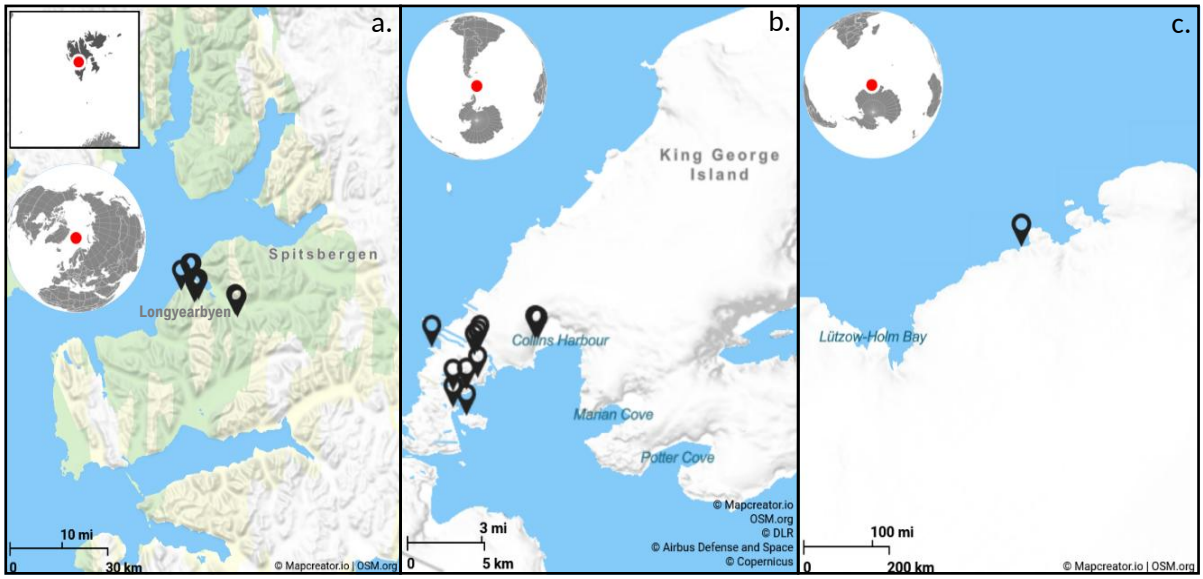

Figure 4. Study areas and sampling sites. (*a)* Svalbard, is located within the Arctic Circle. Antarctica: (*b)* King George Island, in the South Shetland archipelago; (*c)* Thala Hills Oasis, in Enderby Land.

2.1.1. Environmental characteristics and biodiversity

Svalbard (the Arctic)—Located in the Arctic Ocean, the Svalbard archipelago comprises all islands, islets, and reefs situated between 74° and 81°N, and 10° and 35°E, as defined in the Svalbard Treaty. Spitsbergen, the largest island, is home to the capital Longyearbyen, administrated by Norway (Jensen, 2020). Although entirely within the High Arctic, and with a correspondingly severe climate, Svalbard is considerably milder, wetter, and cloudier than the average for the latitude due to atmospheric heat and moisture transport associated with the Icelandic low and the warm West Spitsbergen Current (Adakudlu et al., 2019). The annual mean temperature in Longyearbyen increased from -5.9°C (1971-2000) to -2.5°C (2010-2020), with a mean rainfall of 249 mm in the latter period (Norwegian Meteorological Institute, 2022). This trend is consistent across the entire archipelago, as temperatures have risen by 3 to 5°C in the last decades. Fine-scale simulations project a further temperature

increase of 4 to 7°C by 2100 under different scenarios (RCP2.6 and RCP8.5, respectively). Alongside and consequently, the frequency of heavy rainfalls, glacier ice loss, and annual runoff (mainly caused by enhanced glacier melt), have increased (Adakudlu et al., 2019). About 16% of Svalbard's land area consists of vegetated peninsulas and valleys (Burnett et al., 2023; Johansen et al., 2012).

The vegetation comprises ca. 204 recorded vascular plants (Brožová et al., 2023), 740 lichens (Øvstedal et al., 2009), 380 mosses (Prestø et al., 2014), and at least one hundred algal species (Borchhardt, et al., 2017a; Rippin et al., 2018). Permafrost covers the entire landmass of Svalbard, and only the top meter of the earth thaws during the summer. The flora survives in relatively barren ground soil, and is subject to a very short growing season, with periods of continuous daylight and darkness ranging from 120 to 140 days (Øvstedal et al., 2009).

King George Island, Maritime Antarctica (hereafter, Antarctic Peninsula)—The South Shetland archipelago is located northwest of the Antarctic Peninsula, between 61 and 63°S, and 54 and 63°W. Strongly influenced by the Antarctic Circumpolar Current, the region has the mildest climate in Antarctica (Borchhardt, et al., 2017b), characterized by cold, maritime, and moist conditions (Garrido-Benavent et al., 2020). The Fildes Peninsula, situated in the southwest of King George, the archipelago's largest island, covers an area of 29 km^2 (Boy et al., 2016), and is the island's largest ice-free zone (Michel et al., 2014). The mean annual temperature, recorded in Bellinghausen Station, has increased from -2.3°C (1961-2010) to -1.9°C (2012-2022). Similar to Svalbard, mean annual air temperatures are rising throughout Antarctica, with the most pronounced warming occurring in the Peninsula (Pasik et al., 2021). In the 2012-2022 period, the mean annual precipitation in the region was 660 mm (NOAA National Centers for Environmental Information - NCEI).

The vegetation in Fildes consists of 40 described mosses (Henriques et al., 2018), 119 lichens species (Andreyev, 1989), and two species of flowering plants, namely *Deschampsia antarctica* Desv. and *Colobanthus quitensis* (Kunth) Bart (So et al., 2023). Moreover, a species richness of 830 algal OTUs was recently described.

Molodezhnaya, Thala Hills Oasis of Enderby Land, Continental Antarctica (hereafter, Continental Antarctica)—Enderby Land extends from 38° 30' E to 57°E and 67°S and borders the Cosmonauts Sea in the west and the Sea of Cooperation in the east. The Thala Hills (or Molodezhny) encompass the Molodezhnaya base and cover ca. 41 km^2. They form a coastal oasis with ice-free areas amidst a predominantly glacial landscape and belong to the low-lying coastal Antarctic oases, common along the coasts of continental Antarctica. The oasis has a more severe climate than others at similar latitudes in East Antarctica. The average air temperature registered at Molodezhnaya station of −11.0 °C (1963-1998; Dolgikh et al., 2015), has persisted in recent years (2017-2022; NOAA National Centers

for Environmental Information-NCEI). The recorded annual precipitation is 484 mm water equivalent (Lukashanets et al., 2021).

Soil vegetation cover in the Thala Hills is sparse. Fifty-one lichen and nine moss species are documented (Lukashanets et al., 2021), while the recorded algae diversity is limited to eight green algae and two diatom species (Ohtani et al., 2000).

2.2. Sample collection

Samples were collected in Svalbard in July and in the two Antarctic regions in February and March, corresponding to Arctic and Austral mid- and late-summer, respectively. The warmer temperatures, continuous daylight, and increased humidity (Dolgikh et al., 2015; Norwegian Meteorological Institute, 2022; Pasik et al., 2021) support photosynthesis and increase metabolic activity and abundance in microbial communities, resulting in shifts in community composition (Darby & Neher, 2016). Increased liquid water availability, a critical driver of microbial richness and composition in polar soils (Borchhardt, Baum, et al., 2017; Colesie, Green, et al., 2014), is caused by snow and glacier melt runoff, permafrost thaw, and increased rainfall (Romanowicz & Kling, 2022). Biological activity in general varies seasonally, driven by the reproductive cycles of flora and fauna and the presence of migratory bird populations, which contribute to nutrient inputs (Chown & Convey, 2007).

Polar regions are most accessible during summer when ice cover recedes, weather conditions stabilize, and daylight extends operational hours (Lyu et al., 2024). *In contrast*, logistical challenges during winter, such as extreme cold, darkness, and ice cover, often preclude year-round sampling. However, focusing solely on summer campaigns may limit insights into year-round soil functioning. (Lyu et al., 2024). Temporal variations in environmental conditions must be carefully considered when interpreting cross-sectional microbial association networks and broader ecological dynamics.

Sites with early and mature stages of soil crust development were selected. At each site, five replicates were collected, ensuring a minimum separation of one meter. Sampling consisted of pressing the opening of a sterile plastic Petri dish into each biocrust and lifting it gently with a spatula disinfected with 70% Ethanol. Next, the samples were air-dried for one to three days before sealing the Petri dishes with parafilm. Finally, the soil crusts were transported to the University of Cologne, Germany, for analysis.

Svalbard—The sampling campaign took place in July 2021. Sampling sites comprised glacial moraines and other rocky terrains with sparse vegetation, where bird feces were present. Various bird species, including terns, skuas, and ptarmigans, were observed nesting in the area. Forty-five soil crust samples

were collected at nine sampling sites in the vicinity of Longyearbyen. Three sites west of Longyearbyen, four in the periglacial area of Longyearbreen glacier, and three on the Breinosa mountain were sampled (Fig. 5).

King George Island—The sampling took place from January to March 2022. Fifty soil crust samples were collected in 10 sampling sites, chosen in areas with low visible human disruption. The sites featured arenosols, cryosols, leptosols, and fluvisols (Lupachev et al., 2020), which had bird droppings from the various species of skuas, gulls, terns, petrels, and penguins that visit or nest in the area. Four sites were located in the vicinity of Collins station and three in "*Meseta*" (North-Davis Heights), all of them in the periglacial area of Collins. Three additional samples originated from areas ranging from 300 m to 2 km in distance from Bellinghausen station.

Thala Hills Oasis—The sampling campaign was conducted in February 2022. The terrain comprised rocky hills with weathered rock formations, occasionally accumulating bird feces (Adélie penguins and South Polar skuas nest in the area). Twenty soil crust samples were collected at four sampling sites located between 700 m to 3.2 km in the vicinity of the Molodezhnaya station.

Figure 5. Sampling sites in Svalbard.

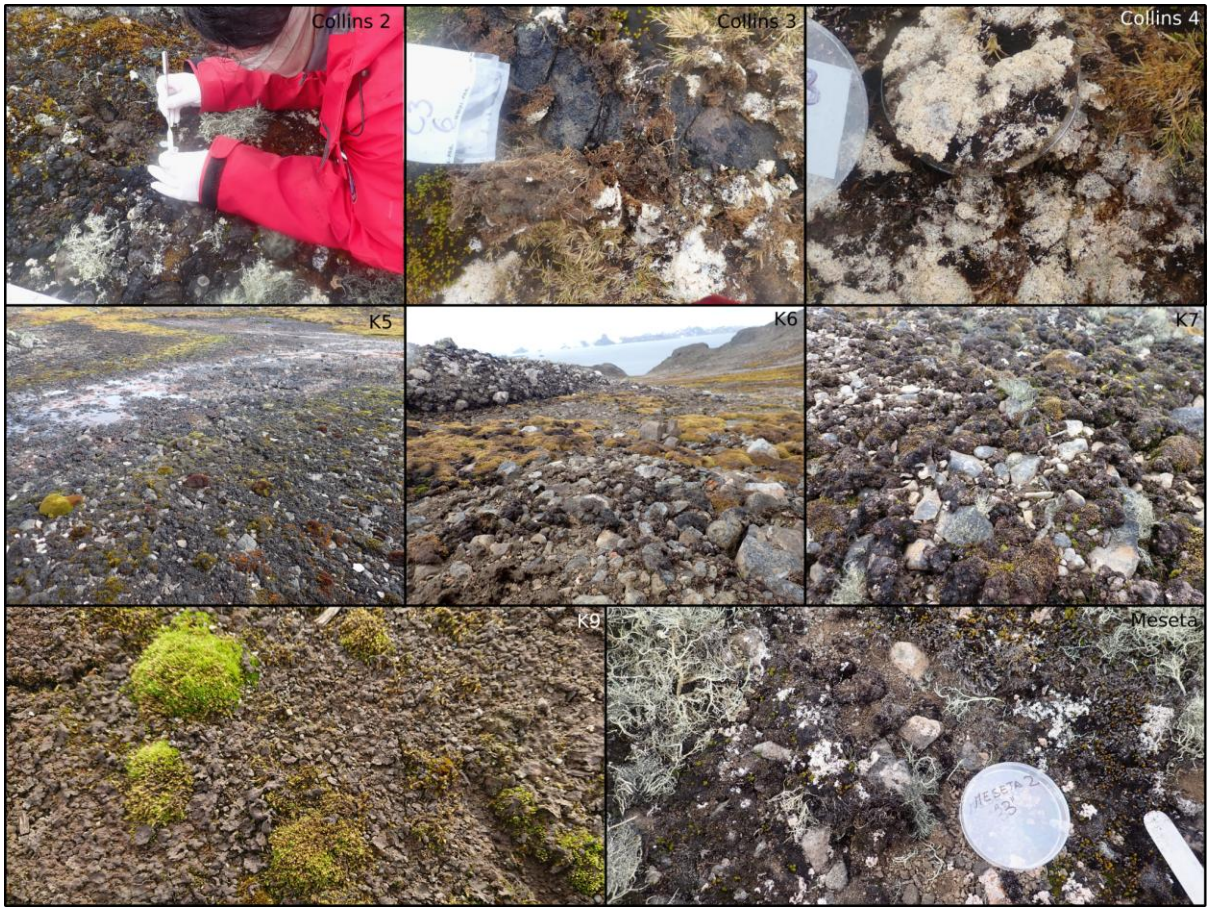

Figure 6. Sampling sites in King George Island.

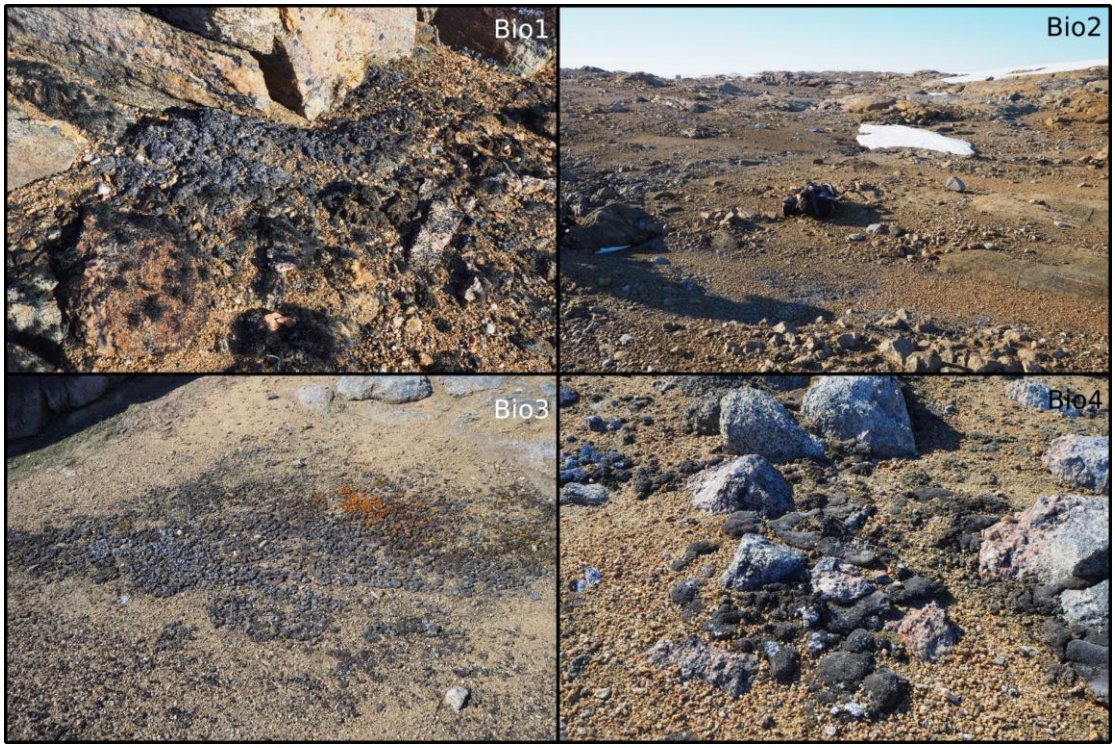

Figure 7. Sampling sites in the Thala Hills Oasis.

2.3. Chemical properties of biocrusts

The chemical properties of the biocrust samples were analyzed as described by Khanipour Roshan et al. (2021). Total organic carbon (TOC), total nitrogen (TN), total phosphorus (TP), and pH were determined from dried and milled biocrust material, using standard methodologies. TOC and TN were measured with a CHNS Analyzer (VARIO EL III, Elementar Analysensysteme, Hanau, Germany) after acidification with 10% HCl to remove inorganic carbon (Blume et al., 2011). TP was measured photometrically using molybdenum blue as a color indicator (Berthold et al., 2015). Specifically, TP analysis involved the digestion of the biocrust powder in acid persulfate (1.5 mL; prepared with 5 g $K_2S_2O_8$ and 5 mL 9 N H_2SO_4 in 100 mL ultrapure water) in an oven at 90 °C for 24 hours. The digested samples were neutralized with 1 N HCl, alkalized with nitrophenol (0.8 g in 100 mL distilled water), and titrated with NaOH (1 M) and HCl (1 M) before being filtered (25 mm, Whatman). The TP concentration was then measured at 885 nm with a spectral photometer (Hach-Lange, DR 3900, Düsseldorf, Germany) using reference standards. The pH was determined in a 0.01 M $CaCl_2$ solution at a 1:2.5 soil-to-solution ratio.

2.4. Development of metabarcoding protocols for terrestrial green algae and ochrophytes

2.4.1. Method and locus selection

The use of universal eukaryotic primers in environmental sequencing typically leads to libraries that inadequately represent the true microbial diversity. Certain genetic loci may not efficiently capture all taxonomic members or exhibit biases (Hall et al., 2010), often producing non-saturated data. Therefore, taxon-specific primers for green algae and diatoms (and other ochrophytes) were designed, which are two potential prey of Cercozoa in polar biocrusts. A metabarcoding approach using tagged versions of the primers was chosen as it enables the simultaneous analysis of multiple samples while reducing costs. Furthermore, it allows a targeted analysis and ensures data saturation, taxonomic resolution, and sensitivity. The method has the potential to detect low-abundance taxa, which may not be uncovered by other omic techniques that offer broader but less sensitive insights into microbiomes. Protocol development followed the methodology that Fiore-Donno et al. (2018) applied for designing Cercozoa-specific primers.

The V4 region of the 18S rRNA-encoding gene was targeted due to its suitability as a marker region for diatom analyses (Guo et al., 2015; Visco et al., 2015). Although no single marker has yet proven ideal across all green algae lineages (Hall et al., 2010), while having a length suited for Illumina MiSeq sequencing, and a rich sequence-library availability, 18S sequencing was applied as it provides

sufficient coverage and insight into terrestrial taxa at genus level. Universal eukaryotic primers (Van Borm & Boomsma, 2002), primers for green algae (Bradley et al., 2016; S.-R. Lee et al., 2010; Stoeck et al., 2010), and diatoms (Guo et al., 2015; Visco et al., 2015; Zimmermann et al., 2011) were evaluated for their suitability for being subjected to terrestrial habitats.

Although the protocol was initially designed with diatoms in mind, further testing revealed its potential to amplify a broader range of ochrophytes—a diverse class that includes diatoms and other closely related phototrophic lineages. This versatility enhances the utility of the primers for studying the trophic dynamics of microbial ecosystems in these environments. Therefore, in this study, I will refer to ochrophytes rather than diatoms to reflect this expanded focus.

2.4.2. Primer design and *in silico* evaluation

Ochrophyte 18S sequences of the Diat.barcode database (v. 9; Rimet et al., 2019) were aligned with MAFFT (v. 7.221) using the L-INS-i algorithm (gap opening penalty =3; Katoh & Standley, 2013). The alignment was refined manually using UGENE (v. 37; Okonechnikov et al., 2012), and only sequences with high coverage of the 18S and which were low in ambiguous bases were kept, resulting in an alignment of 1988 sequences. A subset of the alignment was selected, keeping only 1077 of the sequences. These sequences were chosen according to the diversity of ochrophyte families previously found in terrestrial habitats (Borchhardt, Schiefelbein, et al., 2017; Ettl & Gärtner, 2014; Foets et al., 2021). Likewise, an alignment was generated for green algae. A selection of 18S sequences from the PR^2 database (v. 4.12.0; Guillou et al., 2013) was aligned and refined as earlier described, obtaining an alignment of 4855 sequences. Since the primers were designed to evaluate microbial biodiversity in soil biocrusts, terrestrial ochrophyte sequences were used to assess their specificity and coverage in retrieving ochrophyte targets from terrestrial ecosystems. Likewise, for green algae, high coverages of terrestrial taxa were intended. Thus, it was aimed to reach a specially high coverage of the Chlorophyta taxa Chlorophyceae, Trebouxiophyceae, Ulvophyceae, and the charophyte taxon Zygnematophyceae (Borchhardt, Schiefelbein, et al., 2017; Darienko & Pröschold, 2017; Ettl & Gärtner, 2014).

Literature primers and designed potential primers were subjected to analysis in the OligoEvaluator (Sigma-Aldrich) and the OligoAnalizer Tool (Integrated DNA Technologies), to confirm that the primers met selection criteria, namely: melting temperatures (Tm>54°C), nucleotide composition (40-60% GC content), primer length (18 to 24 bp), the and avoidance of primer duplexes and secondary structures.

TestPrime 1.0 on the non-redundant SILVA database r138.1 (no mismatches allowed; Klindworth et al., 2013) was used to test the primers' specificity and coverage and compare them with existing ones. After meeting the primer selection criteria, the primers that showed the highest relative coverage on

SILVA and the respective reference alignments were selected. One forward and two reverse primers target a region of approximately 290-358 base pairs in a two-step semi-nested PCR protocol for ochrophyte identification. For green algae, the same forward primer and three reverse primers target a region with an approximate length of 304-383 base pairs, with the same PCR scheme, as mentioned before (Table 1).

Table 1. Metabarcoding protocols used in this study

Taxon	Semi-nested PCR	Primers		Ta[+] °C	≈ Length (bp)
		Forward (5'-3')	Reverse (5'-3')		
Cercozoa[1]	1[ST] PCR	S616F_Cerco[1]: TTAAAAAGCTCGTAGTTG	S963R_Cerco[1]: CAACTTTCGTTCTTGATTAAA	50	
	2[ND] PCR	S616F_Cerco[1]	S947R_Cerco[1]: AAGAAGACATCCTTGGTG	50	320-345
Ochrophytes[3]	1[ST] PCR	EukF1[2]: AGCAGCCGCGGTAATTCC	Diat_Rv2[3]: CACCTCTGACAATGRAATAC	64	
	2[ND] PCR	EukF1[2]	Diat_Rv1[3]: CCTCTGACAATGRAATACGAATAC	64	290-358
Green algae[3]	1[ST] PCR	EukF1[2]	Chlphy_RV1[3]: GACTAKGACGGTATCTAA	58	
	2[ND] PCR	EukF1[2]	GreenAl_RV1[3]: CTGACAAYGAAATACGAATGC	56	304-383

[+]Ta: annealing temperature. [1]Fiore-Donno et al., 2018. [2]Van Borm & Boomsma, 2002. [3]This study.

Two-step (semi-nested) PCR protocols were chosen to enrich specific amplicons, enhance reproducibility, and minimize diversity biases (Álvarez-Fernández, 2013; Berry et al., 2011). A metabarcoding sequencing approach was selected, which allows a single Illumina library to comprise different samples to be run simultaneously on an Illumina sequencer. This scheme is both time and cost-efficient, increasing multiple sample analyses while reducing a single assay's experimental cost (Zhou et al., 2015). Adaptors for sample identification were designed for the second semi-nested PCR primers, using a code-containing selection approach (Frank, 2009) to guarantee they met the selection criteria (Table 2). For this, flanking, self-dimer, and cross-dimer tests were applied to avoid complementarity with the template strand and dimerization. The tests were carried out in R (v. 4.0.3), following the criteria presented in Table 2. The adaptors consist of eight-nucleotide barcode sequences appended to the 5'-ends of both primers, as detailed in Tables 3 and 4. Barcoded primers were ordered for NGS sequencing to Microsynth (Wolfurt, Austria).

Table 2. Barcode selection criteria. Taken from: Bystrykh, 2012; Fiore-Donno et al., 2018; Shokralla et al., 2012.

Parameter	Criteria
Sequence	- Barcodes should be anticomplementary to the consensus of the reference alignment on the primers' 5' flanking region. - They should be substantially different from one another to prevent cross-mutation of sample tags into each other, which can cause cross-contamination of the samples. - No more than two identical successive nucleotides were allowed within a unique barcode. - Sequence redundancy and the presence of palindromes were avoided. - Barcodes did not show self or cross-dimerization.
Length	- Tags should be relatively short to save most of the space for the sample sequencing. A length of eight nucleotides was considered optimal.
Nucleotide composition	- A balanced nucleotide composition was ensured.

Table 3: List of ochrophyte primers and tags designed in this study

		Forward 5'-3'		Reverse 5'-3'
Primer	*EukF1*	AGCAGCCGCGGTAATTCC	*Diat_Rv1*	CCTCTGACAATGRAATACGAATAC
Tag	A	TTCTATCG	A	TACTTAGC
	B	TAGTGAGA	B	TCTTAGTG
	C	TCCTCAAT	C	TCTCTTAG
	D	TCGTACCT	D	AACAATGC
	E	TGATTGAG	E	AACCTTAG
	F	TGGACTAT	F	AAGTTACG
	G	ACACACCT	G	CTGAATAG
	H	AGCAGATA	H	CGAATGCC
	I	CTAACGTA	I	GTGAACCG
	J	CATACTCA	J	GTGCTACG
	K	GAAGCGTT	K	GCTTACCG
	L	GACCGGAA	L	GCGAAGTG

Table 4: List of green algae primers and tags designed in this study

		Forward 5'-3'		Reverse 5'-3'
Primer	*EukF1*	AGCAGCCGCGGTAATTCC	*GreenAl_RV1*	CTGACAAYGAAATACGAATGC
Tag	A	TTATGAGG	A	TTACATCC
	B	TATCCACT	B	TAATACGC
	C	TAGGATTG	C	TCGTCACG
	D	TCGCTGTT	D	TGTTCGCA
	E	TGATGGTA	E	TGCCGTCA
	F	ATTCACCT	F	TGGTCTTA
	G	ATAGGACT	G	AACCAAGA
	H	AATCTGCA	H	AAGGACCA
	I	AAGTTGCG	I	AGACACGG
	J	AAGAAGTG	J	CTTGTATG

	Forward 5'-3'		Reverse 5'-3'
K	ACATACCT	K	CTTGACTA
L	ACGCCTAA	L	CAAGGCAC
M	CAATTCGA	M	GATGCAGC
N	CCTATCTA	N	GCACTCAA
O	GAGTCGTT	O	GCACAACC

2.4.3. Protocols' test and optimization

Sample collection for testing—Two environmental samples were collected for preliminary testing of the primers. One soil sample originated from a grass field in Cologne, Germany (50.927205, 6.936057) and was collected by removing the first three millimeters of the soil crust using a blade. A sediment sample was collected from an artificial pond at the University of Cologne (50.926944, 6.936111). Clonal cultures of *Nitzschia communis* and *Characium* sp. raised in SiO_3-enriched Waris-H medium (pH 7; Mcfadden & Melkonian, 1986) were used for primer testing.

PCR optimization—PCRs were conducted in two steps. A temperature gradient was applied during PCR to identify the optimal annealing temperatures for both steps. PCR mixtures of 11 µl and 17 µl for the first and second PCR rounds were prepared in 200 µl PCR tubes. The following final concentrations were employed: DreamTaq Green DNA polymerase 0.01 units, and DreamTaq Green Buffer 1x (Thermo Scientific); dNTP 0.2 mM and primers one µM each. One ng of extracted DNA template was incorporated on each reaction of the first PCR and 1 µl of the resulting amplicons as a template for the following semi-nested PCR. Negative controls were included in every run. The cycle number was kept at 24 in both PCRs since replication becomes prone to errors and less efficient as the reaction exits the log-linear phase (around the 26^{th} cycle; V. Potapov & Ong, 2017; Wong & Medrano, 2005). Both thermocycling protocols included an initial denaturation step at 95°C (2 min), followed by 24 cycles consisting of denaturation at 95°C (30 s), annealing (refer to Table 1 Ta°; 30 s), and elongation at 72°C (30 s). A final elongation step at 72°C for 5 min preceded a storing step at 4°C. After each amplification step, the size and quantity of resulting PCR products were analyzed via electrophoresis gel.

Cloning and transformation—Cloning in competent *Escherichia coli* cells was conducted to isolate and amplify individual PCR products, e.g., single-sequence templates of ochrophytes or green algae, to enable accurate identification through Sanger sequencing. The PCR products were cloned to test the primers' specificity and efficiency in retrieving ochrophyte and green algae 18S sequences from the environmental soil sample. One hundred microliters of the PCR products were subjected to purification with the GeneJET PCR purification kit (Thermo Fischer Scientific, Dreieich, Germany). PCR

products were ligated into pGEM-T Easy Vector Systems (Promega, GmbH, Mannheim, Germany), following the manufacturer's instructions, except for the use of the following reagent volumes: 2.5 µl 2X Rapid Ligation Buffer, 0.5 µl pGEM® -T Easy Vector, 0.5 µl T4 DNA Ligase, 0.5 µl H_2O and one µl of the purified PCR product. Subsequently, reactions were incubated for 1 hour at room temperature. The recombinant plasmids were transformed into competent *E. coli* JM109 cells (Promega) following the same protocol, with the following few changes: only 250 µl of SOC medium were added to the transformation reactions, and a 45 min incubation sufficed.

LB agar plates were prepared by dissolving 9.6 g of LB agar according to Miller (AppliChem, Darmstadt, Germany) in 300 ml of deionized water. The mixture was autoclaved for 15 min at 121°C. Next, 175 µl of Ampicillin (100 mg/ml), 300 µl 100 mM IPTG (Thermo Fisher Scientific, Dreieich, Germany), and 600 µl X-Gal Solution (Thermo Fisher Scientific, Dreieich, Germany) were added to the liquid agar after it cooled down to approximately 50°C. The agar solution was poured onto Petri dishes under a sterile cabinet and left uncovered for drying. Volumes of 50 µl and 150 µl of the transformed cultures were plated onto LB agar plates. LB cultures were incubated overnight at 37°C.

Approximately 50 clones from each sample were picked with a sterile toothpick and directly subjected to amplification. PCR mixtures of 10 µl were prepared for each colony with the following reagent volumes: 0.3 µl 10 µM of the M13-40 forward primer and 0.3 µl 10 µM M13R reverse primer; 0.3 µl 10 mM dNTPs, one µl Thermo Scientific DreamTaq Green Buffer, 0.1 µl DreamTaq polymerase and eight µl water. The thermocycling protocol used was the following: initial denaturation at 95°C (2 min), followed by 30 cycles consisting of denaturation at 95°C (30 s), annealing at 52°C (30 s), and elongation at 72°C (2 min). A final elongation step at 72°C for 5 min preceded a cooling step at 4°C. The size and quantity of the resulting PCR products were analyzed by gel electrophoresis. The PCR products were purified by the addition of 0.15 µl of Exonuclease, 0.9 µl FastAP, and 1.95 µl water to 8 µl of the first PCR product. The purification reaction was heated for 30 min at 37°C, and followed by 20 min at 85°C.

Sanger sequencing—Performed using the Big Dye Terminator Cycle Sequencing Kit (Thermo Fisher Scientific, Dreieich, Germany) and the bacterial forward M13-40 or reverse M13R vector primers. DNA was sequenced using an ABI 3730 sequencer (Applied Biosystems), and the service was provided by the Cologne Center for Genomics. Chromatograms were checked for sequencing errors using UGENE as a visualization tool. Sequences with multiple adjacent miscalled nucleotides were excluded from further analysis. The obtained sequences were identified in the PR^2 database using BLAST+ (v. 2.2.31; Camacho et al., 2009) with an e-value of $1e^{-50}$, and the first best hit from the search was kept.

2.5. Molecular analysis of polar biocrusts

2.5.1. DNA extraction

Surface sections (2–3 mm) of each biocrust sample were separated from the adhering soil using a razor blade until a weight of 0.15 to 0.30 g was obtained. DNA was extracted using the Quick-DNA™ Fecal/Soil Microbe Midiprep kit (Zymo Research, Irvine, CA, USA) according to the manufacturer's instructions. A FastPrep®-24 bead beater (MP Biomedicals, USA), equipped with a 2 ml tube holder assembly, was used for the bead-beating process, which entailed a single cycle at 4.5 m/s for 20 s. The kit includes a cleaning and concentration step, and the final elution volume was 100 µL.

2.5.2. PCR amplification, library preparation and sequencing

Taxon-specific metabarcoding approaches were employed to obtain saturated data while significantly reducing sequencing costs by pooling all samples into a single sequencing run per taxon. After the design and successful testing, amplicons were generated using the semi-nested PCR approaches detailed in Table 1. PCR mixtures of 11 and 17 µl were employed for the first and second PCR, respectively. The final concentrations for all three metabarcoding protocols were as follows: 0.01 units of DreamTaq Green DNA polymerase and 1x DreamTaq Green Buffer (Thermo Fisher Scientific, Dreieich, Germany); 0.2 mM dNTPs, and 1 µM of each primer. One ng of extracted DNA was incorporated on the first PCR, and 1 µl of the resulting amplicons was used as a template for the second. The amplification conditions for the three protocols initiated with denaturation at 95°C (2 min), followed by 24 cycles of the 3-step process of denaturation (95°C, 30 s), annealing (Table 1; 30 s), and elongation (72°C, 30 s), and concluded with an elongation step at 72°C (5 min). After the second PCR, successful amplification and correct PCR product size were checked with an electrophoresis gel.

Amplicons, including internal standards (Table 5), were purified and normalized using the SequalPrep Normalization Plate Kit (Invitrogen GmbH, Karlsruhe, Germany), to achieve a concentration of 1–2 ng/µl per sample, and finally pooled. Sequencing was performed by the Cologne Center for Genomics (Cologne, Germany) on an Illumina MiSeq platform (Illumina Inc., San Diego, CA, USA). Using the v3 Reagent kit, and 2 × 300 cycles, 300 bp long paired-end reads were produced.

Table 5. Cercozoa, green algae, and ochrophytes included in the internal standards of each run

ID	Taxonomic assignment	Genus/Species
Cercozoa		
K92[1]	Imbricatea/Krakenida	*Kraken carinae*
CCAP1943[1]	Thecofilosea/Tectofilosida	*Fisculla terrestris*
RC[1]	Thecofilosea/Cryomonadida	*Rhogostoma pseudocylindrica*
M01[1]	Thecofilosea/Cryomonadida	*Rhogostoma minus*
C12[1]	Sarcomonadea/Glissomonadida	Sandonid

ID	Taxonomic assignment	Genus/Species
C70[1]	Sarcomonadea/Glissomonadida	Sandonid
C4[1]	Sarcomonadea/Glissomonadida	Allapsid
C31[1]	Sarc./Paracercomonadida	Paracercomonad
C15[1]	Sarc./Cercomonadida	Neocercomonad
Green algae		
1EA6[2]	Chlorophycea/Sphaeropleales	*Bracteacoccus bullatus*
1EA9[2]	Chlorophycea/Sphaeropleales	*Neocystis brevis*
A10[2]	Chlorophycea/Sphaeropleales	*Coelastrella oocystiformis*
9BA1[2]	Chlorophycea/Chlamydomonadales	*Chlamydomonas/Chloromonas*
1EA12[2]	Trebouxiophyceae/Prasiolales	*Deuterostichococcus epilithicus*
A2.1[2]	Trebouxiophyceae/Chlorellales	*Auxenochlorella* sp.
A9.1[2]	Trebouxiophyceae/Trebouxiales	*Myrmecia bisecta*
7CA3[2]	Klebsormidiophyceae/Klebsormidiales	*Klebsormidium elegans*
Ochrophytes		
7CA4[2]	Bacillariophyceae/Naviculales	*Pinnularia borealis*
3EA8[2]	Bacillariophyceae/Naviculales	*Pinnularia* sp.
7CA12[2]	Bacillariophyceae/Naviculales	*Sellaphora seminulum*
7CA9[2]	Bacillariophyceae/Bacillariales	*Nitzschia perminuta*

Provided by: [1]AG Bonkowski, University of Cologne. [2]This study.

2.6. Analysis of the metabarcoding data

2.6.1. Sequence processing

Reads processing, as described by Fiore-Donno et al. (2020), can be summarized as follows: Raw reads underwent a quality check with the FastX Toolkit (v. 0.0.13; Hannon Laboratory, 2010). Contigs were assembled by pairing reads using MOTHUR (v.1.45.3; Schloss et al., 2009), allowing no differences in the primer sequences. Sequences with minimal overlap of 200 bp and a minimum length of 290 bp for green algae and ochrophytes, and 300 bp for Cercozoa were selected, and those with ambiguities and more than one mismatch were removed. Sequences were demultiplexed via the detection of their unique primer adapters, which were then removed from the reads. Subsequently, and before conducting read clustering for the samples, the internal standard was analyzed and used to define filtering thresholds for quality filtering and to minimize the inclusion of erroneous sequences. According to those results, sequences were clustered into Operational Taxonomic Units (OTUs) in MOTHUR, using the abundance-based greedy clustering (agc) of Vsearch (Rognes et al., 2016), and a similarity threshold of 97%. Next, the sequences were taxonomically assigned with the PR^2 database using BLAST+ with an e-value of 1e-50, and only the best hit was kept. Non-target taxa, including potential contaminants, were excluded to focus on taxa relevant to the study objectives. However, Endomyxa and Chrysophyceae were retained in downstream analyses due to their ecological relevance—Endomyxa for its close phylogenetic relationship to Cercozoa and similar feeding

strategies, and Chrysophyceae for its widespread presence in the dataset. The latter included the removal of two OTUs representing streptophytic microalgae (*Interfilum* sp. and *Cylindrocystis* sp.), which were subsequently excluded from further analysis. Cercozoan reads were then aligned to reference alignments (Fiore-Donno et al., 2018). Green algal and ochrophyte reference alignments comprise 150 representative sequences originating from the Diat.barcode database (v. 9; Rimet et al., 2019) and 399 sequences from the PR^2 database, respectively. Both alignments were made with MAFFT (v. 7.221) using the L-INS-I algorithm (gap opening penalty = 3; Katoh & Standley, 2013). Next, using the reference alignments, replicated sequences and chimeras were identified, with the latter being detected through the implementation of UCHIME (Edgar et al., 2011) in MOTHUR. Misaligned, replicated, and chimeric sequences were subsequently filtered out from the dataset. Analyses of the internal standard revealed that OTUs represented by fewer than 250 (Cercozoa), 305 (green algae), and 285 (ochrophytes) reads, and occurring in less than three samples, could be considered low-abundance artifacts and were removed accordingly, ensuring that only biologically relevant sequences were retained. The final OTU counts served as the basis for downstream analyses, encompassing the calculation of diversity indexes, network analyses, and the confirmation of predation as a key functional trait of heterotrophic protists in polar biocrusts.

2.6.2. Biodiversity statistical analysis

All statistical analyses were performed using R (v. 4.3.0; R Core Team, 2023). Diversity analyses were calculated with *vegan* (v. 2.6-4; Oksanen et al., 2022) and data manipulation and visualization were achieved using the core *tidyverse* packages (v. 2.0.0; Wickham et al., 2019), *RColorBrewer* (v. 1.1-3; Neuwirth, 2022), and *ggrepel* (v. 0.9.5; Slowikowski et al., 2024). Initially, rarefaction curves were calculated with vegan::rarecurve, demonstrating that all sample replicates reached sufficient saturation (Figs. S3-S5). For downstream analysis of the data, the read counts were transformed into relative abundances per sample. Data were then screened to identify differences in community structure across the three regions and to detect outliers. Non-Metric Multidimensional Scaling (NMDS) was chosen for its ability to effectively capture beta diversity by reducing multidimensional community data into interpretable ordinations, facilitating comparisons across regions and edaphic factors. NMDS plots were computed using vegan::metaMDS based on Bray-Curtis dissimilarities (beta diversity), calculated using vegan::vegdist. P-values were adjusted for multiple comparisons using the Benjamini & Hochberg method (Benjamini & Hochberg, 1995). Two sampling sites (10 samples) were identified as outliers and, consequently, were excluded from further analyses, resulting in a dataset of 23 sampling sites and 116 samples for the three regions (Svalbard, N=46; Antarctic Peninsula, N=45; Continental Antarctica, N=20). Edaphic factors, namely TOC (%), TN (%), TP (g/kg), CN ratio, pH, and sampling region were incorporated into the NMDS plots using the vegan::envfit function. Biotic

factors, specifically the community compositions of Cercozoa, green algae, and ochrophytes, were used as determinants of community structure to evaluate their role as shaping factors and further support the hypothesized predator-prey interactions. For this purpose, principal coordinates analyses (PCoA) were calculated for each data set using vegan::capscale, with community compositions serving as input. The PCoAs showed that the first two axes explained 19.3% and 11.2%, 20.7% and 14.25%, and 19.0% and 12.3% of the variation in the cercozoan, green algal, and ochrophyte communities, respectively. The first axis (PCoA1) of each taxon's community was used to predict those of the others. To assess differences in beta diversity across sampling regions and edaphic factors, Permutational Multivariate Analyses of Variance (PERMANOVA) with vegan::adonis2 using 999 permutations was applied.

Venn diagrams were used to visualize the overlap of OTUs among regions, providing insights into shared and unique microbial taxa contributing to the community composition, and were generated with *ggvenn* (v. 0.1.10; Yan, 2023), and the final figures were plotted to approximately depict OTU abundances using *eulerr* (online v. 6.1.1; Larsson et al., 2022). Alpha diversity metrics were calculated with *vegan*, and statistical comparisons were conducted using ANOVA and Tukey HSD posthoc tests, with the packages *ggpubr* (v. 4.3.1; Kassambara, 2023b) and *rstatix* (v. 4.3.1; Kassambara, 2023a).

2.7. Cross-kingdom co-occurrence network inference

Putative biotic interactions were detected and visualized via the calculation of cross-kingdom co-occurrence and correlation networks among the three investigated taxa. The analysis aimed to infer the role of cercozoan predation in shaping microalgae communities. To achieve this, two complementary approaches were employed:

2.7.1. FlashWeave

FlashWeave is a probabilistic graphical modeling tool designed for inferring high-resolution interaction networks from large and heterogeneous microbial sequencing datasets, based on co-occurrence or co-abundance patterns (Tackmann et al., 2019). It is particularly well-suited for microbiome data due to its ability to account for compositional effects characteristic of sequencing data (Gloor et al., 2017), and to handle sparse datasets, explicitly considering zeros to prevent indirect associations (spurious edges) between taxa with similar absence patterns (Deutschmann et al., 2023). Additionally, FlashWeave integrates metadata, including environmental factors, as additional nodes in the network, enabling the differentiation of direct microbial associations from indirect ones driven by shared environmental effects (Deutschmann et al., 2021; Faust, 2021).

Network calculation was preceded by two pre-processing steps to enhance the reduction of indirect associations, following the approach outlined by Freudenthal et al. (Freudenthal et al., 2022). Firstly, the influence of environmental factors on the microbial communities was assessed, namely TOC (%), TN (%), TP (g/kg), CN ratio, pH, and sampling region. Non-metric multidimensional scaling (NMDS) plots were generated for all data, and the environmental variables were fitted onto the ordinations (refer to 2.6.2, "Biodiversity statistical analysis", for details on software and methods). Permutational Multivariate Analysis of Variance (PERMANOVA) was performed to test differences in community composition across regions and edaphic parameters. Statistically significant environmental vectors, scaled by their correlation values, were added to the NMDS plots to visualize their influence on microbial community composition. The analysis identified region as the variable exerting the strongest influence on the communities, and consequently, network analyses were conducted separately for each region. Secondly, spurious edges caused by rare species were minimized by applying prevalence filters to exclude rare taxa, removing OTUs present in fewer than 10% of the samples in each dataset.

Correlation network construction was performed using FlashWeave (v. 0.19.0; Tackmann et al., 2019) to infer the microbial putative interactions, using the Julia environment (v. 1.7.3; Bezanson et al., 2017) and employing the sensitive mode with default settings. To further control for data compositionality, a centered-log-ratio transformation was applied separately to each of the three taxa abundance datasets. The resulting networks were visualized in Cytoscape (v. 3.10.1; Shannon et al., 2003). Significant putative interactions between taxa (nodes) were aggregated at the order level to simplify interpretation. Node sizes corresponded to the total number of reads for each order, and node color denoted the number of aggregated genera. Edges represented individual putative interactions, with line thickness denoting the number of interactions between two orders, and edge colors indicating positive (blue) or negative (red) correlations. This visualization approach facilitated the interpretation of key taxonomic interactions. Thus, by integrating region-specific analyses, filtering for rare taxa, and employing a robust network inference tool, the approach minimized spurious putative interactions and generated ecologically meaningful networks that were further validated experimentally.

2.7.2. Hierarchical Modeling of Species Communities (HMSC)

To further validate the robustness of the findings and confirm predator-prey correlations identified by FlashWeave, Hierarchical Modeling of Species Communities (HMSC), a Bayesian multivariate form of the Joint Species Distribution Modeling (JSDM) framework, framed with generalized linear model (GLM) principles, was employed (Tikhonov et al., 2020). The following three reasons were instrumental in selecting this framework. First, HMSC allows the disentanglement of environmental

correlations (shared species responses to environmental predictors) from residual associations (interactions not explained by environmental factors), providing insights into potential biotic interactions (Ovaskainen & Abrego, 2020). Second, HMSC extends other JSDM models by explicitly incorporating hierarchical random effects to model nested or spatially structured data (Ovaskainen & Abrego, 2020). Given the design of the study, which involves multiple levels of spatial replication (e.g., replicates within sites and multiple sites across three polar regions), HMSC's ability to capture such dependencies makes it particularly well-suited to this dataset. Third, HMSC allows the inclusion of functional traits to refine inferences on species interactions. In this study, the nutritional mode (e.g., autotrophs, eukaryvores, omnivores) was integrated to understand how this functional role influence community structure and ecological networks.

The data was subjected to the HMSC workflow and the networks were constructed using a hurdle model to generate species-to-species association matrices using the R package Hmsc (v. 3.0-13; Tikhonov, Ovaskainen, et al., 2022). While zero-inflated models are not currently implemented in HMSC, a hurdle model can address this characteristic of sequencing data, and consists of two components: one for modeling presence-absence and another for modeling abundance conditional on presence (Ovaskainen & Abrego, 2020). As both components are statistically independent, the approach enables separate exploration of environmental covariates driving species occurrence versus those influencing species abundance (Tikhonov, Opedal, et al., 2022). To model co-occurrence, data were truncated to presence-absence (retaining zeros and setting non-zeros to one) and fitted the matrix with a probit (binomial) model. To model co-abundance, zeros were treated as missing values, and the original abundances were analyzed using a normal model. Prevalence filters were applied to exclude rare taxa, removing OTUs present in fewer than 10% of samples (as done with FlashWeave), resulting in a unique dataset for the three phyla.

Null models, which include only sequencing depth as a covariate, captured a combination of co-occurrence patterns from shared environmental preferences. Full models include fixed explanatory variables, namely TOC (%), TN (%), TP (g/kg), pH, and sampling region, with the log-transformed sequencing depth added as a continuous variable to control for variation in sequencing effort (Odriozola et al., 2021). The sampling site and sample code were incorporated as random effects to capture unexplained variation due to spatial structure and unmeasured covariates (Ovaskainen & Abrego, 2020). To account for the influence of species traits on interspecific interactions, functional traits such as nutritional mode (e.g., autotroph, eukaryvore, omnivore) and phylum were included in the models as input parameters for the estimation of species niches (Odriozola et al., 2021). Species-to-species association matrices were built for null models (using sequencing depth only) and full models (including all explanatory variables). Null model matrices reflect habitat-driven and interactive

co-occurrence patterns, while full model matrices isolate patterns more indicative of direct interactions by accounting for environmental effects (Odriozola et al., 2021). The models were sampled using Markov Chain Monte Carlo (MCMC) algorithms with four parallel chains. Each chain was run for 150,000 iterations, with the first 50,000 iterations discarded as burn-in. The remaining iterations were thinned by retaining every 100th sample, resulting in 1,000 posterior samples per chain and 4,000 posterior samples in total. Convergence was assessed through the effective sample sizes (ESS) and potential scale reduction factors (PSRF). Model fit was evaluated using predicted values, with explanatory and predictive power quantified as AUC for presence-absence models and R^2 for abundance models.

2.8. Establishment of a biocrust-associated culture collection

In order to support the indirect evidence of predator-prey relationships raised by the network analyses, direct evidence was desired. Therefore, potential algal prey and predatory cercozoans were cultured for subsequent food range experiments. The cultures were established and identified in cooperation with Olivia Piasecki, Pablo Navarro, Natalie Kamischke, and Stefan Rein, during their Bachelor Theses.

Before isolation, small portions of each soil crust (ca. 50 mg) were enriched with SiO_3-enriched Waris-H medium (pH 7). To establish monoclonal cultures, individual cells were isolated using glass pipettes under an inverted microscope (Nikon Eclipse TS 100) and placed into 24-well plates. Green algae and ochrophytes were cultured in Waris-H medium. Depending on their required prey, heterotrophs were cultured in wheatgrass medium (WGM) or Waris-H medium, using bacteria or Saccharomyces cerevisiae as prey, respectively. A detailed list of the generated cultures can be found in Tables 6 and 7. The cultures were stored at 15°C, with a light regime of 14/10 hours light/dark, and a light intensity of about 6.5 PPFD (6500 K lamp). All cultures were barcoded by targeting the 18S rRNA-encoding gene.

2.8.1. DNA extraction and molecular identification of cultures

For Cercozoa, cells were directly added to the tubes without any additional lysis, as their cell structure did not necessitate it. In contrast, for green algae and ochrophytes**,** the cultures were processed using the following methodology, which was modified from (Pawlowski, 2000):

A volume of 0.3–1 ml of a monoclonal algae culture medium was transferred into a 1.5 ml Eppendorf tube with a rounded bottom. For low-density cultures, a larger volume was centrifuged in a falcon tube, and the resulting pellet was transferred to a 1.5 ml Eppendorf tube. The samples were centrifuged at 14,000 rpm for 20 minutes to precipitate the cells and form a visible pellet. The

supernatant was discarded, and 50 µl of Guanidine lysis buffer was added to the pellet along with a single bead for cell disruption. (The lysis buffer was handled in a fume hood due to its hazardous nature). The tubes were then subjected to repeated freezing at -80℃ for three minutes and heating at 65℃ for three minutes in a heat block, a cycle repeated up to six times to enhance cell lysis. The cells were mechanically lysed using a Retsch Mixer Mill MM 400 for 20 seconds at 20 Hz. The lysate was briefly centrifuged, and the content was transferred to a clean tube, with the bead washed with 50 µl of water and the wash added to the new tube. The mixture was centrifuged again at 14,000 rpm for five minutes, and the supernatant was transferred to another clean tube, where an equal volume of isopropanol was added to precipitate the DNA. The samples were incubated at -20℃ for at least two hours before centrifuging at 15,000 rpm for 15 minutes to collect the DNA pellet. The pellet was washed twice with 200 µl of 70% ethanol, with each wash followed by centrifugation at 15,000 rpm for five minutes. The pellet was then dried at room temperature or on a heating block at ≤35℃ to prevent overdrying. Finally, the DNA was dissolved in 30 µl of water and stored at -20℃ for further use.

The cultures were identified using the primers established in this study, and Sanger sequencing was performed as detailed in Section 2.4.3.

Table 6. Cercozoa cultures established in this study.

	Code	Genus	Species	Class	Matched accession	Percent identity	Region
1	1AH1*	*Euglypha*	*rotunda*	Imbricatea	KP728379.1	97.22	Arctic
2	3EH1	*Neocercomonas/ Cercomonas*	sp. *plasmodialis*		MG775618.1/ AF411268.1	95.15	Arctic
3	3EH3	*Rhogostoma*	*schussleri*	Thecofilosea	HQ121430.1	99.34	Arctic
4	4BH1	*Neocercomonas/ Cercomonas*	sp./ sp.	Cercomonadidae	MG775599.1/ HM536151.1	100.00	Arctic
5	7CH7	*Fisculla*	*terrestris*	Thecofilosea	KP728379.1	98.77	Arctic
6	9BH5*	*Fisculla*	*nemoris*	Thecofilosea	KT809361.1	100	Arctic
7	C2.2 H5*	*Cercomonas*	*celer*	Cercomonadidae	FJ790710	99.04	An. Pen.
8	C2.2 H6*	*Cercomonas*	*plasmodialis*	Cercomonadidae	AF411268	99.68	An. Pen.
9	C2.2 H7	*Neocercomonas*	*tuberculata*	Cercomonadidae	MG775594	98.12	An. Pen.
10	B2.5 H2	*Sandona*	*limna*	Sandonidae	HQ918177	100	Con. An.
11	B2.5 H3	*Bodomorpha*	sp.	Viridiraptoridae	DQ211596	99.37	Con. An.
12	B2.5 H4	*Spongomonas*	*minima*	Imbricatea	AF411280	98.03	Con. An.
13	B2.5 H6	*Cercomonas*	*plasmodialis*	Cercomonadidae	AF411268	100	Con. An.
14	B2.5 H9	*Euglypha*	*rotunda*	Imbricatea	AJ418784	99.58	Con. An.
15	B3.3 H1	*Rhogostoma*	*epiphylla*	Thecofilosea	KY905095	99.69	Con. An.
16	B3.5 H2*	*Rhogostoma*	*schussleri*	Thecofilosea	HQ121430.1	99.00	Con. An.
17	B3.5 H1	*Neocercomonas*	sp.	Cercomonadidae	MG775612.1	99.68	Con. An.
18	B4.2 H2	*Rhogostoma*	*epiphylla*	Thecofilosea	KY905095.1	98.37	Con. An.
19	B4.2 H4	*Cercomonas*	*plasmodialis*	Cercomonadidae	AF411268.1	99.67	Con. An.
20	B4.2 H5	*Euglypha*	*rotunda*	Imbricatea	AJ418784.1	100	Con. An.
21	B4.2 H7	*Heteromita*	sp.	Sarcomonadea	HM536169.1	100	Con. An.

*Cultures used in the validation of network associations.

Table 7. Algae and ochrophyte cultures established in this study.

	Code	Genus	Species	Class	Matched accession	Percent identity	Region
1	3EA8	*Pinnularia*	sp.	Bacillariophyceae	KM350088.1	99.31	Arctic
2	7CA11	*Sellaphora*	*seminulum*	Bacillariophyceae	CP024866.1	78.99	Arctic
3	7CA4	*Pinnularia*	*borealis*	Bacillariophyceae	MN940518.1	99.28	Arctic
4	7CA9	*Nitzschia*	*perminuta*	Bacillariophyceae	MN696726.1	99.64	Arctic
5	1EA1	*Gloeocystis*	sp.	Chlorophyceae	GU117588.1	98.17	Arctic
6	1EA10	Radiococcaceae	sp.	Chlorophyceae	JX169836.1	96.72	Arctic
7	1EA11	*Chlamydomonas*	*moewusii*	Chlorophyceae	FR865525.1	98.93	Arctic
8	1EA6	*Bracteacoccus*	*bullatus*	Chlorophyceae	MG582205.1	98.83	Arctic
9	3EA3	*Dictyococcus*	*varians*	Chlorophyceae	KF673359.21/ HQ292768.1	98.55	Arctic
10	3EA5	*Bracteacoccus*	*bullatus*	Chlorophyceae	MG582205.1	95.29	Arctic
11	3EA6	*Dictyococcus/ Pseudomuriella*	sp.	Chlorophyceae	KF673359.1/ MW075327.1	98.04	Arctic
12	6DA1	Haematococcaceae		Chlorophyceae	EF023280.1	98.56	Arctic
13	7CA21	*Chlamydomonas/ Chloromonas*	sp.	Chlorophyceae	LC639358.1/ MT735204.1	98.34	Arctic
14	9BA1	*Chlamydomonas/ Chloromonas*	sp.	Chlorophyceae	MG022664.1/ MK912145.1	100.0/ 100.0	Arctic
15	7CA15	*Vischeria*	*vischeri/ punctata*	Eustigmatophyceae	KM020046.1/ EU878374.1	99.26/ 99.26	Arctic
16	1EA2	*Klebsormidium*	*elegans*	Klebsormidiophyceae	MK262904.1	98.95	Arctic
17	7CA3	*Klebsormidium*	*elegans*	Klebsormidiophyceae	MK262904.1	95.02	Arctic
18	7CA8	*Tetrasporopsis*	*moei*	Phaeosacciophyceae	MT582122.1	98.34	Arctic
19	1EA12	*Deuterostichococcus*	*epilithicus*	Trebouxiophyceae	MT078166.1	99.08	Arctic
20	1EA13	Chlorellales	sp.	Trebouxiophyceae	KX094778.1	98.59	Arctic
21	1EA14	*Coccomyxa*	*subellipsoidea*	Trebouxiophyceae	HG972973.1	100.00	Arctic
22	1EA16	Chlorellales	sp.	Trebouxiophyceae	KX094778.1	100.00	Arctic
23	1EA8	Chlorellales	sp.	Trebouxiophyceae	KX094778.1	98.58	Arctic
24	7CA12	*Lobosphaera/ Parietochloris*	sp.	Trebouxiophyceae	KT072976.1	94.47	Arctic
25	7CA16	*Parietochloris*	*bilobata/ pseudoalveolaris*	Trebouxiophyceae	FJ858973.1/ FJ858971.1	98.97/ 98.97	Arctic
26	7CA6	*Coccomyxa*	*subellipsoidea*	Trebouxiophyceae	AC277064.1	98.68	Arctic
27	7CA7	*Chlorella*	*lewinii*	Trebouxiophyceae	FM205861.1	95.31	Arctic
28	1EA15	*Pleurochloris*	*meiringensis*	Xanthophyceae	AJ579340.1	97.55	Arctic
29	1EA17	*Heterococcus/ Mischococcus*	sp.	Xanthophyceae	AM490820.1/ AF083400.1	93.87/ 93.87	Arctic
30	1EA18	*Excentrochloris/ Botrydiopsis*	sp.	Xanthophyceae	HE573277.1/ AJ579339.1	98.96/ 98.96	Arctic
31	1EA7	*Botrydiopsis*	*constricta*	Xanthophyceae	AJ579339.1	98.96	Arctic
32	3EA2	*Heterococcus*	*caespitosus/ protonematoides*	Xanthophyceae	AM490820.1/ AJ579334.1	97.39	Arctic
33	3EA7	*Xanthonema*	sp.	Xanthophyceae	AM491615.1	97.49	Arctic
34	7CA1	*Xanthonema*	sp.	Xanthophyceae	AM491615.1	98.24	Arctic
35	7CA2	*Tribonema*	*minus*	Xanthophyceae	MT809603.1	98.22	Arctic
36	7CA5	*Cylindrocystis*	*brebissonii*	Zygnemophyceae	MT901370.1	99.66	Arctic
37	C 2.2 A10	*Coelastrella*	*oocystiformis*	Chlorophyceae	MH176105	100	An. Pen.
38	C 2.2 A11	*Macrochloris*	*radiosa*	Chlorophyceae	KM020104	100	An. Pen.
39	C 2.2 A8	*Chlamydomonas*	*mutabilis*	Chlorophyceae	AB701537	97.25	An. Pen.
40	C 2.2 A12	*Leptosira*	*erumpens*	Trebouxiophyceae	Z68696	99.66	An. Pen.

	Code	Genus	Species	Class	Matched accession	Percent identity	Region
41	C 2.2 A2	*Auxenochlorella*	sp.	Trebouxiophyceae	KP081390	99.36	An. Pen.
42	C 2.2 A4	*Coccomyxa*	*subellipsoidea*	Trebouxiophyceae	HG972973	100	An. Pen.
43	C 2.2 A6	*Stichococcus*	sp.	Trebouxiophyceae	KX094817	98.98	An. Pen.
44	C 2.2 A9	*Myrmecia*	*bisecta*	Trebouxiophyceae	LC366918	100	An. Pen.
45	K 5.2 A5	*Chlorella*	sp.	Trebouxiophyceae	MN960178.1	98.34	An. Pen.
46	B 1.3 A6	Chlamydomonadales	sp.	Chlorophyceae			Con. An.
47	B 2.5 A3	*Macrochloris*	*rubrioleum*	Chlorophyceae	AB983624	100	Con. An.
48	B 2.5 A7	*Bracteacoccus*	*bullatus*	Chlorophyceae	MG582205	100	Con. An.
49	B 4.2 A1	*Bracteacoccus*	*bullatus*	Chlorophyceae	AF513377.1	100	Con. An.
50	B 3.5 A5	*Chlorella*	sp.	Chlorophyceae	MN960178.1	98.34	Con. An.
51	B 2.5 A1	Chlorellales	sp.	Trebouxiophyceae	KX094778	96.94	Con. An.

2.8.2. Phylogenetic analysis

One tree was inferred for the cercozoan heterotrophs cultured. The sequences were aligned with MAFFT using the L-INS-i algorithm (Katoh & Standley, 2013) and manually adjusted with UGENE. The sequenced taxa, their best BLAST results, and the nearest outgroups were added into inferred phylogenetic trees using RAxML (Stamatakis, 2014). Outgroup sequences were obtained from the PR^2 database. The inferred trees were visualized in iTOL (Letunic & Bork, 2021) to enhance interpretability and refined using Inkscape for publication-quality presentation.

2.9. Experimental confirmation of predation

2.9.1. Experimental set-up

Co-culture experiments were performed using cercozoan predator and algal prey combinations selected based on network analysis results and the availability of cultures generated in this study, enabling targeted experimental validation. Initially, 11 network-indicated putative interactions were qualitatively tested to confirm predation. Interactions that passed the preliminary testing were subsequently subjected to experiments aimed at quantifying predator feeding rates. Algal cultures not older than one month, cultivated in SiO_3-enriched Waris-H medium, were incubated in the dark a week prior to use. Algal inocula were standardized in their abundance using a Neubauer chamber for both experimental and control sets. The experiments were set up in triplicate sets in 24-well plates employing Waris-H medium and at 15°C. The nitrogen-free medium and dark incubation conditions were chosen to inhibit algal growth, ensuring that fluorescence changes were primarily attributable to predation. Subsequently, approximately 20 cercozoan cells were manually transferred to each well, thus, reducing the chance to transfer previous prey of cercozoans. Active predator counts were documented over a period between 20 to 30 days. Chlorophyll autofluorescence intensity served as a proxy for cell density and was measured with a microplate reader (Varioskan Flash, Thermo Fisher

Scientific, Waltham, MA, USA). Fluorescence measurements were obtained at 430 nm excitation, 665 nm emission, and a 12 nm bandwidth, using the multipoint setting at 121 reads per well. Fluorescence was recorded at four to six time points, and read averages were calculated. Additionally, fluorescence calibration curves were established for each alga, incorporating increasing algae densities determined with a Neubauer chamber. Algal fluorescence was transformed to algal densities for the final plots.

2.9.2. Data analysis

Analyses of covariance (ANCOVA) were employed on the fluorescence measurements generated with the feeding rate experiments, to assess whether changes in algae densities and predator counts were influenced by time, experimental conditions, or their interaction. The assumptions of homogeneity of regression slopes, homogeneity of variances, and normality of residuals were assessed. P-values underwent multiple-testing correction using the Benjamini & Hochberg method. Visualization was conducted using *scales* v. 1.2.1 (Wickham et al., 2023) in addition to the core *tidyverse* packages.

The growth rates (G) of the cercozoan predators were calculated as described by (Heinbokel, 1978): $G = [\ln(D_{t1}) - \ln(D_{t0})]/t$. D (mean predator concentration) is $(D_{t1}-D_{t0})/[\ln(D_{t1}) - \ln(D_{t0})]$, in which D_{t0} and D_{t1} are the initial and final predator concentrations (in cells per milliliter), respectively. t represents the co-culture experimental time interval. Growth rates calculated from predator-prey co-culture experiments were correlated to different network topological features, such as stress and betweenness centrality, with the aim of associating the experimental quantitative data with the network analysis derived from FlashWeave network processing.

2.10. Data and code accessibility

The analyzed sequencing data was submitted to NCBI GeneBank under the accession numbers SRR30143040, SRR30143041, and SRR30143042. Additionally, the environmental data supporting this study are accessible via the PANGAEA repository at https://doi.pangaea.de/10.1594/PANGAEA.972738. All scripts and workflows required to replicate the analyses presented in this study are publicly available on GitHub at https://github.com/CrstnM/EnhancingMicrobialPredator-PreyDetection_MartinezRendon_etal. This repository includes detailed documentation, metadata, and supplementary resources to facilitate reproducibility and transparency in the analytical pipeline.

3. Results

3.1. Performance of designed metabarcoding protocols

The metabarcoding protocols developed in this study were designed to enhance the detection of green algae (Archaeplastida) and ochrophytes (Heterokontophyta), putative prey groups for predator cercozoans in microbial biocrust ecosystems. Through *in silico* evaluation, the selected primer sets demonstrated high specificity and coverage, effectively amplifying target taxa while minimizing the recovery of non-target organisms.

3.1.1. Protocols' *in silico* evaluation

Green algae—*In silico*, the protocol demonstrated high specificity in detecting terrestrial green algae, as 60.1% of all green algae accessions of the non-redundant SILVA database were covered with minimal amplification of non-target taxa. The coverage was particularly high within the phylum Chlorophyta and the class Zygnematophyceae. Notably, only 1.1% of embryophyte sequences were amplified, confirming the protocol's specificity and its suitability for assessing microalgae in biocrusts without contamination from land plants. Additionally, it matched very low percentages of non-targeted major protist taxa, excluding most alveolates (<0.1%), stramenopiles (<0.1%), and amoebozoans (5.3%), highlighting its selectivity for green algae over other eukaryotic groups.

The individual primer coverage was also high, with the reverse primers Chlphy_RV1 and GreenAl_RV1 achieving 95.0% and 70.6% coverage, respectively, when paired with the forward primer EukF1 (Fig. 8). Compared to the broad-spectrum primers of Stoeck et al. (2010), which target a wide range of microbial eukaryotes, this protocol matched nearly sixfold fewer accessions on the SILVA database, further underscoring its specialization for green algae detection. Nevertheless, despite its high specificity, the protocol did not target *in silico Klebsormidiophyceae*, one important terrestrial lineage. Temperature optimization experiments identified optimal annealing temperatures of 58°C for the first semi-nested reaction and 56°C for the second. These settings produced bright, well-defined amplification bands with no mispriming events (Fig. S1).

Ochrophytes—Although originally designed for diatoms, the protocol successfully amplified a broader range of ochrophytes. *In silico*, the protocol matched 35.2% of all ochrophyte accessions in the SILVA database, including 53% of diatom accessions, which accounted for 98.8% of the amplified ochrophytes. This represents a 4.7% increase in coverage compared to the reference protocol (Visco et al., 2015). Moreover, the protocol showed particularly strong performance for key terrestrial taxa

within the Bacillariophyceae and Mediophyceae classes (Fig. 1), surpassing the reference protocol for these groups.

Despite its broad coverage, the protocol maintained specificity, recovering only 21 non-diatom ochrophyte genera, about half of which were classified as Chrysophyceae. These organisms are closely related to diatoms and are likely relevant to the studied ecosystem. Importantly, the protocol demonstrated negligible amplification of non-target taxa, recovering only seven accessions outside Ochrophyta.

The primers achieved high coverage for terrestrial ochrophytes, according to the reference alignment, with the reverse primers Diat_Rv2 and Diat_Rv1 reaching coverage rates of 79.6% and 63.3%, respectively, when paired with the forward primer EukF1 (Fig. 9). The two designed reverse primers share similarities with the reference protocol but differ at both 5' and 3' ends. Despite the protocol's specificity, for the class Coscinodiscophyceae, one of the primer pairs was slightly outcompeted by the reference protocol. Temperature optimization experiments identified optimal annealing at 64°C for both semi-nested reactions, yielding consistently well-defined PCR products of the expected sizes (290–358 bp) without evidence of mispriming (Fig. S2).

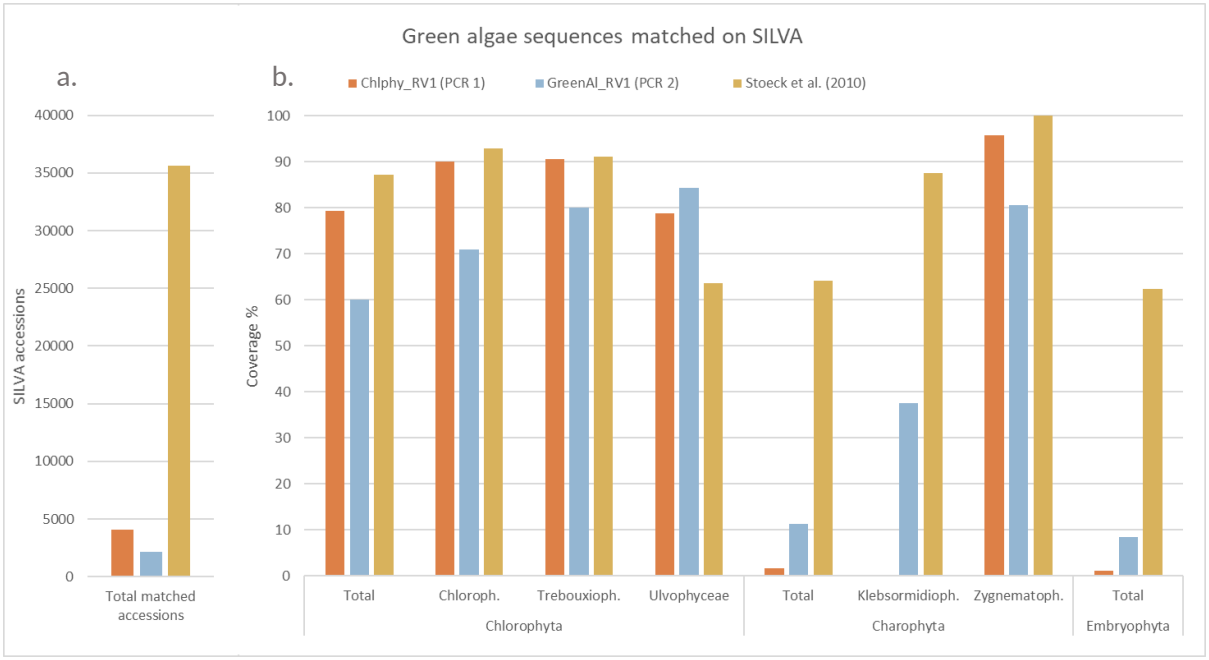

Figure 8. *In silico* comparison of amplification efficiency of green algae primers. PCR1 and PCR2 tests were conducted using the forward primer EukF1. (*a*) Total matched accessions of every tested PCR. The non-redundant SILVA database had 1,908 Chlorophyta and 4,738 Charophyta sequences at the time of the study. The compared methodology (Stoeck et al., 2010) comprises general eukaryotic primers, which expectedly matched a large number of eukaryotic accessions. (*b*) Major terrestrial microalgae taxa are shown within each phylum. Total matched accessions belonging to Embryophyta are also shown. Since the developed protocol was intended for microalgae analysis, the aim was to develop specific primers to avoid the amplification of embryophytes. Results are based on a perfect match (0 mismatches) on the SILVA database.

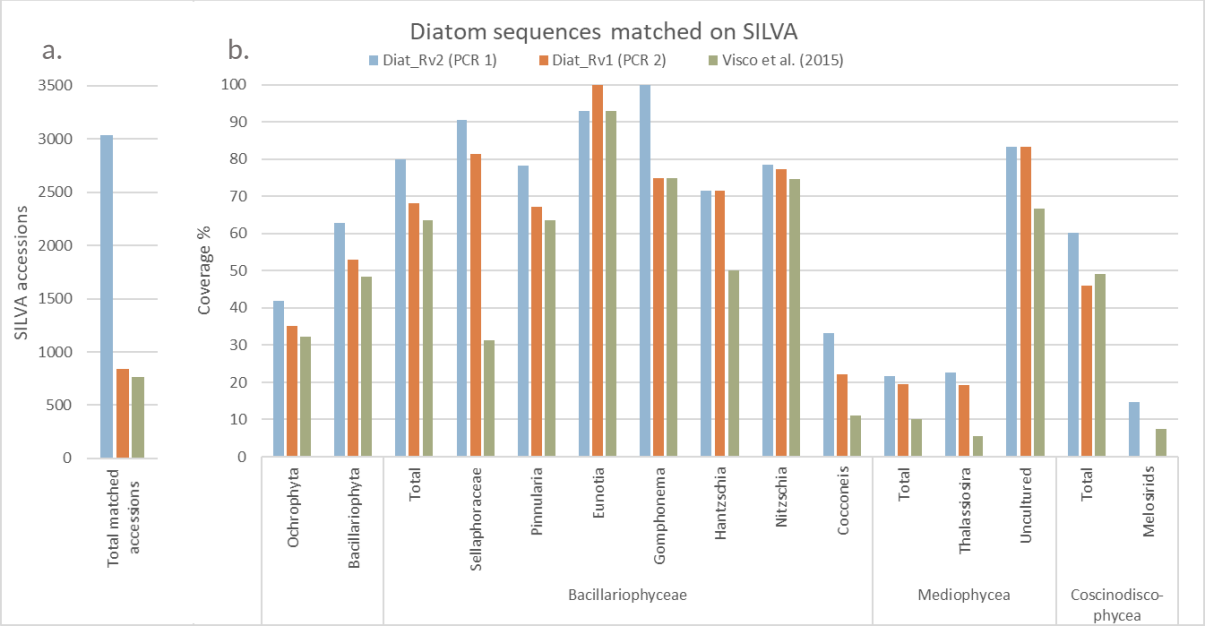

Figure 9. *In silico* comparison of amplification efficiency of primers for ochrophytes. PCR1 and PCR2 tests were conducted using the forward primer EukF1. (*a*) Total matched accessions of every tested PCRAt the time of the study, the non-redundant SILVA database contained 1,571 sequences classified within the Bacillariophyta. (*b*) Total matches for Ochrophyta are shown alongside the total matches for Bacillariophyta and major terrestrial taxa within three representative classes of this phylum. Results are based on a perfect match criterion (0 mismatches) using the SILVA database.

3.1.2. Protocols' preliminary *in situ* validation

The initial *in situ* application of the protocols yielded promising results, validating their effectiveness for detecting green algae and ochrophytes in environmental samples.

For green algae, 35 sequenced clones demonstrated the protocol's good performance in detecting terrestrial taxa. The majority of sequences (86%) were identified as *Spirogyra* sp., a taxon typically associated with freshwater environments but occasionally reported in soil. Additional sequences included two trebouxiophyceans, *Oocystis solitaria* and *Hindakia tetrachotoma*, as well as one chlorophycean sequence from an uncultured *Chlamydomonadales* species (Fig. 10). Importantly, no non-target taxa were amplified during the validation, highlighting the protocol's reliability for downstream ecological studies of polar biocrusts.

For ochrophytes, 38 clones were sequenced, with 47% assigned to Bacillariophyta and 41% to other Ochrophyta, primarily Chrysophyceae and Synurophyceae (Fig. 11a). Notably, nine diatom species spanning seven genera were identified (Fig. 11b), with *Nitzschia acidoclinata* and *Navicula cryptocephala* being the most frequently amplified taxa. The amplification of non-target taxa was minimal, with only a few matches to Chlorophyceae, Embryophyta, and fungi.

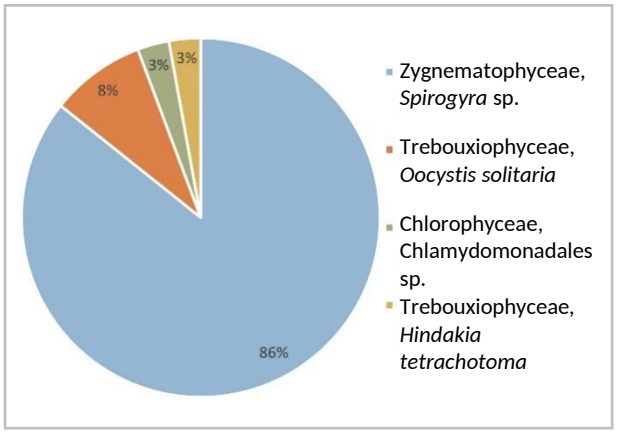

Figure 10. The relative contribution of each sequenced clone in green algae *in situ* evaluation. The taxonomical assignment is based on the best hit by BLAST on the PR[2] database.

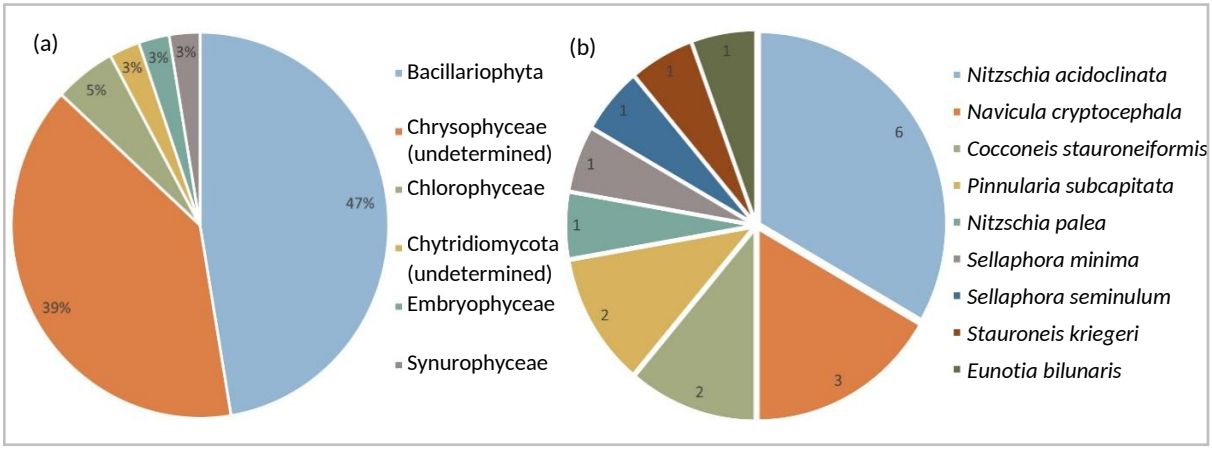

Figure 11. The relative contribution of each sequenced clone of *in situ* evaluation of ochrophytes. The taxonomical assignment is based on the best hit by BLAST on the PR[2] database. (*a*) Diatom sequencing results at high levels (division, phylum, or class). Undetermined refers to environmental sequences in the reference database that could not be assigned to an identified taxon. (*b*) Relative abundance of diatom species according to the sequencing results.

3.1.3. Application of the protocols to polar analysis[1]

The first aim of this study was to produce multiple, independent metabarcoding datasets of a predator group (Cercozoa) and their respective putative prey (here green algae and Ochrophyta). Applying the metabarcoding methodology established by Fiore-Donno et al. (2018), 10.0 million paired reads for Cercozoa were generated. Furthermore, using the newly developed metabarcoding protocols for green algae and ochrophytes, 12.4 million and 10.7 million paired reads were produced, respectively. The specificity of the respective sequencing approaches for Cercozoa and green algae was high with 96.1% and 80.6% of the sequences representing respective target taxa. For ochrophytes, only 28.7% stemmed from the targeted taxa, comprising Bacillariophyta (diatoms) and Chrysophyceae in almost

[1] The current section includes content from "Enhancing Microbial Predator-Prey Detection with Network and Trait-Based Analyses," authored by Martínez Rendón et al., published in *Microbiome*.

equal proportions. Of the remaining OTUs in the ochrophyte dataset, 39% represented green algae, 18.5% streptophytes, and 13.6% fungi, and all non-targeted taxa were removed. Despite considerable non-target amplification in the ochrophyte dataset, saturation was reached in all datasets, for all sites and replicates (Figs. S3-S5), rendering all datasets suitable for further analyses. In total, 604 cercozoan, 191 green algal, and 80 ochrophyte unique OTUs were generated across 116 samples. On average, each sample contained 76 cercozoan OTUs (range: 13-164, ±3.1), 40 green algal OTUs (15-81, ±1.4), and 11 ochrophyte OTUs (2-33, ±0.6; detailed OTU counts and taxonomic affiliations are available online as detailed in section 2.10).

3.2. Biodiversity of biocrust protists

To illustrate whether the newly developed protocol produced distinguishable and representative results, alpha diversity analyses were conducted for each dataset, along with interregional comparisons of community composition and local diversity.

Cercozoa—Sarcomonadea dominated the relative abundance of cercozoans, with 70% of the total 604 OTU count (39 genera). Imbricatea and Thecofilosea followed with 11% (26 genera), and 9% (17 genera), respectively (Fig. 12a; Supplementary Fig. S6 displays genera names). Numerous OTUs in all datasets were identified only at broader taxonomic levels, a common limitation that often stems from incomplete reference databases. Among 352 Cercozoa OTUs that could not be identified up to genus level, 65% were equally assigned to the families Allapsidae and Sandonidae (Glissomonadida). Moreover, 24% of OTUs, most of which were representing Sarcomonadea, were present across all three regions (Fig. 12b). Alpha diversity metrics indicated that Svalbard exhibited the highest cercozoan diversity across the three metrics, namely OTU richness (F=10.368, p=7.34e-5), exponential Shannon (F=8.809, p=0.000278), and inverse Simpson (F=4.955, p=0.009; Fig. 12c; Table S2). Thus, these results demonstrate that Svalbard harbors not only the highest species richness but also a more evenly distributed community compared to the Antarctic regions.

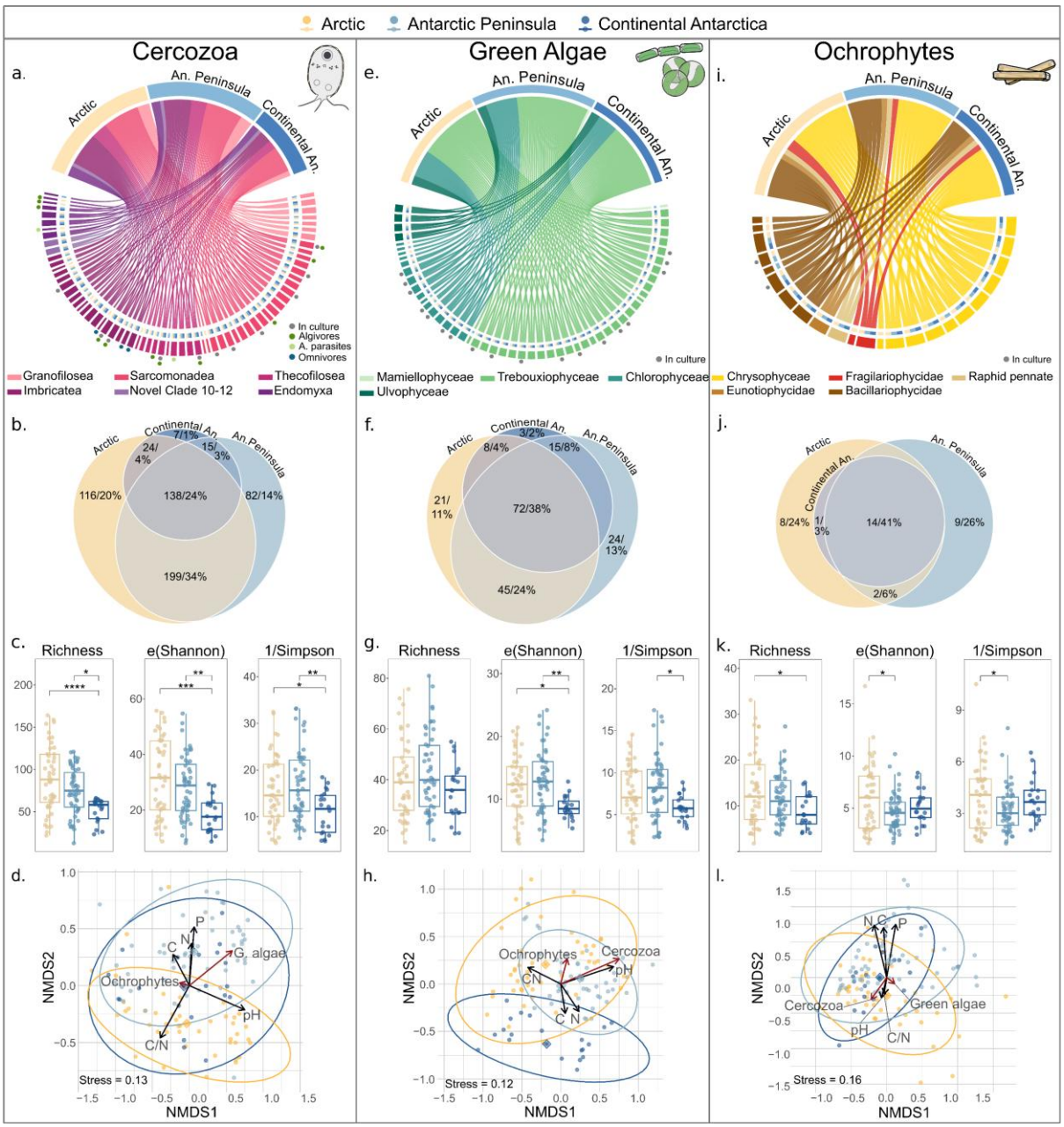

Figure 12. Diversity measures of Cercozoa, green algae, and ochrophytes across three Polar regions. Chord plots (*a*, *e*, and *i*) depict genus richness identified for all regions within the targeted taxa. The chords connect the regions (yellow and blue shades) with the corresponding genera, while different chord colors represent distinct classes. Circles next to the taxon names indicate cultivated taxa (gray), specifically highlighting algivores (dark green), and algae parasites (light green) in Cercozoa. Chord plots in the Supplementary Figs. S6-S8 display genera names. Venn diagrams (*b*, *f*, and *j*) represent unique and shared OTUs within and between sampling regions. Globe sizes are approximately proportional to their abundance. Box plots (*c*, *g*, and *k*) display three α-diversity indices: (1) OTU richness, (2) e(Shannon) for Exponential Shannon, and (3) Inverse Simpson. Significance codes indicate differences between means calculated by ANOVA and subsequent Tukey-HSD test and are denoted as follows: *= $p < 0.05$, **= $p < 0.01$, ***= $p < 0.001$, and ****= $p < 0.0001$. Non-metric multidimensional scaling ordinations (NMDS, *d*, *h*, and *l*) based on Bray-Curtis dissimilarities for the three taxa. The structures (PCoA1) of each of the three communities, used as predictors for the other two, are indicated by red arrows. For instance, the structures of green algae and ochrophytes were used to predict the structure of Cercozoa, and similar predictive analyses were conducted for green algae and ochrophytes. Diamonds indicate region centroids and follow the same color coding as the legend. The confidence ellipses were drawn at the 0.95 level, indicating the regions within which 95% of the data points are expected to lie. The influence

of abiotic variables (pH, C, N, P, and C/N ratio) with the highest correlation to the ordination axes are indicated by black arrows. Scaling was performed using k=3 dimensions; only the two first dimensions are visualized.

Green algae—Trebouxiophyceae dominated the relative abundance of green algae, representing 71% of the total 191 OTUs across 28 genera. Chlorophyceae contributed 24% of OTUs, whereas Ulvophyceae and Mamiellophyceae accounted for seven and one OTU, respectively (Fig. 12e, Supplementary Fig. S7). While 37% of OTUs appeared in all three regions, most Trebouxiophyceae and Ulvophyceae genera occurred widespread. Most of the unique genera (eight) were observed in both Antarctic regions, including the only sequenced Monomastigaceae, while two green algal genera appeared exclusively in Svalbard. Moreover, 17% of OTUs were identified until class or order levels. The OTU richness did not vary among regions (F=1.853, p=0.162). Contrastingly, both, the inverse Simpson (F=3.88, p=0.023; Fig. 12g; Table S2) and exponential Shannon metrics (F=3.88, p=0.003), supported by subsequent Tukey tests (p=0.017 and p=0.0017, respectively), revealed differences between the two Antarctic regions. Additionally, results for exponential Shannon highlighted a higher diversity in Svalbard than in Continental Antarctica (Tukey test, p=0.0191). Thus, these findings reveal a consistent OTU richness across regions but indicate a more uneven community distribution in Continental Antarctica compared to Svalbard and the Antarctic Peninsula.

Ochrophytes—The ochrophyte sequencing yielded 80 OTUs, with the class Bacillariophyceae dominating the diatom relative abundance. The latter encompassed 34 OTUs across 12 genera (Fig. 12i, Supplementary Fig. S8). Forty-one percent of all diatom OTUs within seven genera were common in all regions, whereas 26% and 23% of OTUs were unique to the Antarctic Peninsula and Svalbard, respectively (Fig. 12j). Nevertheless, most genera occurred widespread, with only three being unique to Svalbard and one to the Antarctic Peninsula. Nine OTUs were classified under the taxonomically uncertain operational categoric name 'Raphid Pennates,' corresponding to Bacillariophyceae. Of the latter, five were found in all regions, while four were unique to the Antarctic Peninsula. Among the 41 chrysophyte OTUs, half were assigned to five genera, dominated by *Spumella* (50%) and *Ochromonas* (25%). The remaining 21 taxa were only assigned to clades. While most chrysophyte clades and genera appeared across the three regions, *Paraphysomonas* was only found in Svalbard. Svalbard's Ochrophyta OTU richness was higher than in Continental Antarctica (Tukey test, p=0.011). Additionally, both exponential Shannon and inverse Simpson demonstrated differences between Svalbard and the Antarctic Peninsula (Tukey tests, p=0.0191 and p=0.037, respectively; ANOVA results in Table S2). Taken together, these findings demonstrate higher species richness and evenness in Svalbard for the studied ochrophytes.

3.3. Correlation of biotic and abiotic factors on biocrust microbial communities

To evaluate the role of the hypothesized predator-prey interactions in shaping these microbial communities, beta diversity analyses were performed with emphasis on biological factors as determinants (Fig. 12d, 12h, 12l). The analyses revealed a substantial biotic impact of Cercozoa on green algal community composition, explaining solely 5.4% of the green algal community composition (R^2 = 0.0537, $p < 0.001$; refer to Table S3 for PERMANOVA results). Conversely, the green algal community composition explained some variation in Cercozoa, albeit to a lower extent (3.5%; R^2 = 0.0348, $p < 0.001$). The ochrophyte community also influenced Cercozoa and green algae to a limited degree, explaining 2.1% and 3.0% of their variation, respectively (R^2 = 0.0206, $p < 0.001$; R^2 = 0.0307, $p < 0.001$). Finally, the structuring effects of Cercozoa and green algae on ochrophytes were marginal, explaining only 2.2% and 1.7% of the variation (R^2 = 0.0224, $p < 0.001$; R^2 = 0.0169, $p < 0.001$).

In addition to these biotic interactions, and to compare the extent to which biological variables affect the community composition of the investigated taxa with the impact of abiotic factors, additional analyses quantified to which extent the respective community compositions are affected by abiotic variables. Among the abiotic factors, region had the strongest impact on Cercozoa (R^2 = 0.1208, $p < 0.001$) and green algal communities (R^2=0.1429, $p < 0.001$), explaining 12.1% and 14.3% of the variation, respectively. While region also influenced the ochrophyte community, its effect was comparatively weaker, explaining 5.7% of the variation (R^2 = 0.0571, $p < 0.001$). Furthermore, pH emerged as a significant driver of community composition across all taxa, accounting for 10.6%, 8.2%, and 4.7% of the variation in Cercozoa, green algae, and ochrophytes, respectively. In contrast, other abiotic factors, such as TOC (%), TN (%), TP (g/kg), and the CN ratio contributed to a lower extent, accounting for marginal contributions (< 3.7%) in the three ordinations.

3.4. Hypothesizing predator-prey interactions with cross-kingdom association networks

To explore specific putative interactions between Cercozoa and their prey, co-occurrence network analyses were employed as a means of estimating a microbial food web structure. These analyses aimed to provide a mechanistic link between community composition and potential predator-prey relationships.

3.4.1. FlashWeave network analysis

Using FlashWeave, 407 putative interactions (edges, Fig. 13) were identified among 306 taxa in Svalbard, 422 among 303 taxa in the Antarctic Peninsula, and 140 among 135 taxa in Continental Antarctica. On the class level, these corresponded to 30, 28, and 23 nodes, respectively. The total

class-level aggregated putative interactions were 157, 153, and 71 for Svalbard, the Antarctic Peninsula, and Continental Antarctica, respectively, reflecting the lower richness of Cercozoa and ochrophytes in Continental Antarctica.

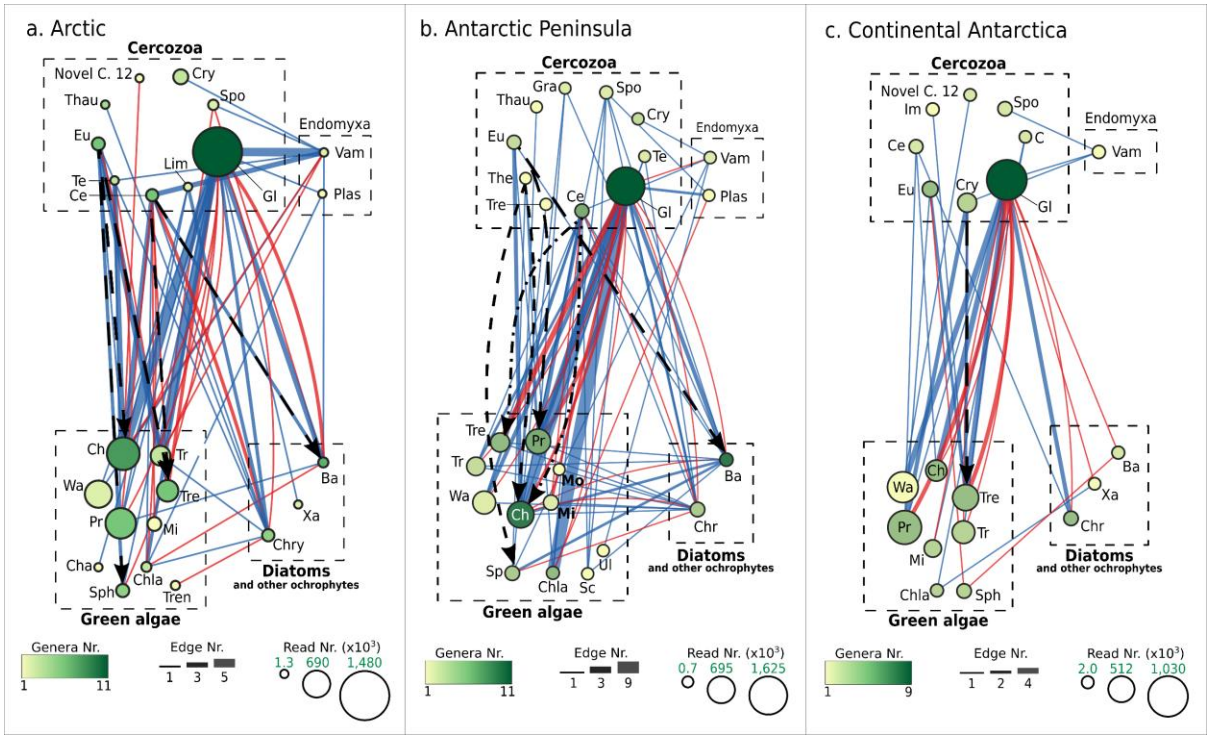

Figure 13. Cross kingdom co-occurrence networks of Cercozoa, green algae, and ochrophytes across three Polar regions, as an indicator for putative food web interactions**.** Significant positive and negative putative interactions detected between taxa are depicted for the three studied regions. Nodes represent genera grouped at order level; node size is proportional to the total number of reads for each order, and node color indicates the number of genera aggregated. Edges represent putative interactions between taxa (blue lines–positive putative interactions; red lines–negative putative interactions). Edge thickness represents the number of individual aggregated edges. Black dashed arrows indicate experimentally tested putative predator-prey relationships. Abbreviations: Novel C. 12, Novel Clade 12; Gra, Granofilosea X; Thau, Thaumatomonadida; Eu, Euglyphida; The, Thecofilosea X; Tre, Tremulida; Te, Tectofilosida; Ce, Cercomonadida; Lim, Limnifida; Gl, Glissomonadida; Spo, Spongomonadida; Cry, Cryomonadida; C, Cercozoa X; Vam, Vampyrellida; Plas, Plasmodiophorida; Ch, Chlorellales; Wa, Watanabeales; Tre, Trentepohliales; Tr, Trebouxiophyceae X; Pr, Prasiolales; Cha, Chaetophorales; Sph, Sphaeropleales; Chla, Chlamydomonadales; Mi, Microthamniales; Tre, Trebouxiales; Sc, Scotinosphaerales; Ul, Ulotrichales; Mo, Monomastigales; Ba, Bacillariophyceae; Xa, Xantophyceae; Chry, Chrysophyceae.

Network topological features were calculated at both the OTU and order levels (Table S4). Here, results at the order level are highlighted, as taxonomic orders resemble approximately functional groups with few exceptions. For example, the class Glissomonadida predominantly includes bacterivores, with exceptions like the algivorous family Viridiraptoridae. The connectivity of the networks, as indicated by the average edge degree, was lower in Continental Antarctica (~six interactions) compared to Svalbard and the Antarctic Peninsula (~10–11 interactions). Additionally,

the Antarctic Peninsula exhibited the highest average clustering coefficient and network density, and the shorter average path lengths, whereas Continental Antarctica displayed the opposite trend. Taken together, these results demonstrate that the Antarctic Peninsula harbors a more tightly connected, denser, and potentially more stable network compared to the other regions.

Intra-domain putative interactions dominated across the three regions, comprising 310 (78.1%), 290 (68.7%), and 89 (63.6%) in Svalbard, the Antarctic Peninsula, and Continental Antarctica, respectively. Inter-domain interactions predominantly involved cercozoan taxa in all regions. Specifically, Cercozoa exhibited 72 (17.7%) putative interactions at the OTU level with algae in Svalbard. However, only 26, i.e. 6.4% of the respective interactions, included algivorous Cercozoa and thus represented putative predator-prey interactions. In the Antarctic Peninsula, 20 interactions (4.7% of 422) corresponded to putative predator-prey interactions, while in Continental Antarctica, there were 13 interactions (9.3% of 140) of such. Notably, the Glissomonadida occupied at least half of the total putative interactions in each region, despite the vast majority of Glissomonadida species do not prey on algae. Interestingly, few putative interactions were found between green algae and ochrophytes across all three regions, particularly in Continental Antarctica. Taken together, these findings suggest that Cercozoa plays a crucial role in structuring microalgal communities. However, predation may not be the sole interaction explaining the found correlations.

3.4.2. HMSC network analysis

To validate the results obtained with FlashWeave and further investigate potential predator-prey interactions, an HMSC hurdle modeling approach was applied, allowing to disentangle environmental and biotic drivers while constructing co-occurrence and co-abundance species-to-species association matrices (Fig. 14). Overall, the full models exhibited a more structured distribution of correlations compared to the null models, indicating that incorporating environmental and trait-based data refined the detection of meaningful associations.

Notably, the presence-absence models identified substantially more associations than those based on abundance data, with higher explanatory and predictive power (Supplementary Table S6). Additionally, the proportion of interactions between algivorous cercozoans and their potential prey (Fig. 14*a-d*) was higher than that of bacterivores with green algae and ochrophytes (Fig. 14*e-h*). Furthermore, HMSC networks identified a similar proportion of predator-prey interactions as FlashWeave, with 7.5% and 4.8% of associations attributed to co-occurrence and co-abundance, respectively (Supplementary Table S5). However, the co-abundance networks yielded significantly fewer overall associations, reinforcing the idea that presence-absence data provide a more comprehensive view of microbial interactions in these systems.

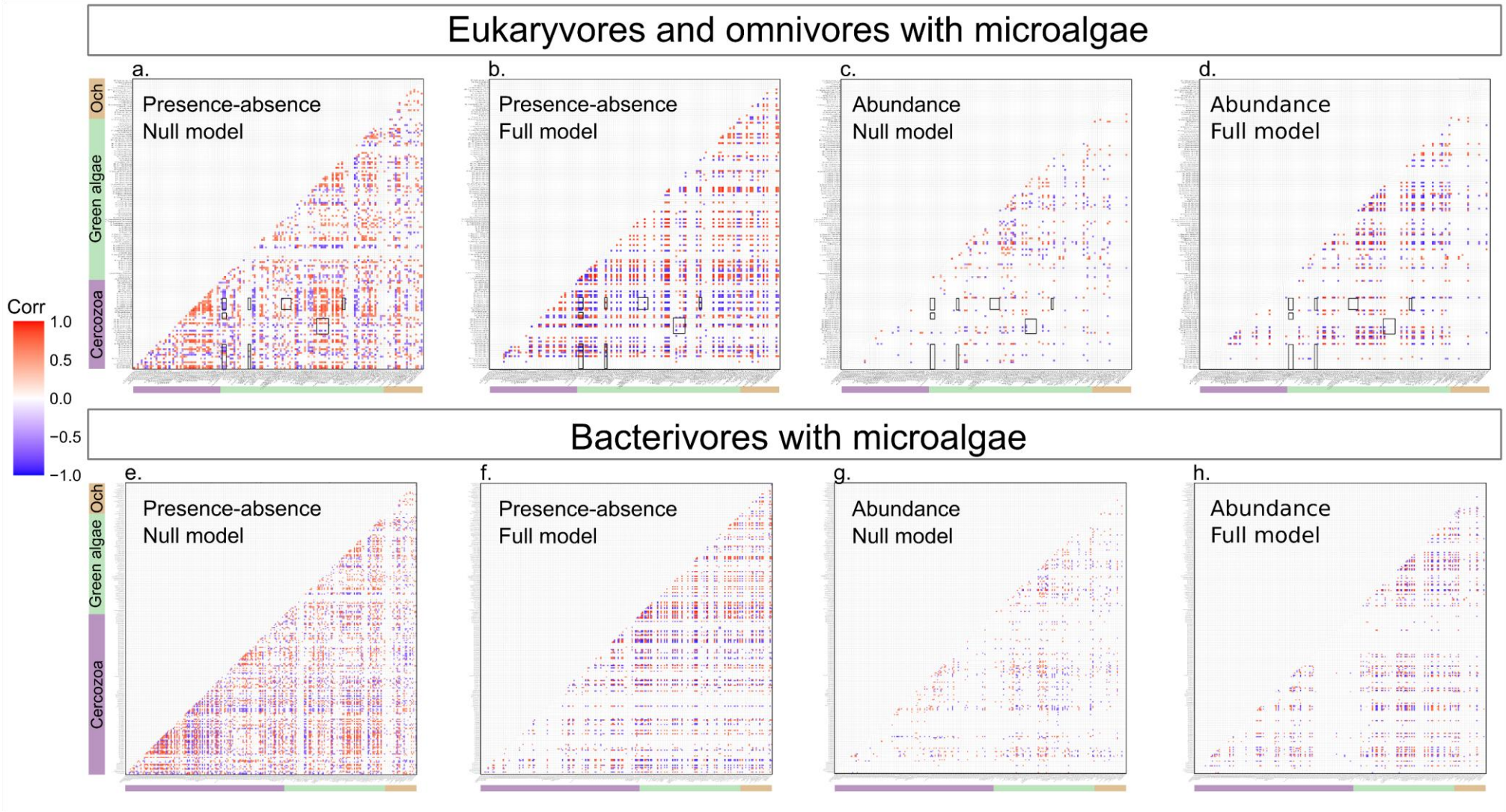

(See legend on the next page)

(See figure on the previous page)

Figure 14. HMSC species-to-species co-occurrence and correlation networks for Cercozoan algivores and bacterivores with microalgae, inferred using presence-absence and abundance models. Panels (*a*–*d*) depict associations between cercozoan eukaryvores and omnivores with green algae and ochrophytes, while panels (*e*–*h*) show associations between cercozoan bacterivores and microalgae. The presence-absence models (*a*, *b*, *e*, *f*) were inferred using a probit model, whereas the abundance models (*c*, *d*, *g*, *h*) were based on a normal model. Each model includes both a null version (*a*, *c*, *e*, *g*) to represent random patterns and a full version (*b*, *d*, *f*, *h*) that incorporates environmental covariates. The correlations marked with black squares represent interactions validated through laboratory testing.

3.5. Identity of isolated biocrust protists

Potentially algivorous taxa and their respective prey were isolated and barcoded (Tables 6 and 7). Sequencing results indicated that algivorous *Cercomonas*, *Rhogostoma*, *Fisculla*, *Assulina*, and *Euglypha* were common across all study regions. Additional taxa, such as *Rhizaspis*, *Viridiraptor*, and were present in Svalbard and the Antarctic Peninsula but absent in Continental Antarctica. Among algivorous Endomyxa, *Vampyrella* and *Thalassomyxa* were exclusively detected in Svalbard, while *Leptophrys* was identified in the two Antarctic regions. Cultures of algivorous *Cercomonas*, *Rhogostoma*, *Fisculla*, and *Euglypha* were successfully established, barcoded, and later subjected to experiments.

The isolation and culturing of prey for subsequent testing resulted in 38 cultures of barcoded green algae (Table 7). The isolated algae predominantly belonged to the classes Chlorophyceae (18 isolates) and Trebouxiophyceae (17 isolates). Additionally, two isolates of Klebsormidiophyceae (*Klebsormidium elegans*) and one isolate of Zygnemophyceae (*Cylindrocystis brebissonii*) were recovered. No representatives from Mamiellophyceae or Ulvophyceae were observed or successfully cultured. Most cultures were identified to the genus or species level, while eight were classified only to higher taxonomic ranks, including the orders or families Chlamydomonadales, Chlorellales, Chlorellaceae, Radiococcaceae, and Haematococcaceae.

Fourteen ochrophyte cultures were established from Arctic isolates. These included four diatoms: two *Pinnularia* spp. isolates from distinct sites, one *Nitzschia perminuta*, and one *Sellaphora seminulum*, all of which were also detected in the environmental sequencing results. In addition, ten other ochrophyte algae were isolated, comprising eight xanthophytes, one Phaeosacciophyceae (*Tetrasporopsis moei*), and one Eustigmatophyceae (*Vischeria sp.*), from which no sequencing results were obtained.

3.5.1. Phylogenetic placement of isolated Cercozoa

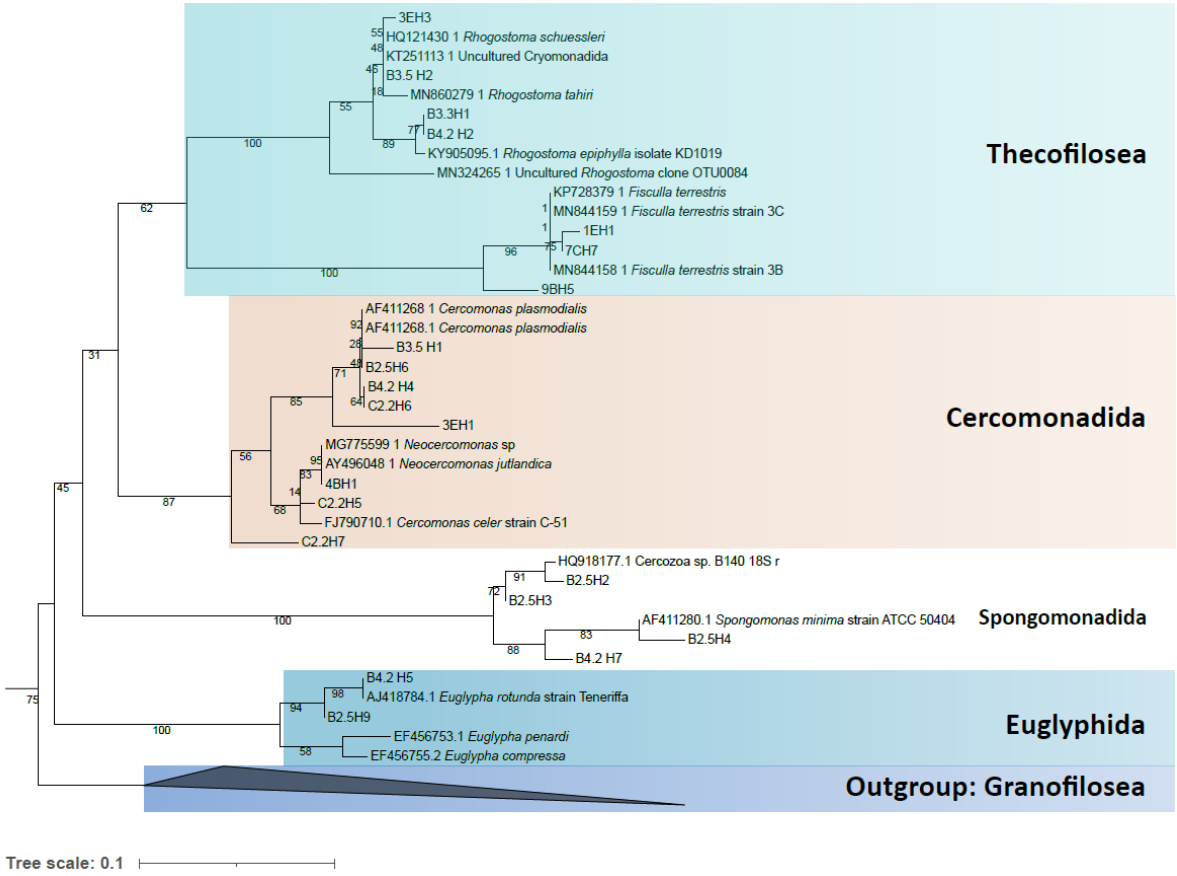

Figure 15. Phylogenetic tree of cercozoan taxa detected in this study, based on the V4 region of the 18S rRNA gene. The tree shows relationships among identified taxa within the classes Thecofilosea, Euglyphida, and Cercomonadida, with the Granofilosea serving as an outgroup. Bootstrap values are indicated by circle size, with larger circles representing higher support values. Taxa identified in this study are highlighted and include species such as Rhogostoma epiphylla, Euglypha rotunda, and Cercomonas celer, aligning with known cercozoan sequences from GenBank. This phylogeny provides a preliminary overview of the cercozoan diversity present in polar biocrusts, although it is not fully conclusive due to the limited resolution of the V4 region of the 18S rRNA gene.

3.6. Experimental validation of predator-prey interactions

To experimentally validate the hypothesized predator-prey relationships and quantify their ecological significance, feeding experiments were conducted with selected heterotrophic Cercozoa and their potential algal prey. These experiments provided direct evidence of prey capture and allowed the measurement of feeding rates under controlled conditions.

3.6.1. Verification and quantification of putative predator-prey interactions

To provide direct evidence for the hypothesized predator-prey interactions identified through network analyses, feeding experiments were conducted using algivorous predators and their putative algal prey. The FlashWeave correlation network guided the selection of interactions for experimental validation and served as a framework for hypothesizing predator-prey relationships. Complementary

insights were obtained from HMSC models, which accounted for environmental covariates, species traits, and hierarchical dependencies, further refining the ecological context of these associations.

The cultures generated in this study enabled the testing of 11 network-indicated putative predator-prey relationships (Fig. 16). Initially, all putative interactions underwent qualitative testing to confirm predation. Notably, two putative predator-prey interactions could not be confirmed, namely, the interactions involving the highly motile alga *Chloromonas* with the cercozoan *Cercomonas* and *Fisculla* were not validated. Subsequently, quantitative feeding rate experiments were conducted for the remaining nine verified predator-prey interactions. ANCOVA analyses of predator count slopes demonstrated considerable growth in eight of the tested putative interactions, except for *Euglypha* feeding on *Stichococcus* (Fig. 16e, Table S14). Microscopic observations confirmed the presence of food vacuoles in all predators, containing algal cells at various stages of digestion (Fig. 17). Algal abundance slopes decreased significantly in five interactions (Table S15), suggesting that predation was detectable but had a limited impact on the overall algal abundance under these experimental conditions.

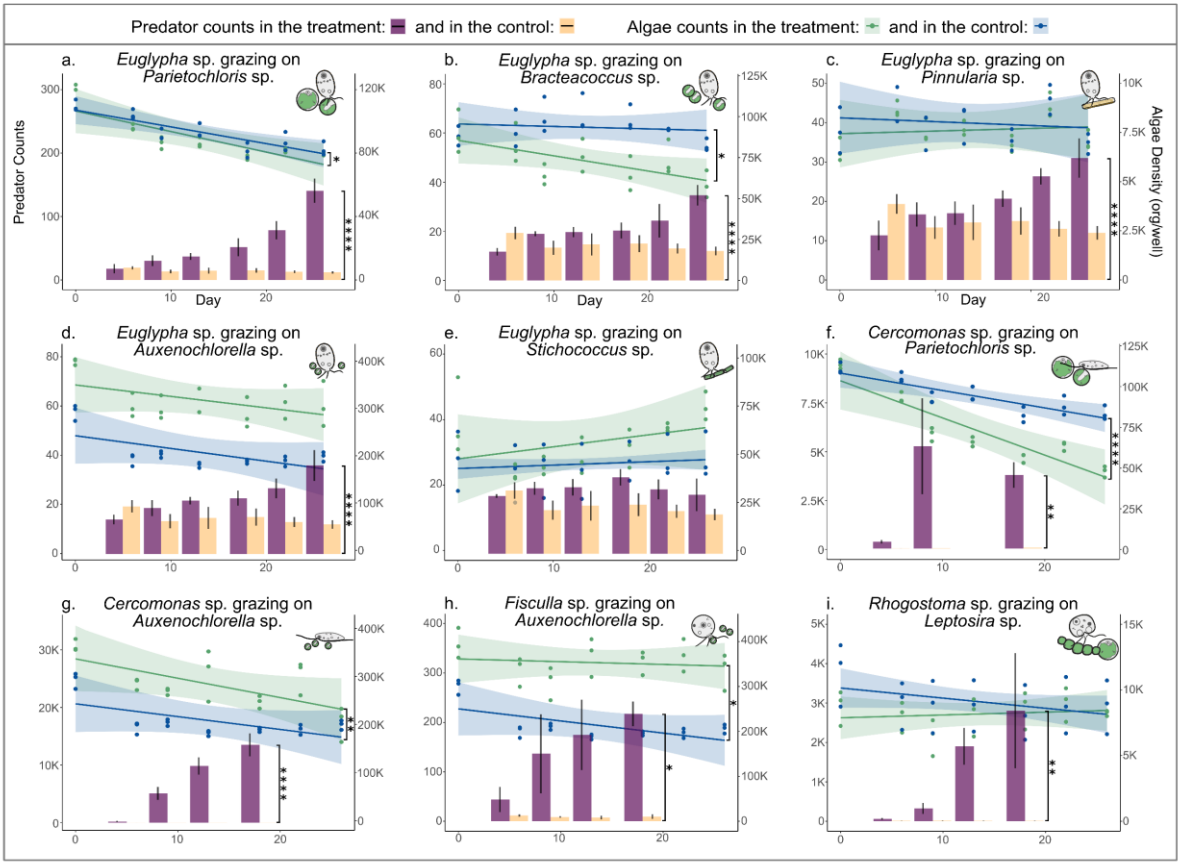

Figure 16. Experimental validation of putative predator-prey interactions. Yellow bars represent predator counts for control conditions, while purple bars depict their counts in co-culture with algal prey (left y-axis). Blue lines represent algae counts in control conditions, while green lines indicate algae counts under predation pressure (right y-axis). Error bars accompanying each bar display standard deviations. Significance codes derived from ANCOVA analyses indicate

differences between the treatment and control slopes for both predator counts (Table S14) and algae fluorescence (Table S15). The codes are denoted as follows: *= p < 0.05, **= p < 0.01, ***= p < 0.001, and ****= p < 0.0001.

Finally, various correlations between network topological features and the calculated predator growth rate of each verified predator-prey interaction were explored, aiming to associate this experimental quantitative data with the network analysis derived from network processing. Two key node topological features, stress and betweenness centrality were found to increase with higher predation growth rates (Fig. 17). Both topological features are centrality measures that highlight the critical roles of certain taxa within a network. Stress centrality quantifies a node's importance based on the number of times it acts as a bridge along the shortest paths of other nodes (Wu et al., 2016), while betweenness centrality indicates a node's influence on the interactions between other nodes in the network (K. K. Lee et al., 2022). Thus, these findings imply a potential relationship between predation growth rate and the importance of predators in the food web, suggesting that more effective predators are likely to be more central and play critical roles in maintaining the network's stability and functionality.

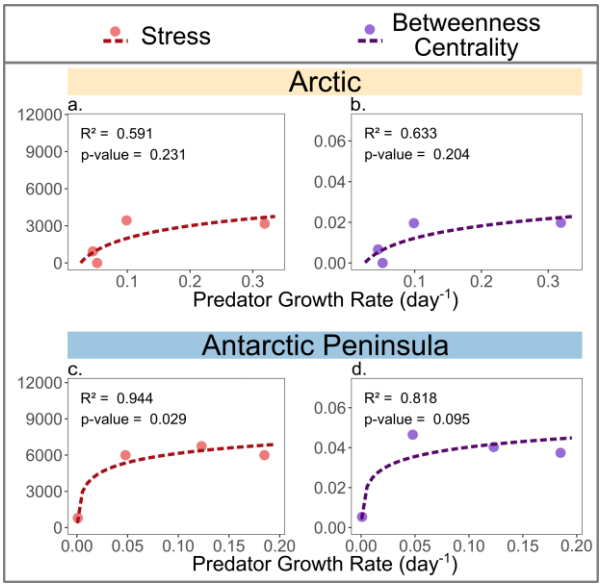

Figure 17. Correlations between two network topological features: predator growth rate between (1) stress (*a* and *c*), and (2) betweenness centrality (*c* and *d*). Each topological feature is represented by its calculated value (y-axes), while predator growth rates were calculated as the exponential increase of predator populations per day (x-axes).

3.6.2. Observations on predatory behavior

This section provides an account of some observed feeding trends of the studied cercozoan predators during co-culture experiments. An inverted microscope Nikon i90 was used at 6000x magnification. The interactions between predators and their algal prey, including the intake and digestion processes, were documented using microscopy (Fig. 18). Below is a summary of some observations:

A. *Rhogostoma epiphylla* and *Auxenochlorella* sp.: Up to four algal cells were observed within the cytoplasm of *Rhogostoma* cells, which primarily swam actively during feeding (Fig. 18A).
B. *Fisculla* sp. *and Auxenochlorella* sp.: Similar to *Rhogostoma*, up to four algal cells were ingested. *Fisculla* was observed both swimming and resting at the bottom of the culture dish during feeding (Fig. 18B).
C. *Cercomonas celer* and a Chlorellales alga: One to three algal cells were visible within the predator's cytoplasm. *Cercomonas* alternated between swimming while digesting and attaching to the bottom of the culture dish (Fig. 18C).
D. *Euglypha rotunda* and *Leptosira* sp.: he alga exhibits a broad phenotypic variability throughout its life cycle (see (Lukešová, 1991) for an overview). *Euglypha* was observed interacting with large algal aggregates, selectively feeding on smaller cells that emerged from protective gelatinous vesicles. The predator appeared to have ruptured the vesicles to gain access to the smaller algae, ingesting up to six cells at a time (Fig. 18D).
E. *Euglypha rotunda* and *Stichococcus* sp.: Predators displayed one to four vacuoles containing algae in various digestion stages (Fig. 18E).
F. *Euglypha rotunda* and *Stichococcus* sp.: Predators displayed one to four vacuoles containing algae in various digestion stages (Fig. 18E).
G. *Euglypha rotunda* and Chlorellales alga: Up to a dozen algal cells were observed within the predator's cytoplasm, suggesting active feeding on dense algal populations (Fig. 18G).
H. Euglypha rotunda and *Bracteacoccus*: Five or more algal cells at different stages of digestion were present in the cytoplasm. Egested food vacuoles containing digested material were also observed being expelled from *Euglypha* cells (Fig. 18H).
I. *Euglypha rotunda* and *Parietochloris* sp.: Up to six algal cells were observed in various digestion stages. Egestion of digested content was also noted (Fig. 18I).
J. *Rhogostoma epiphylla* and *Leptosira* sp.: Algal cells were relatively large compared to the predator. *Rhogostoma* cells typically ingested one algal cell, or two smaller ones, with advanced digestion stages resulting in smaller algal fragments (Fig. 18F).
K. *Euglypha rotunda* and *Pinnularia*: No consistent ingestion of diatoms was observed, likely due to their large size and rigid frustules. *Euglypha* cells appeared to grow slowly, possibly subsisting on dead diatoms. Only one instance of diatom cell ingestion was recorded, but the algal content was not extracted from the frustules.

These observations provide insights into the diverse predatory behaviors of cercozoans. They also highlight prey-specific feeding strategies, such as selective ingestion of smaller algae and difficulties in handling large or physically protected prey.

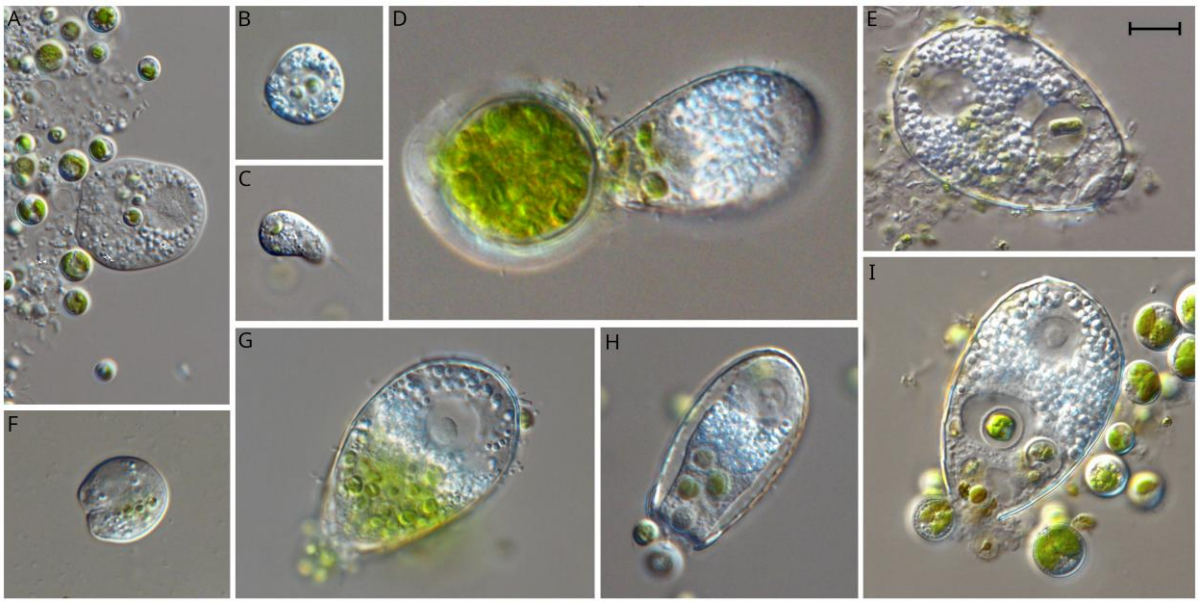

Figure 18. Algivorous cercozoans and their ingested prey. (*A*) *Rhogostoma* sp. with ingested cells of *Auxenochlorella* sp. (*B*) *Fisculla terrestris* with two ingested cells of *Auxenochlorella* sp. (*C*) *Cercomonas celer* with food vacuoles containing Chlorellales cells. *Euglypha rotunda* (*D*, *E*, *G*, *H*, and *I*) with food vacuoles containing (*D*) *Leptosira* sp.; (*E*) *Stichococcus* sp.; (*G*) an undetermined Chlorellalles; (*H*) *Bracteacoccus* sp., and (*I*) *Parietochloris* sp. (*F*) *Rhogostoma* sp. with food vacuoles containing *Leptosira* sp. cells. The scale represents 10 µm.

4. Discussion

The process of inferring biotic microbial interactions—spanning from hypothesizing relationships based on systematic co-occurrence (presence-absence) or co-abundance patterns in environmental sequencing data, to experimentally validating true ecological interactions—should involve the experimental validation of genuine ecological interactions (Faust & Raes, 2012). Using cross-kingdom network inference, that framework was leveraged to investigate predatory relationships between cercozoans and their putative prey, specifically green algae and ochrophytes. The predictions, derived from comprehensive network analyses, were experimentally validated through co-culture experiments, with nine out of 11 tested interactions confirming predatory traits. The results underscore the value of combining *in silico* analyses with experimental approaches to uncover microbial food web dynamics.

The sequencing data obtained via the DNA-based metabarcoding methods developed for algae and diatoms generated robust datasets, which combined with an existing method for cercozoan metabarcoding (Fiore-Donno et al., 2019), ensured comprehensive coverage and served as the foundation for my cross-kingdom network analyses. Importantly, the protocols achieved saturation across all three datasets, eliminating the need for rarefaction and enhancing the reliability of downstream analyses. Together, these methodologies allowed the prediction and validation of interactions with high confidence, bridging computational predictions with experimental evidence. This integrative approach not only reinforces the utility of network inference but also highlights its potential to provide new insights into the ecological interactions shaping polar biocrust communities.

4.1. Evaluation of performance of novel metabarcoding protocols

Green algae—The protocol demonstrated strong performance in capturing the diversity of green algae across the studied regions, showcasing high specificity and minimal non-target amplification. It successfully retrieved a total of 439 OTUs, representing 80.6% of green algal diversity across all sampled regions. A key strength of the protocol lies in its ability to minimize reads assigned to Embryophytes; only 8.7% of the 76 non-target taxa OTUs were identified as Embryophytes. This is a marked improvement compared, for example, to Pushkareva et al. (2022), who reported Embryophyte contamination levels ranging from 18.3% to 23.7% in biocrusts of Svalbard using Stoeck's primers (2010). Furthermore, the protocol retrieved 17 OTUs assigned to Ulvophycea which spanned four genera and one OTU within Zygnemophyceae (*Cylindrocystis)*. One OTU assigned to an unknown

Monomastigaceae (Mamiellophyceae) was found, representing an unconventional reported instance in polar biocrusts, given Monomastigales' typical confinement to freshwater or coastal environments (Tragin et al., 2018).

Despite its robust performance in avoiding non-target taxa, the protocol retrieved only one OTU for Klebsormidiophyceae (*Interfilum* strain SSK), aligning with *in silico* results that predicted limited coverage of this class. This low recovery may stem from primer mismatches with Klebsormidiophyceae genetic regions or reflect patchy distribution in the sampled biocrusts. This is notable given Klebsormidium's frequent presence in biocrusts across all three regions studied (Borchhardt, Baum, et al., 2017; Borchhardt, Schiefelbein, et al., 2017; Pushkareva et al., 2024). Nevertheless, isolation efforts successfully retrieved Klebsormidiophyceae on several occasions, leading to the establishment and sequencing of two unialgal cultures (Table 7). These results underscore the importance of integrating complementary approaches to capture the full spectrum of biocrust diversity. However, refinements in primer design and methodological adjustments are necessary to enhance the detection of taxa like Klebsormidiophyceae, which play an ecologically significant role in biocrust systems.

Ochrophytes—As indicated by the *in silico* results, the protocol amplified a broader range of Ochrophytes when applied to polar biocrust samples. However, only 28.7% of the 536 OTUs determined by the protocol were identified as ochrophytes, while the remainder comprised green algae (39%), embryophytes (16.9%), and fungi (13.6%). A closer look at the retrieved chlorophytes and trebouxiophytes revealed considerable overlap with the taxa identified using the green algae protocol. Notably, four genera within Zygnemophyceae—*Cylindrocystis*, *Cosmarium*, and *Mesotaenium*—were sequenced, two more genera than those retrieved by the green algae protocol. Similarly, three OTUs of the Klebsormidiophyceae (the same *Interfilum* SKK strain), also found by the green algae protocol, were retrieved. Interestingly, this protocol also detected only a single metazoan OTU (Annelida), underscoring its utility for excluding metazoans in favor of Ochrophytes and other microbial taxa. This metabarcoding protocol, utilizing primers similar to those designed by Visco et al. (2015) for diatom sequencing, demonstrates its robustness in targeting microbial taxa while effectively excluding Metazoa.

Among ochrophytes, the protocol identified a diverse array of taxa, including 79 OTUs of diatoms**,** 63 of chrysophytes**,** 12 of xanthophytes**,** and one eustigmatophycean**.** Within diatoms**,** 12 genera and 10 undetermined taxa were identified (refer to Supplementary Figure S8) several of which were consistent with prior studies (Borchhardt, Schiefelbein, et al., 2017; Pushkareva et al., 2021; Rippin, Lange, et al., 2018; Thompson et al., 2020). Notable additions included genera *Achnanthidium*, *Achnanthes*, and *Licmophora*, which were not previously reported in similar contexts. Similarly, the chrysophytes identified were consistent with Rippin et al. (Rippin, Lange, et al., 2018), with the

addition of *Chromophyton*, *Chrysocapsa*, and *Paraphysomonas*. These findings highlight the protocol's capability to capture a broad range of ochrophytes while contributing to the taxonomic richness previously documented in polar biocrusts.

4.2. Protist diversity in polar biocrusts

Species richness and evenness for Svalbard and the Antarctic Peninsula were consistently higher, especially for cercozoans and green algae when compared to Continental Antarctica (Fig. 12). Despite this disparity, over half of the OTUs were shared among all regions, while specialist OTUs accounted for 1% to 26% of the total composition. This overlap is likely attributable to the presence of cosmopolitan or (bi)polar species, alongside some degree of endemicity. Notably, comparisons of polar and temperate microbial communities have revealed similar trends, with polar microbial communities being more similar to each other than to temperate sites and sharing over 30% of their OTUs (Kleinteich et al., 2017). This overlap was attributed to natural or anthropogenically mediated dispersal, coupled with environmental filtering, which promotes the establishment of overlapping microbial taxa across polar regions. Furthermore, these results align with previous studies that indicated that the Antarctic Peninsula supports higher protistan biodiversity relative to the harsher and more arid conditions of Continental Antarctica, such as those found in the Thala Hills (Dolgikh et al., 2015; J. R. Lee et al., 2017; Thompson, 2021; Y. Zhang et al., 2018).

Differences in species richness and evenness across polar biocrust regions have important implications for the structure and stability of microbial food webs. Higher species richness and evenness, as observed in Svalbard and the Antarctic Peninsula, are often linked to more complex and resilient food webs due to the presence of diverse trophic interactions and functional redundancy (McCann, 2000). In such systems, a greater variety of prey taxa can buffer predatory species against fluctuations in prey availability, thereby stabilizing predator populations (McCann, 2000). In contrast, the comparatively lower richness and evenness observed in Continental Antarctica may lead to simpler, less resilient food webs, leaving these systems more susceptible to environmental perturbations, such as shifts in climate or the colonization and invasion by non-native species (Convey, 2010). Notably, the phylogenetic analysis of cercozoan taxa (Fig. 15) revealed substantial genetic divergence among the detected lineages, suggesting the potential for novel species within these polar ecosystems. This highlights the need for further taxonomic and functional characterization to better understand the diversity and ecological roles of these protists. However, all three regions share a common vulnerability: their native biota are typically constrained by adversity-selected life history strategies, which prioritize survival over competition, leaving them ill-equipped to respond to rapid changes or

the introduction of more competitive species (Convey, 2010). These dynamics emphasize the vital role of biodiversity in sustaining ecosystem functions, particularly in extreme environments where food web simplifications could amplify the effects of warming, nutrient shifts, and other environmental changes. Understanding how these disparities influence ecosystem resilience and biogeochemical cycling remains a key challenge in polar microbial ecology.

Beta diversity analyses highlighted distinct microbial assemblages across the three regions and identified this parameter as the primary driver of community variation. Associations with abiotic soil factors suggested that, while environmental variables had varying effects on community structure, pH consistently emerged as the second most influential factor. However, a limitation of this study is the exclusion of water availability as an explanatory factor, as it was not measured. Water availability is a well-documented determinant of microbial community composition in polar biocrusts (Pushkareva et al., 2022, 2024). Collectively, these findings indicate that local climatic conditions and soil parameters play significant roles in shaping protist communities, in agreement with prior research (Chu et al., 2020; Oliverio et al., 2020).

The diversity of protist communities across polar biocrusts underscores the ecological complexity of these systems, with distinct assemblages driven by both abiotic factors and local climatic conditions. However, diversity alone does not fully explain the underlying processes shaping these communities. To delve deeper into ecological dynamics, it is crucial to examine the role of biotic factors that directly impact community composition, population dynamics, and nutrient cycling. Next, the influence of predation on microbial assemblages was explored, building on the observed diversity patterns to explore how predator-prey interactions shape microbial community dynamics and ecosystem functions.

4.3. Impact of biotic factors on microbial communities

Predation is a fundamental ecological process within microbial ecosystems, influencing population dynamics, shaping community structures, and driving adaptive resistance mechanisms (Burian et al., 2022; Hiltunen & Laakso, 2013; Nguyen et al., 2023). Recognizing its significance, this study aimed to validate inferred predator-prey interactions using experimental methods. As a next step after generating datasets and estimating diversity, the reciprocal impacts of predator and prey communities were quantified, and network analyses were subsequently conducted to infer potential interactions.

Beta diversity analyses identified biotic interactions as a key factor in shaping microbial communities, closely following region and soil pH as dominant environmental influences. The interactions between

cercozoans and green algae were particularly noteworthy. The community composition of green algae exerted a 1.5-fold greater structuring influence on Cercozoa than *vice versa*, highlighting the impact of cercozoan predation on green algae populations. In comparison, the structuring effect of ochrophytes on the green algal community was approximately 1.8-fold stronger than that of green algae over ochrophytes.

The interplay between cercozoans and ochrophytes was comparatively limited, with small but detectable mutual impacts on community composition. Notably, cercozoans exerted more than twice the structuring effect on green algae compared to ochrophytes, suggesting distinct predator-prey dynamics between these groups. These findings highlight the more pronounced interactions between cercozoans and green algae relative to ochrophytes. Such trends are further reflected in the subsequent network analyses, which will be discussed in detail in the following section, providing insights into the predicted frequency and nature of these interactions.

Beyond influencing community composition, predation likely drives nutrient cycling and microbial resistance mechanisms within biocrusts. Amoebal grazing experiments have shown that protist predation on algae can restructure microbial communities by reducing algal biomass and indirectly stimulating bacterial growth through egested organic residues (Jahnke et al., 2007). Similarly, cercozoans may accelerate the turnover of algal-derived organic matter, making carbon and nitrogen more bioavailable for decomposers and influencing trophic interactions within biocrust ecosystems. The extent of these effects likely depends on prey traits; green algae exhibiting rapid growth or high nutrient content may be preferentially targeted, whereas those with defense mechanisms such as mucilage production or morphological plasticity could exhibit greater resilience to predation (Mugnai et al., 2020). The limited impact of ochrophytes on cercozoans was unexpected, raising questions about potential indirect interactions or resource-mediated effects within the microbial ecosystem.

These findings emphasize the important role of biotic factors, particularly predation, in structuring microbial communities within polar biocrusts. They highlight the shaping role of biotic interactions over microbial assemblages, consistent with previous research emphasizing the importance of trophic and other biotic interactions, along with environmental effects, in structuring microbial communities (Freilich et al., 2018; Berry & Widder, 2014; Li et al., 2013). The observed complexity and diversity of associations underscore the multifaceted nature of these ecosystems, where both abiotic and biotic processes collectively dictate community composition. To further elucidate these dynamics, the following section evaluates the application of network and trait-based approaches, offering critical insights into the functional and structural implications of predator-prey interactions within these microbial networks.

4.4. Evaluation of the network and trait-based approaches

To enable a basis for comparison, a goal of this study was to generate three replicated networks from comparable but sufficiently distinct communities, derived from the biodiversity observed in Svalbard, the Antarctic Peninsula, and Continental Antarctica. Using FlashWeave, I leveraged the significant variation in community composition between regions to construct robust and replicable microbial networks, despite some shared taxa, offering insights into predator-prey dynamics while allowing the assessment of the reproducibility and predictive accuracy. To further validate these findings, HMSC models were employed, strengthening network predictions and disentangling biotic interactions from environmental effects.

Microbial interaction networks provide an opportunity to detect ecological relationships and population dynamics, as microbial survey datasets are expected to exhibit signatures of such interactions (Berry & Widder, 2014). In this study, cross-kingdom network analyses of polar biocrusts enabled predictions of predator-prey interactions among cercozoans, green algae, and ochrophytes. Across all regions, positive inter-domain putative interactions dominated, accounting for 81%, 79%, and 76% of correlations in Svalbard, the Antarctic Peninsula, and Continental Antarctica, respectively. Remarkably, this trend also extended to putative predator-prey interactions, suggesting that both positive and negative correlations must be considered to fully understand these ecological relationships. While predator-prey interactions are often expected to be negatively correlated due to prey depletion by predators, this assumption does not always hold in microbial systems. For instance, predators and prey can positively correlate at some spatial scales that allow predators to maximize prey encounters (Freilich et al., 2018), or may exhibit positive correlations because they share microhabitats where conditions favor both groups (Levins & Schultz, 1996). Furthermore, predator-prey interactions may be time-lagged due to population and environmental changes (Faust & Raes, 2012), making real-time sequencing snapshots less likely to capture direct depletion effects. Thus, the pervasive occurrence of positive putative interactions across all three regions, particularly among potential predator-prey interactions, underscores the complexity of microbial networks, where correlations cannot be directly attributed to specific biological functions without further validation.

Associations with taxa within Glissomonadida accounted for a substantial portion of putative interactions in each region, despite the order being predominantly bacterivorous (Dumack et al., 2020). This result suggests that Glissomonadida likely functions as a hub taxon within these ecosystems. Known for their rapid growth under favorable conditions, glissomonads can become highly abundant in the soil matrix, potentially explaining their prevalence. The observed association between glissomonads and algae, if not predatory, may instead stem from shared environmental preferences or indirect interactions mediated by the broader microbial community. Alternatively,

glissomonads might be attracted towards microalgae, which dominate carbon fixation in polar areas with sparse or absent higher plant life (Rippin, Lange, et al., 2018), and release exudates rich in carbon compounds into the environment (Kuehn et al., 2014). Glissomonads may exploit these compounds as osmotrophs (Dumack et al., 2020; Howe et al., 2011) or feed on algae-associated carbon-scavenging bacteria, paralleling the microbial loop observed in plant ecosystems (Bonkowski, 2004).

The analysis with FlashWeave revealed that only a small fraction of the total correlations represented potential predator-prey interactions between predatory protists and green algae or ochrophytes, with 72 (17.7%), 86 (20.4%), and 46 (32.9%) such interactions identified in Svalbard, the Antarctic Peninsula, and Continental Antarctica, respectively. Notably, only a minor subset of Cercozoa involved in these correlations were algivores, accounting for 6.4%, 4.7%, and 9.3% of the total correlations in Svalbard, the Antarctic Peninsula, and Continental Antarctica, respectively. Similarly, HMSC networks yielded comparable proportions of predator-prey interactions, with 7.5% for co-occurrence and 4.8% for co-abundance. Interestingly, while the co-occurrence results from HMSC's full model closely aligned with FlashWeave, the co-abundance networks produced significantly fewer associations overall. Moreover, all correlations between cercozoans and their prey detected in FlashWeave were confirmed in the full model for co-occurrence, with at least one or more corresponding correlations in the species-to-species matrix at the genus level (Fig. 14, black squares). Thus, this suggests that HMSC's co-occurrence networks effectively captured key predator-prey relationships, even if co-abundance data yielded sparser connections.

The discrepancy between co-occurrence and co-abundance models is well recognized but often yields contrasting results depending on the ecological system and modeling framework. Some studies suggest that abundance models generally provide improved explanatory power, particularly for common species at fine spatial scales, as seen in macroecological datasets (Howard et al., 2014; Johnston et al., 2015). These models often capture more detailed population dynamics and habitat associations than presence-absence models. However, in microbial communities, where many taxa are rare or occur sporadically, presence-absence models can outperform abundance-based approaches in detecting ecological patterns, particularly in datasets with a high proportion of low-abundance taxa, where abundance fluctuations may be driven more by stochastic processes than ecological interactions. In hurdle models within the HMSC framework, presence-absence models often reveal more associations than those based on abundance data, and their explanatory and predictive powers can exceed that of abundance models, as observed in both Odriozola et al. (2021) and this study (Supplementary table S6). In contrast, abundance models may better capture ecological dynamics in communities where species exhibit stable, high-abundance distributions.

The relationship between occurrence and abundance is complex and species-dependent (Johnston et al., 2015). While abundance patterns often follow an "abundant-center" distribution within a species' range, the environmental factors driving abundance may differ from those limiting distribution (Couwenberghe et al., 2013; Nielsen et al., 2005). Presence-absence models can provide useful information about ecological optima but may overestimate the range suitable for high abundance (Couwenberghe et al., 2013) whereas abundance data, when available, can significantly enhance species distribution modeling. Two-stage modeling approaches, separating occurrence and abundance processes, offer a promising method for capturing these complex relationships (Nielsen et al., 2005), as applied in this study using a hurdle model.

FlashWeave explicitly accounts for sequencing data's compositional nature by implementing centered-log-ratio transformations and filtering indirect associations through metadata integration, ensuring that network inferences are not biased by differences in sequencing depth or sample-specific variability (Deutschmann et al., 2021; Tackmann et al., 2019), HMSC does not yet model compositional data explicitly, meaning that species associations derived from HMSC may be influenced by relative abundance constraints inherent to sequencing-based studies. This distinction is critical in microbial ecology, where sequencing counts do not reflect absolute abundances, but rather relative proportions constrained within each sample (Gloor et al., 2017). As a result, species-to-species correlations derived from HMSC may not fully account for the underlying structure of compositional data, whereas FlashWeave provides a more compositionally aware approach for detecting microbial interactions. Nonetheless, to further validate these findings, the HMSC hurdle model workflow was applied to construct co-occurrence and co-abundance networks (Tikhonov, Opedal, et al., 2022). Since both components of the hurdle model are statistically independent, this approach enabled the separate examination of the environmental covariates driving species occurrence versus those influencing species abundance (Tikhonov, Opedal, et al., 2022).

A key advantage of the HMSC approach was the incorporation of a null model, a feature not calculated for FlashWeave. Null models helped distinguish random co-occurrences from true biotic associations by accounting for environmental covariates and refining network interpretations. However, while null models improve confidence in inferred associations, they do not establish causality and must be complemented with experimental validation.

Trait-based approaches enhanced the precision of network analyses by linking specific ecological roles, such as algivory, to predicted interactions. This integration not only improved the accuracy of inferred relationships but also provided critical ecological context. To validate these predictions, experimental testing remains essential. The following section focuses on the experimental

confirmation of these interactions, shedding light on the dynamics between Cercozoa and their algal prey within polar biocrusts.

4.5. Confirmation of predator-prey interactions

While network analyses provide valuable insights into microbial interactions, experimental validation is essential to confirm true predator-prey relationships. Here, network-derived hypotheses were tested using co-culture experiments, where predicted interactions between predatory cercozoans and their potential prey resulted in measurable predation. FlashWeave-guided predictions were further refined with HMSC models, which accounted for environmental covariates, hierarchical dependencies, and functional traits. To ensure ecological relevance, a focus on cercozoan taxa known as obliged or facultative algivores was applied (Dumack, 2017; Seppey et al., 2017), allowing a trait-based selection of interactions for co-culturing.

Out of the 11 tested interactions, nine were confirmed, yielding a validation rate of 82%. In these cases, predator abundance increased substantially, while in eight of these, ANCOVA analyses confirmed significant and consistent predator growth (Fig. 16, Supplementary Table S7). Predation also led to a significant decline in algal abundance in five cases, according to ANCOVA results (Supplementary Table S8). Microscopic examinations confirmed algal ingestion, revealing food vacuoles containing algal cells at various digestion stages across all predators (Fig. 18).

The experiments further revealed that *Cercomonas* sp., *Fisculla* sp., and *Rhogostoma* sp. were the most vicious predators, i.e. the predators with higher growth rates, suggesting they are among the most efficient cercozoan predators. Conversely, two interactions involving *Chloromonas* with *Fisculla* sp. and *Cercomonas* sp. could not be confirmed, likely due to the alga's rapid motility, which may allow it to evade capture in liquid cultures. These results suggest that, as expected, certain algal traits can reduce vulnerability to predation, which here was exemplified by motility but can extend to the production of extracellular polysaccharides or secondary metabolites that deter grazers. Distinct predation strategies emerged across cercozoans. *Rhogostoma* sp. and *Fisculla sp.* displayed active swimming while feeding, ingesting multiple algal cells simultaneously (Fig. 18A–B). *Euglypha sp.* was a generalist predator, feeding on four out of five tested algal species (Fig. 18D, E, G-I). However, interactions with diatoms (*Pinnularia sp.*) were largely unsuccessful; diatom ingestion was only observed once, and their rigid frustules likely limited nutrient extraction. *Cercomonas* sp. alternated between free-swimming predation and substrate attachment (Fig. 18C), suggesting behavioral plasticity in prey acquisition. Taken together, these strategies highlight the complexity of microbial

food webs and suggest that predator-prey interactions are shaped not only by encounter rates and predator-feeding adaptations but also by prey defense mechanisms.

Network analysis also revealed a positive correlation between predation efficiency and node centrality, with predators exhibiting higher stress and betweenness centrality also displaying faster growth rates (Fig. 17). Since stress centrality reflects a taxon's role in bridging multiple trophic interactions, and betweenness centrality indicates its influence on overall network connectivity, these findings suggest that efficient predators occupy key structural positions in microbial food webs, potentially stabilizing trophic dynamics**.**

Despite the strong experimental evidence of predation, the limitations of laboratory conditions must be acknowledged. Factors such as constant temperature (15°C), controlled light regimes, high prey densities, nutrient limitations, and liquid media—absent of competitors or environmental constraints—likely amplified predation rates and behaviors. These optimized conditions contrast with the spatially structured, resource-patchy environments of polar biocrusts, where competition, resource heterogeneity, and spatial constraints significantly shape trophic interactions. The opaque nature of soil complicates direct observation and validation of biotic interactions, necessitating indirect approaches and cautious extrapolation of the results to natural settings.

Additionally, the extreme conditions of polar ecosystems, particularly fluctuating resource availability, may drive shifts in prey preferences and foraging strategies among cercozoans, mirroring patterns observed in other soil ecosystems where species interactions are shaped by transient resource availability and optimal foraging behavior (M. S. Adl & Gupta, 2006). In natural soil ecosystems, competition among predators, reduced prey mobility due to substrate opacity, and fluctuating environmental conditions could all modulate predator-prey interactions. Soil-associated predation events may be sporadic, with trophic dynamics mediated by seasonal changes in moisture availability and nutrient fluxes.

Ultimately, while these findings provide robust evidence for cercozoans' predatory capacity under controlled conditions, their ecological roles in natural ecosystems remain uncertain. Future research should integrate environmental complexities such as substrate heterogeneity, prey dormancy, and multi-trophic interactions. Bridging the gap between controlled experiments and field conditions through direct *in situ* measurements will be essential for capturing the nuanced dynamics of microbial interactions in polar biocrusts.

4.6. The potential role of Cercozoa as a key trophic link in polar biocrusts

Microbial predators play an important role in structuring ecosystems by regulating prey populations, influencing nutrient cycling, and maintaining microbial community stability (McCann, 2000). In polar biocrusts, where higher trophic levels are scarce or absent, microalgal primary production dominates, and microbial grazers—such as cercozoans—constitute key consumers within the ecosystem, likely shaping trophic interactions. My findings demonstrate that cercozoans actively graze on microalgae, positioning them as key players in microbial trophic interactions. While the extent of their impact on algal populations *in situ* remains to be fully quantified, future field-based studies integrating direct measurements of microbial interactions will be crucial for assessing their ecological influence.

Cercozoans were consistently observed in predator-prey associations within network analyses, forming the majority of inter-domain interactions. Their ability to prey on multiple algal taxa suggests a potential top-down effect on algal populations, which could influence microbial community composition. The experimental validation of network-predicted interactions further supports the idea that cercozoans are not just opportunistic grazers but actively exert predation pressure on microalgae. However, whether their predatory impact is strong enough to structure algal populations *in situ* remains an open question.

Beyond direct predation, cercozoans may play a crucial role in microbial food web restructuring by mobilizing carbon and nitrogen stored in algal biomass, making these nutrients more bioavailable for bacterial decomposers. This aligns with broader findings that protists serve as key recyclers in soil ecosystems, linking carbon and nitrogen fluxes (Bonkowski, 2004; Geisen et al., 2018). Their ability to bridge microbial trophic levels suggests that they not only regulate algal populations but, by doing so, might also contribute to bacterial productivity by facilitating organic matter turnover. The observed relationship between predation efficiency and network topological features, such as betweenness centrality and stress, further suggests that efficient predators may exert a disproportionate influence on microbial interactions and resource redistribution.

However, as shown in soil biofilm studies, different algal species exhibit variable susceptibility to predation, with some taxa, such as *Chlamydocapsa*, increasing in response to grazing pressure (Jahnke et al., 2007). These findings underscore the importance of prey defense mechanisms in shaping predator-prey dynamics within polar biocrusts. While cercozoans function as key grazers, their broader impact on microbial food web stability and nutrient cycling likely depends on the specific composition of algal communities and their defensive traits, as well as environmental factors influencing predator-prey interactions.

While cercozoans were here identified as potential primary grazers, they are likely part of a broader microbial predator guild that includes testate amoebae, ciliates, vampyrellids, and heterotrophic flagellates (Thompson, 2021; Thompson et al., 2020). These alternative grazers may interact with cercozoans in trophic cascades, competing for the same prey or even preying upon cercozoans themselves. Additionally, rotifers and nematodes—where present—could further shape microbial trophic interactions. These results highlight the ability of cercozoans to switch between prey types, probably in response to resource availability and seasonal changes, and suggest a level of trophic flexibility that may be key to their persistence in extreme environments. However, cercozoan feeding strategies vary significantly across taxa, ranging from strict bacterivores to facultative or obligate algivores. While some taxa primarily consume bacteria but opportunistically graze on algae when available, others, such as *Rhogostoma* and *Fisculla*, appear here to rely on algivory to some extent. Understanding these functional differences is essential for assessing their broader ecological impact in polar microbial food webs.

The ability of cercozoans to exploit diverse resources likely contributes to their ecological significance in polar biocrusts. Their slender pseudopodia and flexible body shapes enable them to access prey within small soil pores, an adaptation that facilitates foraging in microhabitats with limited resources (Geisen et al., 2018). This versatility not only positions cercozoans as key grazers but also as potential regulators of microbial community structure, shaping population dynamics through predation and nutrient cycling.

While cercozoans have demonstrated their capacity to prey on algae, their interactions with other microbial groups in polar biocrusts remain an area requiring further exploration. For instance, cyanobacteria, which often dominate carbon fixation in polar regions (Boy et al., 2016), may indirectly influence cercozoan dynamics. Although cercozoans are not known as direct grazers of cyanobacteria, they may benefit from shared microhabitats or prey on bacteria that scavenge cyanobacterial exudates. Such interactions resemble the microbial loop observed in terrestrial ecosystems, where plant-associated exudates drive nutrient cycling (Bonkowski, 2004).

Ultimately, these findings establish cercozoans as functionally important microbial predators in polar biocrusts. However, the degree to which they regulate algal populations and influence microbial food web stability remains to be fully understood. Future studies should aim to quantify their *in situ* impact, integrating field observations with experimental and trait-based approaches. Additionally, exploring the functional diversity of cercozoans, including their feeding strategies and metabolic capacities, will be essential for refining their role in biocrust ecosystems. Comparative studies across polar and non-

polar regions could further elucidate the generalizability of these findings and provide broader insights into the functioning of microbial food webs under extreme conditions.

4.7. Methodological considerations and limitations

The methods employed in this study provided high-resolution insights into predator-prey dynamics, offering a valuable starting point for understanding microbial ecosystems in extreme environments. However, as with any experimental design, limitations, and trade-offs exist, which must be acknowledged to refine future approaches.

4.7.1. Strengths of the experimental design

This study's integrative methodology, combining high-resolution network analyses (FlashWeave and HMSC) with experimental validation through trait-based approaches, is a notable strength. Microbial co-occurrence networks are often criticized for identifying correlations that may not reflect true ecological interactions (Shang et al., 2017). By incorporating functional trait data into the analyses, I was able to link taxonomic identity with ecological roles, facilitating the interpretation of putative predator-prey interactions. Such trait-informed analyses have been instrumental in other studies, such as Seppey et al. (2017), which revealed unexpected facultative algivory in *Rhogostoma*.

The design also benefited from its focus on low-diversity environments, which allowed for a high degree of sampling saturation and minimized the confounding effects of community complexity. This approach is particularly effective in polar regions, where environmental constraints shape distinct microbial communities (Fiore-Donno et al., 2018). The integration of FlashWeave, known for its computational efficiency and ability to incorporate metadata, with HMSC, a Bayesian modeling framework that disentangles environmental and biotic effects, further enhanced the robustness of the network analyses. These complementary tools ensured that both direct and indirect interactions were captured, providing a comprehensive view of microbial associations.

Moreover, the application of a hurdle model within the HMSC framework addressed the zero-inflated nature of sequencing data. By modeling presence-absence and abundance separately, the approach allowed for independent exploration of the environmental drivers of species occurrence and abundance (Tikhonov et al., 2022). This dual-model structure added depth to the analysis, although it highlights areas for further methodological refinement.

4.7.2. Limitations and trade-offs

Despite the strengths of the experimental design, certain limitations must be acknowledged.

Network analyses as hypothesis-generating tools

While FlashWeave and HMSC were effective in generating ecologically meaningful networks, it is essential to recognize that these methods remain hypothesis-generating rather than definitive tools. FlashWeave's design, optimized for large and heterogeneous sequencing datasets, to handle compositionality, incorporate metadata, and optimize computational speed (Tackmann et al., 2019), proved well-suited for this study, particularly due to its ability to minimize spurious associations through metadata integration (Deutschmann et al., 2021). However, the inability of HMSC to explicitly model compositional data remains a constraint, limiting their application for high-dimensional sequencing datasets. Employing a multinomial JSDM approach, as suggested by Itter et al. (2024), could enhance the predictive power of future studies by simultaneously modeling compositional data and residual correlations. Moreover, HMSC is computationally intensive, requiring expertise in hierarchical generalized linear mixed models and Bayesian inference, as well as proficiency in Markov chain Monte Carlo sampling strategies. Additionally, its performance depends on comprehensive trait and metadata inputs, which can be challenging to assemble for complex microbial communities. Consequently, FlashWeave remained here the primary guideline for selecting interactions to be experimentally tested, while HMSC provided a complementary perspective by offering insights into community structuring and microbial associations.

Temporal and environmental variability

The networks were constructed based on samples collected during the peak summer months for each region (July for Svalbard and February–March for the Antarctic regions) when favorable conditions such as increased temperatures and humidity prevail (Dolgikh et al., 2015; Norwegian Meteorological Institute, 2022; Pasik et al., 2021). While this approach maximized microbial activity and diversity, the resulting network structures may reflect transient dynamics rather than stable interactions. Temporal replication, extending across different seasons, would allow for a more nuanced understanding of how environmental variability influences microbial networks.

Simplified experimental conditions

The co-culture experiments, designed to validate predicted interactions, were conducted under optimized laboratory conditions, including high prey densities, and nitrogen-limited liquid media. This setup does not account for the complexity of biocrust natural ecosystems, where factors such as competition, spatial heterogeneity, and seasonal dynamics influence community structure and trophic

interactions. While algivory by protists like Cercozoa was confirmed experimentally, the ecological relevance of these interactions under field conditions remains uncertain, given the potential for fluctuating prey availability and environmental constraints.

Unmeasured variables:

Despite efforts to minimize spurious edges in the networks, unmeasured abiotic and biotic factors likely influenced microbial associations. For example, water availability, developmental stage of the biocrusts, microhabitat heterogeneity, UV radiation, time-lagged effects, spatial scales of interaction, competition with other predators, and functional traits beyond feeding strategy were not directly measured but are known to shape microbial interactions in polar biocrusts. Integrating these variables into future network analyses could enhance the accuracy of inferred interactions.

4.7.3. Implications for future studies: integrating multi-omics approaches

The findings of this study underscore the importance of integrating classical culture-based approaches with high-throughput sequencing and trait-based analyses. While this approach has been instrumental in revealing unexpected ecological roles, such as facultative algivory in protists previously considered bacterivorous (Seppey et al., 2017), future studies must address remaining gaps to fully capture the complexity of microbial interactions in polar biocrusts.

One critical avenue for future research lies in improving temporal and spatial replication. Long-term monitoring across multiple seasons and years would provide insights into the stability and variability of microbial interactions under shifting environmental conditions, such as changes in temperature, soil moisture, and nutrient dynamics, linked to global climatic change. Similarly, sampling across diverse microhabitats could capture the spatial heterogeneity of microbial networks, shedding light on how local environmental factors shape biocrust community structure and trophic dynamics.

Another priority is the advancement of *in situ* methodologies. While laboratory experiments provide controlled environments to validate network predictions, they cannot fully replicate the intricacies of natural ecosystems. Emerging tools, such as advanced imaging techniques, microfluidic systems, and real-time environmental monitoring, could enable direct observation of microbial interactions in natural biocrusts. Stable isotope probing and isotope labeling, in particular, could be instrumental in confirming trophic interactions, especially where direct predator-prey relationships remain speculative.

Expanding the scope of trait-based analyses is another critical step. Future studies could incorporate additional functional traits, such as metabolic profiles, enzymatic activities, and prey defense mechanisms, to deepen our understanding of trophic interactions. For example, linking specific algal

traits, like cell wall structure or mucilage production, to predation resistance could reveal nuanced dynamics of predator-prey interactions. Similarly, analyzing bacterial functional traits could illuminate the broader ecological roles of bacterivorous protists, contributing to a more holistic understanding of microbial ecosystem functioning.

Exploring multi-trophic interactions is essential to understanding the interconnected food webs within polar biocrusts. The relationships between cercozoans, algae, bacteria, and cyanobacteria are likely part of a larger, integrated web of interactions that drive nutrient cycling and ecosystem resilience. Investigating how shifts in one trophic level cascade through the microbial community could provide valuable insights into ecosystem stability and adaptability, especially under environmental stressors.

Finally, addressing environmental variability in experimental designs remains a key challenge. Incorporating factors such as seasonal changes, substrate availability, UV radiation, and nutrient dynamics into network analyses would allow for more accurate modeling of microbial interactions. Integrating these variables could help distinguish transient associations from stable ecological interactions, advancing our understanding of microbial food web dynamics in extreme environments.

4.7.4. Advancing microbial interaction studies: Further integrative approaches

The integration of multi-omics approaches represents a promising frontier for studying microbial interactions in polar biocrusts. Techniques such as metagenomics, meta-transcriptomics, and stable isotope probing can provide unprecedented resolution in identifying active microbial processes and linking them to specific taxa (Almela et al., 2019, 2023; Freudenthal et al., 2022). For instance, stable isotope tracing could confirm whether algivorous Cercozoa, observed in these experiments, actively consume algae under field conditions, addressing a key limitation of laboratory-based studies.

Additionally, the application of trait-matching and machine-learning approaches has proven promising for inferring microbial feeding links (Barel et al., 2023). These methodologies leverage functional trait data and predictive algorithms to model potential interactions, offering a scalable and efficient way to uncover trophic networks in complex microbial ecosystems. As these tools continue to evolve, they hold great potential for refining our understanding of predator-prey dynamics, particularly in ecosystems where direct observation remains challenging.

Conclusions and outlook

This study establishes Cercozoa as active microbial predators in polar biocrusts, providing the first experimental validation of their predatory interactions with microalgae in these extreme environments. By integrating network analyses, trait-based functional assignments, and controlled feeding experiments, we demonstrate that cercozoans effectively graze on algal prey, likely contributing to microbial trophic interactions and carbon fluxes in biocrust ecosystems. However, their precise ecological role in situ remains unresolved, as environmental heterogeneity, prey availability, and competitive interactions may shape their impact under natural conditions.

The results highlight the trophic flexibility of cercozoans, with some taxa acting as facultative algivores, potentially shifting between prey types based on resource availability. This adaptability may be crucial in polar ecosystems, where seasonal fluctuations in environmental conditions strongly influence microbial food web dynamics. Additionally, the observed link between predator efficiency and network topology underscores the potential for network-based approaches to predict ecologically significant interactions, offering a powerful framework for future microbial food web research.

Despite these advances, key questions remain. The extent to which cercozoans regulate algal populations in natural biocrusts requires further investigation through *in situ* monitoring and field experiments. Additionally, their interactions with other microbial predators, such as testate amoebae, ciliates, and vampyrellids, remain largely unexplored. Future research should also expand trait-based approaches to incorporate metabolic profiling and stable isotope tracing, which could help clarify the contributions of cercozoans to biogeochemical cycles.

As polar regions continue to experience rapid environmental change, understanding how microbial trophic networks respond to shifting conditions will be critical. By bridging experimental and ecological perspectives, this study provides a foundation for future research on microbial food web dynamics in extreme environments. Further integrating molecular, experimental, and ecological approaches will be essential to refine our understanding of microbial predator-prey relationships and their broader implications for ecosystem function and resilience in a changing world.

Abbreviations

ANCOVA – Analysis of Covariance

BLAST – Basic Local Alignment Search Tool

ESS – Effective Sample Size

HMSC – Hierarchical Modeling of Species Communities

IPTG – Isopropyl β-D-1-thiogalactopyranoside

JSDM – Joint Species Distribution Modeling

MAFFT – Multiple Alignment using Fast Fourier Transform

MCMC – Markov Chain Monte Carlo

NMDS – Non-Metric Multidimensional Scaling

NOAA – National Oceanic and Atmospheric Administration

OTU – Operational Taxonomic Unit

PCoA – Principal Coordinates Analysis

PERMANOVA – Permutational Multivariate Analysis of Variance

PPFD – Photosynthetic Photon Flux Density

PR^2 – Protist Ribosomal Reference Database

PSRF – Potential Scale Reduction Factor

RAxML – Randomized Accelerated Maximum Likelihood

RCP2.6 – Representative Concentration Pathway 2.6

RCP8.5 – Representative Concentration Pathway 8.5

SAR – Stramenopiles, Alveolates, and Rhizaria

TOC – Total Organic Carbon

TN – Total Nitrogen

TP – Total Phosphorus

WGM – Wheatgrass Medium

References

Adakudlu, M., Andersen, J., Bakke, J., Beldring, S., Benestad, R., Bilt, W. van der, Bogen, J., Borstad, C., Breili, K., Breivik, Ø., Børsheim, K. Y., Christiansen, H. H., Dobler, A., Engeset, R., Frauenfelder, R., Gerland, S., Gjelten, H. M., Gundersen, J., Isaksen, K., … Wong, W. K. (2019). *Climate in Svalbard 2100 – a knowledge base for climate adaptation.* [Report]. Norwegian Centre for Climate Services (NCCS) for Norwegian Environment Agency (Miljødirektoratet). https://doi.org/10.25607/OBP-888

Adams, B. J., Bardgett, R. D., Ayres, E., Wall, D. H., Aislabie, J., Bamforth, S., Bargagli, R., Cary, C., Cavacini, P., Connell, L., Convey, P., Fell, J. W., Frati, F., Hogg, I. D., Newsham, K. K., O'Donnell, A., Russell, N., Seppelt, R. D., & Stevens, M. I. (2006). Diversity and distribution of Victoria Land biota. *Soil Biology and Biochemistry*, *38*(10), 3003–3018. https://doi.org/10.1016/j.soilbio.2006.04.030

Adl, M. S., & Gupta, V. S. (2006). Protists in soil ecology and forest nutrient cycling. *Canadian Journal of Forest Research*, *36*(7), 1805–1817. https://doi.org/10.1139/x06-056

Adl, S. M., Bass, D., Lane, C. E., Lukeš, J., Schoch, C. L., Smirnov, A., Agatha, S., Berney, C., Brown, M. W., Burki, F., Cárdenas, P., Čepička, I., Chistyakova, L., Campo, J., Dunthorn, M., Edvardsen, B., Eglit, Y., Guillou, L., Hampl, V., … Zhang, Q. (2019). Revisions to the Classification, Nomenclature, and Diversity of Eukaryotes. *Journal of Eukaryotic Microbiology*, *66*(1), 4–119. https://doi.org/10.1111/jeu.12691

Adl, S. M., Simpson, A. G. B., Lane, C. E., Lukeš, J., Bass, D., Bowser, S. S., Brown, M. W., Burki, F., Dunthorn, M., Hampl, V., Heiss, A., Hoppenrath, M., Lara, E., Le Gall, L., Lynn, D. H., McManus, H., Mitchell, E. A. D., Mozley-Stanridge, S. E., Parfrey, L. W., … Spiegel, F. W. (2012). The revised classification of eukaryotes. *The Journal of Eukaryotic Microbiology*, *59*(5), 429–493. https://doi.org/10.1111/j.1550-7408.2012.00644.x

Almela, P., Rico, E., Velázquez, D., Verleyen, E., & Quesada, A. (2023). Soil moisture drives differences in the diversity and trophic complexity of high Arctic tundra soils. *FEMS Microbiology Ecology*, *99*(6), fiad050. https://doi.org/10.1093/femsec/fiad050

Almela, P., Velázquez, D., Rico, E., Justel, A., & Quesada, A. (2019). Carbon Pathways Through the Food Web of a Microbial Mat From Byers Peninsula, Antarctica. *Frontiers in Microbiology*, *10*. https://www.frontiersin.org/articles/10.3389/fmicb.2019.00628

Álvarez-Fernández, R. (2013). Chapter One—Explanatory Chapter: PCR Primer Design. In *Methods in Enzymology* (Vol. 529, pp. 1–21). Elsevier. https://doi.org/10.1016/B978-0-12-418687-3.00001-X

Anderson, O. (2016). *Experimental evidence for non-encysted, freeze-resistant stages of terrestrial naked amoebae capable of resumed growth after freezethaw events*. *55*, 19–25. https://doi.org/10.4467/16890027AP.16.003.4044

Andreyev, M. P. (1989). The lichens in the vicinity of Bellingshausen station, King George Island. *Polar Geography and Geology*, *13*(1), 42–45. https://doi.org/10.1080/10889378909377379

Anthony, M. A., Bender, S. F., & Van Der Heijden, M. G. A. (2023). Enumerating soil biodiversity. *Proceedings of the National Academy of Sciences*, *120*(33), e2304663120. https://doi.org/10.1073/pnas.2304663120

Bamforth, S. S., Wall, D. H., & Virginia, R. A. (2005). Distribution and diversity of soil protozoa in the McMurdo Dry Valleys of Antarctica. *Polar Biology*, *28*(10), 756–762. https://doi.org/10.1007/s00300-005-0006-4

Barel, J. M., Petchey, O. L., Ghaffouli, A., & Jassey, V. E. J. (2023). Uncovering microbial food webs using machine learning. *Soil Biology and Biochemistry*, *186*, 109174. https://doi.org/10.1016/j.soilbio.2023.109174

Bar-On, Y. M., Phillips, R., & Milo, R. (2018). The biomass distribution on Earth. *Proceedings of the National Academy of Sciences*, *115*(25), 6506–6511. https://doi.org/10.1073/pnas.1711842115

Becking, B. (1934). *Geobiologie of inleiding tot de milieukunde*.

Belnap, J., & Lange, O. L. (2001). Structure and Functioning of Biological Soil Crusts: A Synthesis. In J. Belnap & O. L. Lange (Eds.), *Biological Soil Crusts: Structure, Function, and Management* (Vol. 150, pp. 471–479). Springer Berlin Heidelberg. https://doi.org/10.1007/978-3-642-56475-8_33

Belnap, J., & Lange, O. L. (2013). *Biological Soil Crusts: Structure, Function, and Management*. Springer Science & Business Media.

Benjamini, Y., & Hochberg, Y. (1995). Controlling the False Discovery Rate: A Practical and Powerful Approach to Multiple Testing. *Journal of the Royal Statistical Society: Series B (Methodological)*, *57*(1), 289–300. https://doi.org/10.1111/j.2517-6161.1995.tb02031.x

Bernasconi, S. M. (2008). Weathering, soil formation and initial ecosystem evolution on a glacier forefield: A case study from the Damma Glacier, Switzerland. *Mineralogical Magazine*, *72*(1), 19–22. https://doi.org/10.1180/minmag.2008.072.1.19

Berry, D., Ben Mahfoudh, K., Wagner, M., & Loy, A. (2011). Barcoded Primers Used in Multiplex Amplicon Pyrosequencing Bias Amplification. *Applied and Environmental Microbiology*, *77*(21), 7846–7849. https://doi.org/10.1128/AEM.05220-11

Berry, D., & Widder, S. (2014). Deciphering microbial interactions and detecting keystone species with co-occurrence networks. *Frontiers in Microbiology*, *5*. https://doi.org/10.3389/fmicb.2014.00219

Berthold, M., Zimmer, D., & Schumann, R. (2015). A simplified method for total phosphorus digestion with potassium persulphate at sub-boiling temperatures in different environmental samples. *Rostocker Meeresbiologische Beiträge*, *25*, 7–25.

Bezanson, J., Edelman, A., Karpinski, S., & Shah, V. B. (2017). Julia: A Fresh Approach to Numerical Computing. *SIAM Review*, *59*(1), 65–98. https://doi.org/10.1137/141000671

Bintanja, R. (2018). The impact of Arctic warming on increased rainfall. *Scientific Reports*, *8*(1), 16001. https://doi.org/10.1038/s41598-018-34450-3

Blanchet, F. G., Cazelles, K., & Gravel, D. (2020). Co-occurrence is not evidence of ecological interactions. *Ecology Letters*, *23*(7), 1050–1063. https://doi.org/10.1111/ele.13525

Blume, H.-P., Stahr, K., & Leinweber, P. (2011). *Bodenkundliches Praktikum: Eine Einführung in pedologisches Arbeiten für Ökologen, Land- und Forstwirte, Geo- und Umweltwissenschaftler* (3. Aufl. 2010). Spektrum Akademischer Verlag. https://doi.org/10.1007/978-3-8274-2733-5

Bonkowski, M. (2004). Protozoa and plant growth: The microbial loop in soil revisited. *New Phytologist*, *162*(3), 617–631. https://doi.org/10.1111/j.1469-8137.2004.01066.x

Bonkowski, M., Cheng, W., Griffiths, B. S., Alphei, J., & Scheu, S. (2000). Microbial-faunal interactions in the rhizosphere and effects on plant growth§. *European Journal of Soil Biology*, *36*(3), 135–147. https://doi.org/10.1016/S1164-5563(00)01059-1

Bonkowski, M., Dumack, K., & Fiore-Donno, A. M. (2019). The Protists in Soil—A Token of Untold Eukaryotic Diversity. In J. D. van Elsas, J. T. Trevors, A. S. Rosado, & P. Nannipieri (Eds.), *Modern Soil Microbiology* (3rd ed., pp. 125–140). CRC Press. https://doi.org/10.1201/9780429059186-8

Borchhardt, N., Baum, C., Mikhailyuk, T., & Karsten, U. (2017). Biological Soil Crusts of Arctic Svalbard—Water Availability as Potential Controlling Factor for Microalgal Biodiversity. *Frontiers in Microbiology*, *8*, 1485. https://doi.org/10.3389/fmicb.2017.01485

Borchhardt, N., Baum, C., Thiem, D., Köpcke, T., Karsten, U., Leinweber, P., & Hrynkiewicz, K. (2019). Soil microbial phosphorus turnover and identity of algae and fungi in biological soil crusts along a transect in a glacier foreland. *European Journal of Soil Biology*, *91*, 9–17. https://doi.org/10.1016/j.ejsobi.2018.12.006

Borchhardt, N., Schiefelbein, U., Abarca, N., Boy, J., Mikhailyuk, T., Sipman, H. J. M., & Karsten, U. (2017). Diversity of algae and lichens in biological soil crusts of Ardley and King George islands, Antarctica. *Antarctic Science*, *29*(3), 229–237. https://doi.org/10.1017/S0954102016000638

Bowker, M. A., Maestre, F. T., Eldridge, D., Belnap, J., Castillo-Monroy, A., Escolar, C., & Soliveres, S. (2014). Biological soil crusts (biocrusts) as a model system in community, landscape and ecosystem ecology. *Biodiversity and Conservation*, *23*(7), 1619–1637. https://doi.org/10.1007/s10531-014-0658-x

Boy, J., Godoy, R., Shibistova, O., Boy, D., McCulloch, R., de la Fuente, A. A., Morales, M. A., Mikutta, R., & Guggenberger, G. (2016). Successional patterns along soil development gradients formed by glacier retreat in the Maritime Antarctic, King George Island. *Revista Chilena de Historia Natural*, *89*(1), 6. https://doi.org/10.1186/s40693-016-0056-8

Bradley, I. M., Pinto, A. J., & Guest, J. S. (2016). *Design and Evaluation of Illumina MiSeq Compatible Primers for the 18S rRNA Gene for Improved Characterization of Mixed Phototrophic Communities*. 16.

Breen, K., & Lévesque, E. (2008). The Influence of Biological Soil Crusts on Soil Characteristics along a High Arctic Glacier Foreland, Nunavut, Canada. *Arctic, Antarctic, and Alpine Research*, *40*(2), 287–297. https://doi.org/10.1657/1523-0430(06-098)[BREEN]2.0.CO;2

Brown, M. W., Heiss, A. A., Kamikawa, R., Inagaki, Y., Yabuki, A., Tice, A. K., Shiratori, T., Ishida, K.-I., Hashimoto, T., Simpson, A. G. B., & Roger, A. J. (2018). Phylogenomics Places Orphan Protistan Lineages in a Novel Eukaryotic Super-Group. *Genome Biology and Evolution*, *10*(2), 427–433. https://doi.org/10.1093/gbe/evy014

Brožová, V., Bolstad, J. S., Seregin, A. P., & Eidesen, P. B. (2023). From everywhere all at once: Several colonization routes available to Svalbard in the early Holocene. *Ecology and Evolution*, *13*(3), e9892. https://doi.org/10.1002/ece3.9892

Burian, A., Pinn, D., Peralta-Maraver, I., Sweet, M., Mauvisseau, Q., Eyice, O., Bulling, M., Röthig, T., & Kratina, P. (2022). Predation increases multiple components of microbial diversity in activated sludge communities. *The ISME Journal*, *16*(4), 1086–1094. https://doi.org/10.1038/s41396-021-01145-z

Burki, F., Roger, A. J., Brown, M. W., & Simpson, A. G. B. (2020). The New Tree of Eukaryotes. *Trends in Ecology & Evolution*, *35*(1), 43–55. https://doi.org/10.1016/j.tree.2019.08.008

Burki, F., Sandin, M. M., & Jamy, M. (2021). Diversity and ecology of protists revealed by metabarcoding. *Current Biology*, *31*(19), R1267–R1280. https://doi.org/10.1016/j.cub.2021.07.066

Burki, F., Shalchian-Tabrizi, K., Minge, M., Skjæveland, Å., Nikolaev, S. I., Jakobsen, K. S., & Pawlowski, J. (2007). Phylogenomics Reshuffles the Eukaryotic Supergroups. *PLoS ONE*, *2*(8), e790. https://doi.org/10.1371/journal.pone.0000790

Burnett, H. A., Bieker, V. C., Le Moullec, M., Peeters, B., Rosvold, J., Pedersen, Å. Ø., Dalén, L., Loe, L. E., Jensen, H., Hansen, B. B., & Martin, M. D. (2023). Contrasting genomic consequences of anthropogenic reintroduction and natural recolonization in high-arctic wild reindeer. *Evolutionary Applications*, eva.13585. https://doi.org/10.1111/eva.13585

Bystrykh, L. V. (2012). Generalized DNA Barcode Design Based on Hamming Codes. *PLoS ONE*, *7*(5), 8. https://doi.org/10.1371/journal.pone.0036852

Cadotte, M. W., Carscadden, K., & Mirotchnick, N. (2011). Beyond species: Functional diversity and the maintenance of ecological processes and services. *Journal of Applied Ecology*, *48*(5), 1079–1087. https://doi.org/10.1111/j.1365-2664.2011.02048.x

Camacho, C., Coulouris, G., Avagyan, V., Ma, N., Papadopoulos, J., Bealer, K., & Madden, T. L. (2009). BLAST+: Architecture and applications. *BMC Bioinformatics*, *10*(1), 421. https://doi.org/10.1186/1471-2105-10-421

Canini, F., Geml, J., D'Acqui, L. P., Selbmann, L., Onofri, S., Ventura, S., & Zucconi, L. (2020). Exchangeable cations and pH drive diversity and functionality of fungal communities in biological soil crusts from coastal sites of Victoria Land, Antarctica. *Fungal Ecology*, *45*, 100923. https://doi.org/10.1016/j.funeco.2020.100923

Caron, D. A., & Hu, S. K. (2019). Are We Overestimating Protistan Diversity in Nature? *Trends in Microbiology*, *27*(3), 197–205. https://doi.org/10.1016/j.tim.2018.10.009

Carvalhais, N., Forkel, M., Khomik, M., Bellarby, J., Jung, M., Migliavacca, M., Mu, M., Saatchi, S., Santoro, M., Thurner, M., Weber, U., Ahrens, B., Beer, C., Cescatti, A., Randerson, J. T., & Reichstein, M. (2014). Global covariation of carbon turnover times with climate in terrestrial ecosystems. *Nature*, *514*(7521), 213–217. https://doi.org/10.1038/nature13731

Cary, S., Mcdonald, I., Barrett, J., & Cowan, D. (2010). On the rocks: The microbiology of Antarctic dry valley soils. *Nature Reviews. Microbiology*, *8*, 129–138. https://doi.org/10.1038/nrmicro2281

Cavicchioli, R., Ripple, W. J., Timmis, K. N., Azam, F., Bakken, L. R., Baylis, M., Behrenfeld, M. J., Boetius, A., Boyd, P. W., Classen, A. T., Crowther, T. W., Danovaro, R., Foreman, C. M., Huisman, J., Hutchins, D. A., Jansson, J. K., Karl, D. M., Koskella, B., Mark Welch, D. B., … Webster, N. S. (2019). Scientists' warning to humanity: Microorganisms and climate change. *Nature Reviews Microbiology*, *17*(9), 569–586. https://doi.org/10.1038/s41579-019-0222-5

Chown, S. L., & Convey, P. (2007). Spatial and temporal variability across life's hierarchies in the terrestrial Antarctic. *Philosophical Transactions of the Royal Society B: Biological Sciences*, *362*(1488), 2307–2331. https://doi.org/10.1098/rstb.2006.1949

Chu, H., Gao, G.-F., Ma, Y., Fan, K., & Delgado-Baquerizo, M. (2020). Soil Microbial Biogeography in a Changing World: Recent Advances and Future Perspectives. *mSystems*, *5*(2), e00803-19. https://doi.org/10.1128/mSystems.00803-19

Colesie, C., Gommeaux, M., Green, T. G. A., & Büdel, B. (2014). Biological soil crusts in continental Antarctica: Garwood Valley, southern Victoria Land, and Diamond Hill, Darwin Mountains region. *Antarctic Science*, *26*(2), 115–123. https://doi.org/10.1017/S0954102013000291

Colesie, C., Green, T. G. A., Türk, R., Hogg, I. D., Sancho, L. G., & Büdel, B. (2014). Terrestrial biodiversity along the Ross Sea coastline, Antarctica: Lack of a latitudinal gradient and potential limits of bioclimatic modeling. *Polar Biology*, *37*(8), 1197–1208. https://doi.org/10.1007/s00300-014-1513-y

Colesie, C., Walshaw, C. V., Sancho, L. G., Davey, M. P., & Gray, A. (2023). Antarctica's vegetation in a changing climate. *WIREs Climate Change*, *14*(1), e810. https://doi.org/10.1002/wcc.810

Convey, P. (2010). Terrestrial biodiversity in Antarctica – Recent advances and future challenges. *Polar Science*, *4*(2), 135–147. https://doi.org/10.1016/j.polar.2010.03.003

Couwenberghe, R. van, Collet, C., Pierrat, J. C., Verheyen, K., & Gégout, J.-C. (2013). Can species distribution models be used to describe plant abundance patterns. *Ecography*, *36*, 665–674.

Darby, B., & Neher, D. (2016). *Microfauna Within Biological Soil Crusts* (pp. 139–157). https://doi.org/10.1007/978-3-319-30214-0_8

Darienko, T., & Pröschold, T. (2017). Toward a monograph of non-marine Ulvophyceae using an integrative approach (Molecular phylogeny and systematics of terrestrial Ulvophyceae II.). *Phytotaxa*, *324*(1), 1. https://doi.org/10.11646/phytotaxa.324.1.1

Deutschmann, I. M., Krabberød, A. K., Latorre, F., Delage, E., Marrasé, C., Balagué, V., Gasol, J. M., Massana, R., Eveillard, D., Chaffron, S., & Logares, R. (2023). Disentangling temporal associations in marine microbial networks. *Microbiome*, *11*(1), 83. https://doi.org/10.1186/s40168-023-01523-z

Deutschmann, I. M., Lima-Mendez, G., Krabberød, A. K., Raes, J., Vallina, S. M., Faust, K., & Logares, R. (2021). Disentangling environmental effects in microbial association networks. *Microbiome*, *9*(1), 232. https://doi.org/10.1186/s40168-021-01141-7

Dolgikh, A. V., Mergelov, N. S., Abramov, A. A., Lupachev, A. V., & Goryachkin, S. V. (2015). Soils of Enderby Land. In J. G. Bockheim (Ed.), *The Soils of Antarctica* (pp. 45–63). Springer International Publishing. https://doi.org/10.1007/978-3-319-05497-1_4

Dumack, K. (2017). *Novel Lineages in Cercozoa and Their Feeding Strategies*.

Dumack, K., Fiore-Donno, A. M., Bass, D., & Bonkowski, M. (2020). Making sense of environmental sequencing data: Ecologically important functional traits of the protistan groups Cercozoa and Endomyxa (Rhizaria). *Molecular Ecology Resources*, *20*(2), 398–403. https://doi.org/10.1111/1755-0998.13112

Dumack, K., Pundt, J., & Bonkowski, M. (2018). Food Choice Experiments Indicate Selective Fungivorous Predation in *Fisculla terrestris* (Thecofilosea, Cercozoa). *Journal of Eukaryotic Microbiology*, *66*(3), 525–527. https://doi.org/10.1111/jeu.12680

Edgar, R. C., Haas, B. J., Clemente, J. C., Quince, C., & Knight, R. (2011). UCHIME improves sensitivity and speed of chimera detection. *Bioinformatics*, *27*(16), 2194–2200. https://doi.org/10.1093/bioinformatics/btr381

Ettl, H., & Gärtner, G. (2014). *Syllabus der Boden-, Luft- und Flechtenalgen*. Springer Berlin Heidelberg. https://doi.org/10.1007/978-3-642-39462-1

Falkowski, P. (2012). Ocean Science: The power of plankton. *Nature*, *483*(7387), S17–S20. https://doi.org/10.1038/483S17a

Faust, K. (2021). Open challenges for microbial network construction and analysis. *The ISME Journal*, *15*(11), 3111–3118. https://doi.org/10.1038/s41396-021-01027-4

Faust, K., & Raes, J. (2012). Microbial interactions: From networks to models. *Nature Reviews Microbiology*, *10*(8), Article 8. https://doi.org/10.1038/nrmicro2832

Ferrenberg, S., Reed, S. C., & Belnap, J. (2015). Climate change and physical disturbance cause similar community shifts in biological soil crusts. *Proceedings of the National Academy of Sciences*, *112*(39), 12116–12121. https://doi.org/10.1073/pnas.1509150112

Fierer, N. (2017). Embracing the unknown: Disentangling the complexities of the soil microbiome. *Nature Reviews Microbiology*, *15*(10), 579–590. https://doi.org/10.1038/nrmicro.2017.87

Fiore-Donno, A. M., Richter-Heitmann, T., & Bonkowski, M. (2020). *Contrasting responses of protistan plant parasites and phagotrophs to ecosystems, land management and soil properties* [Preprint]. Ecology. https://doi.org/10.1101/2020.03.22.001768

Fiore-Donno, A. M., Rixen, C., Rippin, M., Glaser, K., Samolov, E., Karsten, U., Becker, B., & Bonkowski, M. (2018). New barcoded primers for efficient retrieval of cercozoan sequences in high-throughput environmental diversity surveys, with emphasis on worldwide biological

soil crusts. *Molecular Ecology Resources*, *18*(2), 229–239. https://doi.org/10.1111/1755-0998.12729

Foets, J., Stanek-Tarkowska, J., Teuling, A. J., Van de Vijver, B., Wetzel, C. E., & Pfister, L. (2021). Autecology of terrestrial diatoms under anthropic disturbance and across climate zones. *Ecological Indicators*, *122*, 107248. https://doi.org/10.1016/j.ecolind.2020.107248

Foissner, W. (2006). Biogeography and Dispersal of Micro-organisms: A Review Emphasizing Protists. *Acta Protozoologica*, *45*, 111–136.

Foissner, W. (2008). Protist diversity and distribution: Some basic considerations. *Biodiversity and Conservation*, *17*, 235–242. https://doi.org/10.1007/s10531-007-9248-5

Frank, D. N. (2009). BARCRAWL and BARTAB: Software tools for the design and implementation of barcoded primers for highly multiplexed DNA sequencing. *BMC Bioinformatics*, *10*(1), 362. https://doi.org/10.1186/1471-2105-10-362

Freckman, D. W., & Virginia, R. A. (1997). Low-Diversity Antarctic Soil Nematode Communities: Distribution and Response to Disturbance. *Ecology*, *78*(2), 363–369. https://doi.org/10.2307/2266013

Freilich, M. A., Wieters, E., Broitman, B. R., Marquet, P. A., & Navarrete, S. A. (2018). Species co-occurrence networks: Can they reveal trophic and non-trophic interactions in ecological communities? *Ecology*, *99*(3), 690–699. https://doi.org/10.1002/ecy.2142

Freudenthal, J., Ju, F., Bürgmann, H., & Dumack, K. (2022). Microeukaryotic gut parasites in wastewater treatment plants: Diversity, activity, and removal. *Microbiome*, *10*(1), 27. https://doi.org/10.1186/s40168-022-01225-y

Garrido-Benavent, I., Pérez-Ortega, S., Durán, J., Ascaso, C., Pointing, S. B., Rodríguez-Cielos, R., Navarro, F., & de los Ríos, A. (2020). Differential Colonization and Succession of Microbial Communities in Rock and Soil Substrates on a Maritime Antarctic Glacier Forefield. *Frontiers in Microbiology*, *11*. https://www.frontiersin.org/articles/10.3389/fmicb.2020.00126

Geisen, S. (2016). The bacterial-fungal energy channel concept challenged by enormous functional versatility of soil protists. *Soil Biology and Biochemistry*, *102*, 22–25. https://doi.org/10.1016/j.soilbio.2016.06.013

Geisen, S., Bandow, C., Römbke, J., & Bonkowski, M. (2014). Soil water availability strongly alters the community composition of soil protists. *Pedobiologia*, *57*(4), 205–213. https://doi.org/10.1016/j.pedobi.2014.10.001

Geisen, S., Hu, S., Dela Cruz, T. E. E., & Veen, G. F. (Ciska). (2021). Protists as catalyzers of microbial litter breakdown and carbon cycling at different temperature regimes. *The ISME Journal*, *15*(2), 618–621. https://doi.org/10.1038/s41396-020-00792-y

Geisen, S., Mitchell, E. A. D., Adl, S., Bonkowski, M., Dunthorn, M., Ekelund, F., Fernández, L. D., Jousset, A., Krashevska, V., Singer, D., Spiegel, F. W., Walochnik, J., & Lara, E. (2018). Soil protists: A fertile frontier in soil biology research. *FEMS Microbiology Reviews*, *42*(3), 293–323. https://doi.org/10.1093/femsre/fuy006

Giachello, S. (2023). Toward a common set of functional traits for soil protists. *Soil Biology and Biochemistry*.

Gloor, G. B., Macklaim, J. M., Pawlowsky-Glahn, V., & Egozcue, J. J. (2017). Microbiome Datasets Are Compositional: And This Is Not Optional. *Frontiers in Microbiology*, *8*, 2224. https://doi.org/10.3389/fmicb.2017.02224

Guillou, L., Bachar, D., Audic, S., Bass, D., Berney, C., Bittner, L., Boutte, C., Burgaud, G., de Vargas, C., Decelle, J., del Campo, J., Dolan, J. R., Dunthorn, M., Edvardsen, B., Holzmann, M., Kooistra, W. H. C. F., Lara, E., Le Bescot, N., Logares, R., … Christen, R. (2013). The Protist Ribosomal Reference database (PR2): A catalog of unicellular eukaryote Small Sub-Unit rRNA sequences with curated taxonomy. *Nucleic Acids Research*, *41*(D1), D597–D604. https://doi.org/10.1093/nar/gks1160

Guo, L., Sui, Z., Zhang, S., Ren, Y., & Liu, Y. (2015). Comparison of potential diatom 'barcode' genes (the 18S rRNA gene and ITS, COI, rbcL) and their effectiveness in discriminating and

determining species taxonomy in the Bacillariophyta. *International Journal of Systematic and Evolutionary Microbiology*, *65*(Pt_4), 1369–1380. https://doi.org/10.1099/ijs.0.000076

Gupta, G., Ndiaye, A., & Filteau, M. (2021). Leveraging Experimental Strategies to Capture Different Dimensions of Microbial Interactions. *Frontiers in Microbiology*, *12*. https://doi.org/10.3389/fmicb.2021.700752

Guseva, K., Darcy, S., Simon, E., Alteio, L. V., Montesinos-Navarro, A., & Kaiser, C. (2022). From diversity to complexity: Microbial networks in soils. *Soil Biology and Biochemistry*, *169*, 108604. https://doi.org/10.1016/j.soilbio.2022.108604

Hall, J., Fu, K., Lo, C., Lewis, L. A., & Karol, K. G. (2010). An assessment of proposed DNA barcodes in freshwater green algae. *Cryptogamie*, *31*(4), 529–555.

Hannon Laboratory. (2010). *FASTX-Toolkit*. http://hannonlab.cshl.edu/fastx_toolkit/index.html

Heinbokel, J. F. (1978). Studies on the functional role of tintinnids in the Southern California Bight. I. Grazing and growth rates in laboratory cultures. *Marine Biology*, *47*(2), 177–189. https://doi.org/10.1007/BF00395638

Henriques, D. K., Silva, B. G. C., Zuñiga, G. E., & Câmara, P. E. A. S. (2018). Contributions to the bryological knowledge of ASPA 125, Fildes Peninsula, King George Island. *Biological Research*, *51*(1), 29. https://doi.org/10.1186/s40659-018-0178-3

Hess, S., & Melkonian, M. (2014). Ultrastructure of the Algivorous Amoeboflagellate Viridiraptor invadens (Glissomonadida, Cercozoa). *Protist*, *165*(5), 605–635. https://doi.org/10.1016/j.protis.2014.07.004

Hiltunen, T., & Laakso, J. (2013). The relative importance of competition and predation in environment characterized by resource pulses – an experimental test with a microbial community. *BMC Ecology*, *13*(1), 29. https://doi.org/10.1186/1472-6785-13-29

Hodkinson, I. D., Coulson, S. J., & Webb, N. R. (2003). Community Assembly along Proglacial Chronosequences in the High Arctic: Vegetation and Soil Development in North-West Svalbard. *Journal of Ecology*, *91*(4), 651–663.

Howard, C., Stephens, P. A., Pearce-Higgins, J. W., Gregory, R. D., & Willis, S. G. (2014). Improving species distribution models: The value of data on abundance. *Methods in Ecology and Evolution*, *5*(6), 506–513. https://doi.org/10.1111/2041-210X.12184

Howe, A. T., Bass, D., Chao, E. E., & Cavalier-Smith, T. (2011). New Genera, Species, and Improved Phylogeny of Glissomonadida (Cercozoa). *Protist*, *162*(5), 710–722. https://doi.org/10.1016/j.protis.2011.06.002

Itter, M. S., Kaarlejärvi, E., Laine, A.-L., Hamberg, L., Tonteri, T., & Vanhatalo, J. (2024). Bayesian joint species distribution model selection for community-level prediction. *Global Ecology and Biogeography*, *33*(5), e13827. https://doi.org/10.1111/geb.13827

Jahnke, J., Wehren, T., & Priefer, U. B. (2007). In vitro studies of the impact of the naked soil amoeba Thecamoeba similis Greef, feeding on phototrophic soil biofilms. *European Journal of Soil Biology*, *43*(1), 14–22. https://doi.org/10.1016/j.ejsobi.2006.11.002

Jansson, J. K., & Hofmockel, K. S. (2020). Soil microbiomes and climate change. *Nature Reviews Microbiology*, *18*(1), 35–46. https://doi.org/10.1038/s41579-019-0265-7

Jensen, Ø. (2020). The Svalbard Treaty and Norwegian Sovereignty. *Arctic Review on Law and Politics*, *11*, 82–107. https://doi.org/10.23865/arctic.v11.2348

Ji, M., Kong, W., Jia, H., Delgado-Baquerizo, M., Zhou, T., Liu, X., Ferrari, B. C., Malard, L., Liang, C., Xue, K., Makhalanyane, T. P., Zhu, Y.-G., Wang, Y., Pearce, D. A., & Cowan, D. (2022). Polar soils exhibit distinct patterns in microbial diversity and dominant phylotypes. *Soil Biology and Biochemistry*, *166*, 108550. https://doi.org/10.1016/j.soilbio.2022.108550

Jiang, M.-Z., Liu, C., Xu, C., Jiang, H., Wang, Y., & Liu, S.-J. (2024). Gut microbial interactions based on network construction and bacterial pairwise cultivation. *Science China Life Sciences*. https://doi.org/10.1007/s11427-023-2537-0

Jiang, M.-Z., Zhu, H.-Z., Zhou, N., Liu, C., Jiang, C.-Y., Wang, Y., & Liu, S.-J. (2022). Droplet microfluidics-based high-throughput bacterial cultivation for validation of taxon pairs in

microbial co-occurrence networks. *Scientific Reports*, *12*(1), 18145. https://doi.org/10.1038/s41598-022-23000-7

Jiang, Y., Li, S., Barnes, A. D., Liu, J., Zhu, G., Luan, L., Dini-Andreote, F., Geisen, S., & Sun, B. (2023). Unraveling the importance of top-down predation on bacterial diversity at the soil aggregate level. *Geoderma*, *439*, 116658. https://doi.org/10.1016/j.geoderma.2023.116658

Johansen, B. E., Karlsen, S. R., & Tømmervik, H. (2012). Vegetation mapping of Svalbard utilising Landsat TM/ETM+ data. *Polar Record*, *48*(1), 47–63. https://doi.org/10.1017/S0032247411000647

Johnston, A., Fink, D., Reynolds, M. D., Hochachka, W. M., Sullivan, B. L., Bruns, N. E., Hallstein, E., Merrifield, M. S., Matsumoto, S., & Kelling, S. (2015). Abundance models improve spatial and temporal prioritization of conservation resources. *Ecological Applications*, *25*(7), 1749–1756. https://doi.org/10.1890/14-1826.1

Kassambara, A. (2023a). *rstatix: Pipe-Friendly Framework for Basic Statistical Tests* (Version 0.7.2) [Computer software]. https://cran.r-project.org/web/packages/rstatix/index.html

Kassambara, A. (2023b). *ggpubr: "ggplot2" Based Publication Ready Plots* (Version 0.6.0) [Computer software]. https://cran.r-project.org/web/packages/ggpubr/index.html

Katoh, K., & Standley, D. M. (2013). MAFFT Multiple Sequence Alignment Software Version 7: Improvements in Performance and Usability. *Molecular Biology and Evolution*, *30*(4), 772–780. https://doi.org/10.1093/molbev/mst010

Keeling, P. J., Burger, G., Durnford, D. G., Lang, B. F., Lee, R. W., Pearlman, R. E., Roger, A. J., & Gray, M. W. (2005). The tree of eukaryotes. *Trends in Ecology & Evolution*, *20*(12), 670–676. https://doi.org/10.1016/j.tree.2005.09.005

Kellogg, C. T. E., McClelland, J. W., Dunton, K. H., & Crump, B. C. (2019). Strong Seasonality in Arctic Estuarine Microbial Food Webs. *Frontiers in Microbiology*, *10*, 2628. https://doi.org/10.3389/fmicb.2019.02628

Khanipour Roshan, S., Dumack, K., Bonkowski, M., Leinweber, P., Karsten, U., & Glaser, K. (2021). Taxonomic and Functional Diversity of Heterotrophic Protists (Cercozoa and Endomyxa) from Biological Soil Crusts. *Microorganisms*, *9*(2), 205. https://doi.org/10.3390/microorganisms9020205

Kleinteich, J., Hildebrand, F., Bahram, M., Voigt, A. Y., Wood, S. A., Jungblut, A. D., Küpper, F. C., Quesada, A., Camacho, A., Pearce, D. A., Convey, P., Vincent, W. F., Zarfl, C., Bork, P., & Dietrich, D. R. (2017). Pole-to-Pole Connections: Similarities between Arctic and Antarctic Microbiomes and Their Vulnerability to Environmental Change. *Frontiers in Ecology and Evolution*, *5*, 137. https://doi.org/10.3389/fevo.2017.00137

Klimešová, J., Prach, K., & Bernardová, A. (2012). Using Available Information to Assess the Potential Effects of Climate Change on Vegetation in the High Arctic: North Billjefjorden, Central Spitsbergen (Svalbard). *AMBIO*, *41*(5), 435–445. https://doi.org/10.1007/s13280-011-0235-4

Klindworth, A., Pruesse, E., Schweer, T., Peplies, J., Quast, C., Horn, M., & Glöckner, F. O. (2013). Evaluation of general 16S ribosomal RNA gene PCR primers for classical and next-generation sequencing-based diversity studies. *Nucleic Acids Research*, *41*(1), e1–e1. https://doi.org/10.1093/nar/gks808

Kuehn, K. A., Francoeur, S. N., Findlay, R. H., & Neely, R. K. (2014). Priming in the microbial landscape: Periphytic algal stimulation of litter-associated microbial decomposers. *Ecology*, *95*(3), 749–762. https://doi.org/10.1890/13-0430.1

Larsson, J., Godfrey, A. J. R., Gustafsson, P., algorithms), D. H. E. (geometric, code), E. H. (root solver, & Privé, F. (2022). *eulerr: Area-Proportional Euler and Venn Diagrams with Ellipses* (Version 7.0.0) [Computer software]. https://cran.r-project.org/web/packages/eulerr/index.html

Lee, J. R., Raymond, B., Bracegirdle, T. J., Chadès, I., Fuller, R. A., Shaw, J. D., & Terauds, A. (2017). Climate change drives expansion of Antarctic ice-free habitat. *Nature*, *547*(7661), 49–54. https://doi.org/10.1038/nature22996

Lee, K. K., Kim, H., & Lee, Y.-H. (2022). Cross-kingdom co-occurrence networks in the plant microbiome: Importance and ecological interpretations. *Frontiers in Microbiology*, *13*, 953300. https://doi.org/10.3389/fmicb.2022.953300

Lee, S.-R., Oak, J. H., Chung, I. K., & Lee, J. A. (2010). Effective molecular examination of eukaryotic plankton species diversity in environmental seawater using environmental PCR, PCR-RFLP, and sequencing. *J Appl Phycol*, *9*.

Letunic, I., & Bork, P. (2021). Interactive Tree Of Life (iTOL) v5: An online tool for phylogenetic tree display and annotation. *Nucleic Acids Research*, *49*(W1), W293–W296. https://doi.org/10.1093/nar/gkab301

Levins, R., & Schultz, B. B. (1996). Effects of Density Dependence, Feedback and Environmental Sensitivity on Correlations Among Predators, Prey and Plant Resources: Models and Practical Implications. *Journal of Animal Ecology*, *65*(6), 802–812. JSTOR. https://doi.org/10.2307/5678

Li, X.-R., Jia, R.-L., Zhang, Z.-S., Zhang, P., & Hui, R. (2018). Hydrological response of biological soil crusts to global warming: A ten-year simulative study. *Global Change Biology*, *24*(10), 4960–4971. https://doi.org/10.1111/gcb.14378

Lima-Mendez, G., Faust, K., Henry, N., Decelle, J., Colin, S., Carcillo, F., Chaffron, S., Ignacio-Espinosa, J. C., Roux, S., Vincent, F., Bittner, L., Darzi, Y., Wang, J., Audic, S., Berline, L., Bontempi, G., Cabello, A. M., Coppola, L., Cornejo-Castillo, F. M., … Raes, J. (2015). Determinants of community structure in the global plankton interactome. *Science*, *348*(6237), 1262073. https://doi.org/10.1126/science.1262073

Logares, R., Audic, S., Bass, D., Bittner, L., Boutte, C., Christen, R., Claverie, J.-M., Decelle, J., Dolan, J. R., Dunthorn, M., Edvardsen, B., Gobet, A., Kooistra, W. H. C. F., Mahé, F., Not, F., Ogata, H., Pawlowski, J., Pernice, M. C., Romac, S., … Massana, R. (2014). Patterns of Rare and Abundant Marine Microbial Eukaryotes. *Current Biology*, *24*(8), 813–821. https://doi.org/10.1016/j.cub.2014.02.050

Lukashanets, D. A., Convey, P., Borodin, O. I., Miamin, V. Y., Hihiniak, Y. H., Gaydashov, A. A., Yatsyna, A. P., Vezhnavets, V. V., Maysak, N. N., & Shendrik, T. V. (2021). Eukarya biodiversity in the Thala Hills, East Antarctica. *Antarctic Science*, *33*(6), 605–623. https://doi.org/10.1017/S0954102021000328

Lukešová, A. (1991). Three filamentous green algae isolated from soil. *Archiv Für Protistenkunde*, *139*(1–4), 69–83. https://doi.org/10.1016/S0003-9365(11)80009-6

Lupachev, A. V., Abakumov, E. V., Goryachkin, S. V., & Veremeeva, A. A. (2020). Soil cover of the Fildes Peninsula (King George Island, West Antarctica). *CATENA*, *193*, 104613. https://doi.org/10.1016/j.catena.2020.104613

Lynn, D. H. (2008). The ciliated protozoa: Characterization, classification, and guide to the literature: Third edition. In *The Ciliated Protozoa: Characterization, Classification, and Guide to the Literature: Third Edition* (p. 605). https://doi.org/10.1007/978-1-4020-8239-9

Lyu, Z., Sommers, P., Schmidt, S. K., Magnani, M., Cimpoiasu, M., Kuras, O., Zhuang, Q., Oh, Y., De La Fuente, M., Cramm, M., & Bradley, J. A. (2024). Seasonal dynamics of Arctic soils: Capturing year-round processes in measurements and soil biogeochemical models. *Earth-Science Reviews*, *254*, 104820. https://doi.org/10.1016/j.earscirev.2024.104820

Maestre, F., Bowker, M., Eldridge, D., Cortina, J., Lazaro, R., Gallardo, A., Delgado-Baquerizo, M., Berdugo, M., Castillo-Monroy, A. P., & Valencia, E. (2016). *Biological Soil Crusts as a Model System in Ecology* (pp. 407–425). https://doi.org/10.1007/978-3-319-30214-0_20

Martin, W. F., Tielens, A. G. M., Mentel, M., Garg, S. G., & Gould, S. B. (2017). The Physiology of Phagocytosis in the Context of Mitochondrial Origin. *Microbiology and Molecular Biology Reviews*, *81*(3), e00008-17. https://doi.org/10.1128/MMBR.00008-17

Matchado, M. S., Lauber, M., Reitmeier, S., Kacprowski, T., Baumbach, J., Haller, D., & List, M. (2021). Network analysis methods for studying microbial communities: A mini review. *Computational and Structural Biotechnology Journal*, *19*, 2687–2698. https://doi.org/10.1016/j.csbj.2021.05.001

McCann, K. S. (2000). The diversity–stability debate. *Nature*, *405*(6783), 228–233. https://doi.org/10.1038/35012234

Mcfadden, G., & Melkonian, M. (1986). Use of HEPES buffer for microalgal culture media and fixation for electron microscopy. *Phycologia*, *25*, 551–557. https://doi.org/10.2216/i0031-8884-25-4-551.1

Michel, R., Schaefer, C., López-Martínez, J., Simas, F., Haus, N., Serrano, E., & Bockheim, J. (2014). Soils and landforms from Fildes Peninsula and Ardley Island, Maritime Antarctica. *Geomorphology*, *225*, 76–86. https://doi.org/10.1016/j.geomorph.2014.03.041

Miner, K. R., Turetsky, M. R., Malina, E., Bartsch, A., Tamminen, J., McGuire, A. D., Fix, A., Sweeney, C., Elder, C. D., & Miller, C. E. (2022). Permafrost carbon emissions in a changing Arctic. *Nature Reviews Earth & Environment*, *3*(1), 55–67. https://doi.org/10.1038/s43017-021-00230-3

Mugnai, G., Pinchuk, I., Borruso, L., Tiziani, R., Sannino, C., Canini, F., Turchetti, B., Mimmo, T., Zucconi, L., & Buzzini, P. (2024). The hidden network of biocrust successional stages in the High Arctic: Revealing abiotic and biotic factors shaping microbial and metazoan communities. *Science of The Total Environment*, *926*, 171786. https://doi.org/10.1016/j.scitotenv.2024.171786

Mugnai, G., Rossi, F., Mascalchi, C., Ventura, S., & De Philippis, R. (2020). High Arctic biocrusts: Characterization of the exopolysaccharidic matrix. *Polar Biology*, *43*(11), 1805–1815. https://doi.org/10.1007/s00300-020-02746-8

Naylor, D., Sadler, N., Bhattacharjee, A., Graham, E. B., Anderton, C. R., McClure, R., Lipton, M., Hofmockel, K. S., & Jansson, J. K. (2020). Soil Microbiomes Under Climate Change and Implications for Carbon Cycling. *Annual Review of Environment and Resources*, *45*(1), 29–59. https://doi.org/10.1146/annurev-environ-012320-082720

Neuwirth, E. (2022). *RColorBrewer: ColorBrewer Palettes*.

Nguyen, T. B.-A., Bonkowski, M., Dumack, K., Chen, Q.-L., He, J.-Z., & Hu, H.-W. (2023). Protistan predation selects for antibiotic resistance in soil bacterial communities. *The ISME Journal*, *17*(12), 2182–2189. https://doi.org/10.1038/s41396-023-01524-8

Nielsen, S. E., Johnson, C. J., Heard, D. C., & Boyce, M. S. (2005). Can models of presence-absence be used to scale abundance? Two case studies considering extremes in life history. *Ecography*, *28*, 197–208.

NOAA National Centers for Environmental Information (NCEI). (n.d.). *Global Surface Summary of the Day—GSOD 1.0. Bellinghausen Station, King George Island*. Retrieved September 25, 2023, from https://www.ncei.noaa.gov/access/metadata/landing-page/bin/iso?id=gov.noaa.ncdc:C00516

Norwegian Meteorological Institute. (2022, April 11). *Annual precipitation in Svalbard, Hopen, Bjørnøya and Jan Mayen, filtered*. MOSJ. https://mosj.no/en/indikator/climate/atmosphere/air-temperature-and-precipitation/

Obbels, D., Verleyen, E., Mano, M.-J., Namsaraev, Z., Sweetlove, M., Tytgat, B., Fernandez-Carazo, R., De Wever, A., D'hondt, S., Ertz, D., Elster, J., Sabbe, K., Willems, A., Wilmotte, A., & Vyverman, W. (2016). Bacterial and eukaryotic biodiversity patterns in terrestrial and aquatic habitats in the Sør Rondane Mountains, Dronning Maud Land, East Antarctica. *FEMS Microbiology Ecology*, *92*(6), fiw041. https://doi.org/10.1093/femsec/fiw041

Odriozola, I., Abrego, N., TlÁskal, V., ZrůstovÁ, P., Morais, D., Větrovský, T., Ovaskainen, O., & Baldrian, P. (2021). Fungal Communities Are Important Determinants of Bacterial Community Composition in Deadwood. *mSystems*, *6*(1), e01017-20. https://doi.org/10.1128/mSystems.01017-20

Ohtani, S., Suyama, K., Yamamoto, H., & Aridomi, Y. (2000). *Distribution of soil algae at the monitoring sites in the vicinity of Syowa Station between austral summers of 1992/1993 and 1997/1998*.

Okonechnikov, K., Golosova, O., Fursov, M., & the UGENE team. (2012). Unipro UGENE: A unified bioinformatics toolkit. *Bioinformatics*, *28*(8), 1166–1167. https://doi.org/10.1093/bioinformatics/bts091

Oksanen, J., Simpson, G. L., Blanchet, F. G., Kindt, R., Legendre, P., Minchin, P. R., O'Hara, R. B., Solymos, P., Stevens, M. H. H., Szoecs, E., Wagner, H., Barbour, M., Bedward, M., Bolker, B., Borcard, D., Carvalho, G., Chirico, M., Caceres, M. D., Durand, S., … Weedon, J. (2022). *vegan: Community Ecology Package* (Version 2.6-4) [Computer software]. https://cran.r-project.org/web/packages/vegan/index.html

Oliverio, A. M., Geisen, S., Delgado-Baquerizo, M., Maestre, F. T., Turner, B. L., & Fierer, N. (2020). The global-scale distributions of soil protists and their contributions to belowground systems. *Science Advances*, *6*(4), eaax8787. https://doi.org/10.1126/sciadv.aax8787

O'Malley, M. A., Simpson, A. G. B., & Roger, A. J. (2013). The other eukaryotes in light of evolutionary protistology. *Biology & Philosophy*, *28*(2), 299–330. https://doi.org/10.1007/s10539-012-9354-y

Ovaskainen, O., & Abrego, N. (2020). *Joint Species Distribution Modelling: With Applications in R*. Cambridge University Press; Cambridge Core. https://doi.org/10.1017/9781108591720

Øvstedal, D., Tønsberg, T., & Elvebakk, A. (2009). The lichen flora of Svalbard. *Sommerfeltia*, *33*(1), 3–393. https://doi.org/10.2478/v10208-011-0013-5

Pacheco, A. R., & Segrè, D. (2019). A multidimensional perspective on microbial interactions. *FEMS Microbiology Letters*, *366*(11), fnz125. https://doi.org/10.1093/femsle/fnz125

Pasik, M., Bakuła, K., Różycki, S., Ostrowski, W., Kowalska, M., Fijałkowska, A., Rajner, M., Łapiński, S., Sobota, I., Kejna, M., & Osińska-Skotak, K. (2021). Glacier Geometry Changes in the Western Shore of Admiralty Bay, King George Island over the Last Decades. *Sensors*, *21*, 1532. https://doi.org/10.3390/s21041532

Pawlowski, J. (2000). Introduction to the Molecular Systematics of Foraminifera. *Micropaleontology*, *46*, 1–12.

Pawlowski, J. (2014). Protist Evolution and Phylogeny. In *eLS*. John Wiley & Sons, Ltd. https://doi.org/10.1002/9780470015902.a0001935.pub2

Pawlowski, J., Audic, S., Adl, S., Bass, D., Belbahri, L., Berney, C., Bowser, S. S., Cepicka, I., Decelle, J., Dunthorn, M., Fiore-Donno, A. M., Gile, G. H., Holzmann, M., Jahn, R., Jirků, M., Keeling, P. J., Kostka, M., Kudryavtsev, A., Lara, E., … de Vargas, C. (2012). CBOL Protist Working Group: Barcoding Eukaryotic Richness beyond the Animal, Plant, and Fungal Kingdoms. *PLoS Biology*, *10*(11), e1001419. https://doi.org/10.1371/journal.pbio.1001419

Philippot, L., Chenu, C., Kappler, A., Rillig, M. C., & Fierer, N. (2024). The interplay between microbial communities and soil properties. *Nature Reviews Microbiology*, *22*(4), 226–239. https://doi.org/10.1038/s41579-023-00980-5

Potapov, A. M., Beaulieu, F., Birkhofer, K., Bluhm, S. L., Degtyarev, M. I., Devetter, M., Goncharov, A. A., Gongalsky, K. B., Klarner, B., Korobushkin, D. I., Liebke, D. F., Maraun, M., Mc Donnell, R. J., Pollierer, M. M., Schaefer, I., Shrubovych, J., Semenyuk, I. I., Sendra, A., Tuma, J., … Scheu, S. (2022). Feeding habits and multifunctional classification of soil-associated consumers from protists to vertebrates. *Biological Reviews*, *97*(3), 1057–1117. https://doi.org/10.1111/brv.12832

Potapov, V., & Ong, J. L. (2017). Examining Sources of Error in PCR by Single-Molecule Sequencing. *PLOS ONE*, 19.

Power, S. N., Thomas, V. A., Salvatore, M. R., & Barrett, J. E. (2024). Habitat suitability of biocrust communities in a cold desert ecosystem. *Ecology and Evolution*, *14*(7), e11649. https://doi.org/10.1002/ece3.11649

Prestø, T., Lueth, M., & Hassel, K. (2014). *Bryophytes of the Longyearbyen area*. https://doi.org/10.13140/RG.2.1.2426.7600

Pushkareva, E., Baumann, K., Van, A. T., Mikhailyuk, T., Baum, C., Hrynkiewicz, K., Demchenko, E., Thiem, D., Köpcke, T., Karsten, U., & Leinweber, P. (2021). Diversity of microbial phototrophs

and heterotrophs in Icelandic biocrusts and their role in phosphorus-rich Andosols. *Geoderma*, *386*, 114905. https://doi.org/10.1016/j.geoderma.2020.114905

Pushkareva, E., Elster, J., Holzinger, A., Niedzwiedz, S., & Becker, B. (2022). Biocrusts from Iceland and Svalbard: Does microbial community composition differ substantially? *Frontiers in Microbiology*, *13*, 1048522. https://doi.org/10.3389/fmicb.2022.1048522

Pushkareva, E., Elster, J., Kudoh, S., Imura, S., & Becker, B. (2024). Microbial community composition of terrestrial habitats in East Antarctica with a focus on microphototrophs. *Frontiers in Microbiology*, *14*, 1323148. https://doi.org/10.3389/fmicb.2023.1323148

Pushkareva, E., Johansen, J. R., & Elster, J. (2016). A review of the ecology, ecophysiology and biodiversity of microalgae in Arctic soil crusts. *Polar Biology*, *39*(12), 2227–2240. https://doi.org/10.1007/s00300-016-1902-5

R Core Team. (2023). *R: The R Project for Statistical Computing*. https://www.r-project.org/

Reed, S. C., Maestre, F. T., Ochoa-Hueso, R., Kuske, C. R., Darrouzet-Nardi, A., Oliver, M., Darby, B., Sancho, L. G., Sinsabaugh, R. L., & Belnap, J. (2016). Biocrusts in the Context of Global Change. In B. Weber, B. Büdel, & J. Belnap (Eds.), *Biological Soil Crusts: An Organizing Principle in Drylands* (pp. 451–476). Springer International Publishing. https://doi.org/10.1007/978-3-319-30214-0_22

Rimet, F., Gusev, E., Kahlert, M., Kelly, M. G., Kulikovskiy, M., Maltsev, Y., Mann, D. G., Pfannkuchen, M., Trobajo, R., Vasselon, V., Zimmermann, J., & Bouchez, A. (2019). Diat.barcode, an open-access curated barcode library for diatoms. *Scientific Reports*, *9*(1), Article 1. https://doi.org/10.1038/s41598-019-51500-6

Rippin. (2018). *Biological Soil Crust Microalgae and Cyanobacteria Key Players in Polar and Alpine Ecosystems*.

Rippin, M., Borchhardt, N., Williams, L., Colesie, C., Jung, P., Büdel, B., Karsten, U., & Becker, B. (2018). Genus richness of microalgae and Cyanobacteria in biological soil crusts from

Svalbard and Livingston Island: Morphological versus molecular approaches. *Polar Biology*, *41*(5), 909–923. https://doi.org/10.1007/s00300-018-2252-2

Rippin, M., Lange, S., Sausen, N., & Becker, B. (2018). Biodiversity of biological soil crusts from the Polar Regions revealed by metabarcoding. *FEMS Microbiology Ecology*, *94*(fiy036). https://doi.org/10.1093/femsec/fiy036

Rodriguez-Caballero, E., Belnap, J., Büdel, B., Crutzen, P. J., Andreae, M. O., Pöschl, U., & Weber, B. (2018). Dryland photoautotrophic soil surface communities endangered by global change. *Nature Geoscience*, *11*(3), 185–189. https://doi.org/10.1038/s41561-018-0072-1

Rognes, T., Flouri, T., Nichols, B., Quince, C., & Mahé, F. (2016). VSEARCH: A versatile open source tool for metagenomics. *PeerJ*, *4*, e2584. https://doi.org/10.7717/peerj.2584

Romanowicz, K. J., & Kling, G. W. (2022). Summer thaw duration is a strong predictor of the soil microbiome and its response to permafrost thaw in arctic tundra. *Environmental Microbiology*, *24*(12), 6220–6237. https://doi.org/10.1111/1462-2920.16218

Röttjers, L., Vandeputte, D., Raes, J., & Faust, K. (2021). Null-model-based network comparison reveals core associations. *ISME Communications*, *1*(1), 1–8. https://doi.org/10.1038/s43705-021-00036-w

Ryšánek, D., Hrčková, K., & Škaloud, P. (2015). Global ubiquity and local endemism of free-living terrestrial protists: Phylogeographic assessment of the streptophyte alga lebsormidium. *Environmental Microbiology*, *17*(3), 689–698. https://doi.org/10.1111/1462-2920.12501

Saleem, M., Fetzer, I., Harms, H., & Chatzinotas, A. (2013). Diversity of protists and bacteria determines predation performance and stability. *The ISME Journal*, *7*(10), 1912–1921. https://doi.org/10.1038/ismej.2013.95

Schloss, P. D., & Handelsman, J. (2006). Toward a Census of Bacteria in Soil. *PLoS Computational Biology*, *2*(7), e92. https://doi.org/10.1371/journal.pcbi.0020092

Schloss, P. D., Westcott, S. L., Ryabin, T., Hall, J. R., Hartmann, M., Hollister, E. B., Lesniewski, R. A., Oakley, B. B., Parks, D. H., Robinson, C. J., Sahl, J. W., Stres, B., Thallinger, G. G., Horn, D. J.

V., & Weber, C. F. (2009). Introducing mothur: Open-Source, Platform-Independent, Community-Supported Software for Describing and Comparing Microbial Communities. *Applied and Environmental Microbiology*, *75*(23), 7537–7541. https://doi.org/10.1128/AEM.01541-09

Schuur, E. A. G., McGuire, A. D., Schädel, C., Grosse, G., Harden, J. W., Hayes, D. J., Hugelius, G., Koven, C. D., Kuhry, P., Lawrence, D. M., Natali, S. M., Olefeldt, D., Romanovsky, V. E., Schaefer, K., Turetsky, M. R., Treat, C. C., & Vonk, J. E. (2015). Climate change and the permafrost carbon feedback. *Nature*, *520*(7546), 171–179. https://doi.org/10.1038/nature14338

Seppey, C. V. W., Singer, D., Dumack, K., Fournier, B., Belbahri, L., Mitchell, E. A. D., & Lara, E. (2017). Distribution patterns of soil microbial eukaryotes suggests widespread algivory by phagotrophic protists as an alternative pathway for nutrient cycling. *Soil Biology and Biochemistry*, *112*, 68–76. https://doi.org/10.1016/j.soilbio.2017.05.002

Severgnini, M., Canini, F., Consolandi, C., Camboni, T., Paolo D'Acqui, L., Mascalchi, C., Ventura, S., & Zucconi, L. (2021). Highly differentiated soil bacterial communities in Victoria Land macro-areas (Antarctica). *FEMS Microbiology Ecology*, *97*(7), fiab087. https://doi.org/10.1093/femsec/fiab087

Shang, Y., Sikorski, J., Bonkowski, M., Fiore-Donno, A.-M., Kandeler, E., Marhan, S., Boeddinghaus, R. S., Solly, E. F., Schrumpf, M., Schöning, I., Wubet, T., Buscot, F., & Overmann, J. (2017). Inferring interactions in complex microbial communities from nucleotide sequence data and environmental parameters. *PLOS ONE*, *12*(3), e0173765. https://doi.org/10.1371/journal.pone.0173765

Shannon, P., Markiel, A., Ozier, O., Baliga, N. S., Wang, J. T., Ramage, D., Amin, N., Schwikowski, B., & Ideker, T. (2003). Cytoscape: A Software Environment for Integrated Models of Biomolecular Interaction Networks. *Genome Research*, *13*(11), 2498–2504. https://doi.org/10.1101/gr.1239303

Shokralla, S., Spall, J. L., Gibson, J. F., & Hajibabaei, M. (2012). Next-generation sequencing technologies for environmental DNA research. *Molecular Ecology*, *21*(8), 1794–1805. https://doi.org/10.1111/j.1365-294X.2012.05538.x

Simoes, C. L., Rosa, K. K. D., Czapela, F. F., Vieira, R., & Simoes, J. C. (2015). Collins Glacier Retreat Process and Regional Climatic Variations, King George Island, Antarctica. *Geographical Review*, *105*(4), 462–471. https://doi.org/10.1111/j.1931-0846.2015.12091.x

Simpson, A. G. B., & Roger, A. J. (2002). Eukaryotic Evolution: Getting to the Root of the Problem. *Current Biology*, *12*(20), R691–R693. https://doi.org/10.1016/S0960-9822(02)01207-1

Simpson, A. G. B., Slamovits, C. H., & Archibald, J. M. (2017). Protist Diversity and Eukaryote Phylogeny. In J. M. Archibald, A. G. B. Simpson, C. H. Slamovits, L. Margulis, M. Melkonian, D. J. Chapman, & J. O. Corliss (Eds.), *Handbook of the Protists* (pp. 1–21). Springer International Publishing. https://doi.org/10.1007/978-3-319-32669-6_45-1

Singer, D., Seppey, C. V. W., Lentendu, G., Dunthorn, M., Bass, D., Belbahri, L., Blandenier, Q., Debroas, D., de Groot, G. A., de Vargas, C., Domaizon, I., Duckert, C., Izaguirre, I., Koenig, I., Mataloni, G., Schiaffino, M. R., Mitchell, E. A. D., Geisen, S., & Lara, E. (2021). Protist taxonomic and functional diversity in soil, freshwater and marine ecosystems. *Environment International*, *146*, 106262. https://doi.org/10.1016/j.envint.2020.106262

Singh, B. K., Bardgett, R. D., Smith, P., & Reay, D. S. (2010). Microorganisms and climate change: Terrestrial feedbacks and mitigation options. *Nature Reviews Microbiology*, *8*(11), 779–790. https://doi.org/10.1038/nrmicro2439

Slowikowski, K., Schep, A., Hughes, S., Dang, T. K., Lukauskas, S., Irisson, J.-O., Kamvar, Z. N., Ryan, T., Christophe, D., Hiroaki, Y., Gramme, P., Abdol, A. M., Barrett, M., Cannoodt, R., Krassowski, M., Chirico, M., Aphalo, P., & Barton, F. (2024). *ggrepel: Automatically Position Non-Overlapping Text Labels with "ggplot2"* (Version 0.9.5) [Computer software]. https://cran.r-project.org/web/packages/ggrepel/index.html

So, J. E., Halda, J. P., Hong, S. G., Hur, J.-S., & Kim, J. H. (2023). The Revision of Lichen Flora Around Maxwell Bay, King George Island, Maritime Antarctic. *Journal of Microbiology*, *61*(2), 159–173. https://doi.org/10.1007/s12275-023-00015-x

Souffreau, C., Vanormelingen, P., Sabbe, K., & Vyverman, W. (2013). Tolerance of resting cells of freshwater and terrestrial benthic diatoms to experimental desiccation and freezing is habitat-dependent. *Phycologia*, *52*, 246–255. https://doi.org/10.2216/12-087.1

Stamatakis, A. (2014). RAxML version 8: A tool for phylogenetic analysis and post-analysis of large phylogenies. *Bioinformatics*, *30*(9), 1312–1313. https://doi.org/10.1093/bioinformatics/btu033

Steven, B., Lionard, M., Kuske, C. R., & Vincent, W. F. (2013). High Bacterial Diversity of Biological Soil Crusts in Water Tracks over Permafrost in the High Arctic Polar Desert. *PLoS ONE*, *8*(8), e71489. https://doi.org/10.1371/journal.pone.0071489

Stoeck, T., Bass, D., Nebel, M., Christen, R., Jones, M. D. M., Breiner, H.-W., & Richards, T. A. (2010). Multiple marker parallel tag environmental DNA sequencing reveals a highly complex eukaryotic community in marine anoxic water. *Molecular Ecology*, *19*(s1), 21–31. https://doi.org/10.1111/j.1365-294X.2009.04480.x

Tackmann, J., Matias Rodrigues, J. F., & von Mering, C. (2019). Rapid Inference of Direct Interactions in Large-Scale Ecological Networks from Heterogeneous Microbial Sequencing Data. *Cell Systems*, *9*(3), 286-296.e8. https://doi.org/10.1016/j.cels.2019.08.002

Thompson, A. R. (2021). Phagotrophic protists (protozoa) in Antarctic terrestrial ecosystems: Diversity, distribution, ecology, and best research practices. *Polar Biology*. https://doi.org/10.1007/s00300-021-02896-3

Thompson, A. R., Geisen, S., & Adams, B. J. (2020). Shotgun metagenomics reveal a diverse assemblage of protists in a model Antarctic soil ecosystem. *Environmental Microbiology*, *22*(11), 4620–4632. https://doi.org/10.1111/1462-2920.15198

Tikhonov, G., Opedal, Ø. H., Abrego, N., Lehikoinen, A., de Jonge, M. M. J., Oksanen, J., & Ovaskainen, O. (2020). Joint species distribution modelling with the r-package Hmsc. *Methods in Ecology and Evolution*, *11*(3), 442–447. https://doi.org/10.1111/2041-210X.13345

Tikhonov, G., Opedal, Ø. H., Abrego, N., Lehikoinen, A., M. J. de Jonge, M., Oksanen, J., & Ovaskainen, O. (2022). *Hmsc 3.0: Getting started with Hmsc: Univariate models* [Software Vignette]. Cran R Project. https://cran.r-project.org/web/packages/Hmsc/vignettes/vignette_1_univariate.pdf

Tikhonov, G., Ovaskainen, O., Oksanen, J., Jonge, M. de, Opedal, O., & Dallas, T. (2022). *Hmsc: Hierarchical Model of Species Communities* (Version 3.0-13) [Computer software]. https://cran.r-project.org/web/packages/Hmsc/index.html

Tragin, M., Zingone, A., & Vaulot, D. (2018). Comparison of coastal phytoplankton composition estimated from the V4 and V9 regions of the 18S rRNA gene with a focus on photosynthetic groups and especially Chlorophyta. *Environmental Microbiology*, *20*(2), 506–520. https://doi.org/10.1111/1462-2920.13952

Treseder, K. K., & Lennon, J. T. (2015). Fungal Traits That Drive Ecosystem Dynamics on Land. *Microbiology and Molecular Biology Reviews*, *79*(2), 243–262. https://doi.org/10.1128/MMBR.00001-15

Van Borm, S., & Boomsma, J. J. (2002). Group-specific polymerase chain reaction amplification of SSU rRNA-encoding gene fragments from 12 microbial taxa. *Molecular Ecology Notes*, *2*(3), 356–359. https://doi.org/10.1046/j.1471-8286.2002.00248.x

Velázquez, D., Jungblut, A. D., Rochera, C., Rico, E., Camacho, A., & Quesada, A. (2017). Trophic interactions in microbial mats on Byers Peninsula, maritime Antarctica. *Polar Biology*, *40*(5), 1115–1126. https://doi.org/10.1007/s00300-016-2039-2

Venter, P. C., Nitsche, F., Domonell, A., Heger, P., & Arndt, H. (2017). The Protistan Microbiome of Grassland Soil: Diversity in the Mesoscale. *Protist*, *168*(5), 546–564. https://doi.org/10.1016/j.protis.2017.03.005

Vimercati, L., Bueno de Mesquita, C. P., Johnson, B. W., Mineart, D., DeForce, E., Vimercati Molano, Y., Ducklow, H., & Schmidt, S. K. (2022). Dynamic trophic shifts in bacterial and eukaryotic communities during the first 30 years of microbial succession following retreat of an Antarctic glacier. *FEMS Microbiology Ecology*, *98*(12), fiac122. https://doi.org/10.1093/femsec/fiac122

Violle, C., Navas, M.-L., Vile, D., Kazakou, E., Fortunel, C., Hummel, I., & Garnier, E. (2007). Let the concept of trait be functional! *Oikos*, *116*(5), 882–892. https://doi.org/10.1111/j.0030-1299.2007.15559.x

Visco, J. A., Apothéloz-Perret-Gentil, L., Cordonier, A., Esling, P., Pillet, L., & Pawlowski, J. (2015). Environmental Monitoring: Inferring the Diatom Index from Next-Generation Sequencing Data. *Environmental Science & Technology*, *49*(13), 7597–7605. https://doi.org/10.1021/es506158m

Wan, X., Gao, Q., Zhao, J., Feng, J., Van Nostrand, J. D., Yang, Y., & Zhou, J. (2020). Biogeographic patterns of microbial association networks in paddy soil within Eastern China. *Soil Biology and Biochemistry*, *142*, 107696. https://doi.org/10.1016/j.soilbio.2019.107696

Wang, X., Chi, Y., & Song, S. (2024). Important soil microbiota's effects on plants and soils: A comprehensive 30-year systematic literature review. *Frontiers in Microbiology*, *15*. https://doi.org/10.3389/fmicb.2024.1347745

Warton, D. I. (2022). *Eco-Stats: Data Analysis in Ecology: From t-tests to Multivariate Abundances*. Springer International Publishing. https://doi.org/10.1007/978-3-030-88443-7

Weber, B., Belnap, J., Büdel, B., Antoninka, A. J., Barger, N. N., Chaudhary, V. B., Darrouzet-Nardi, A., Eldridge, D. J., Faist, A. M., Ferrenberg, S., Havrilla, C. A., Huber-Sannwald, E., Malam Issa, O., Maestre, F. T., Reed, S. C., Rodriguez-Caballero, E., Tucker, C., Young, K. E., Zhang, Y., …

Bowker, M. A. (2022). What is a biocrust? A refined, contemporary definition for a broadening research community. *Biological Reviews*, *n/a*(n/a). https://doi.org/10.1111/brv.12862

Weber, B., Büdel, B., & Belnap, J. (Eds.). (2016). *Biological Soil Crusts: An Organizing Principle in Drylands* (Vol. 226). Springer International Publishing. https://doi.org/10.1007/978-3-319-30214-0

Weiss, S., Van Treuren, W., Lozupone, C., Faust, K., Friedman, J., Deng, Y., Xia, L. C., Xu, Z. Z., Ursell, L., Alm, E. J., Birmingham, A., Cram, J. A., Fuhrman, J. A., Raes, J., Sun, F., Zhou, J., & Knight, R. (2016). Correlation detection strategies in microbial data sets vary widely in sensitivity and precision. *The ISME Journal*, *10*(7), Article 7. https://doi.org/10.1038/ismej.2015.235

Wickham, H., Averick, M., Bryan, J., Chang, W., McGowan, L. D., François, R., Grolemund, G., Hayes, A., Henry, L., Hester, J., Kuhn, M., Pedersen, T. L., Miller, E., Bache, S. M., Müller, K., Ooms, J., Robinson, D., Seidel, D. P., Spinu, V., … Yutani, H. (2019). Welcome to the Tidyverse. *Journal of Open Source Software*, *4*(43), 1686. https://doi.org/10.21105/joss.01686

Wickham, H., Pedersen, T. L., Seidel, D., Posit, & PBC. (2023). *scales: Scale Functions for Visualization* (Version 1.3.0) [Computer software]. https://cloud.r-project.org/web/packages/scales/index.html

Wong, M. L., & Medrano, J. F. (2005). Real-time PCR for mRNA quantitation. *BioTechniques*, *39*(1), 11. https://doi.org/10.2144/05391rv01

Wu, L., Yang, Y., Chen, S., Zhao, M., Zhu, Z., Yang, S., Qu, Y., Ma, Q., He, Z., Zhou, J., & He, Q. (2016). Long-term successional dynamics of microbial association networks in anaerobic digestion processes. *Water Research*, *104*, 1–10. https://doi.org/10.1016/j.watres.2016.07.072

Yan, L. (2023). *ggvenn: Draw Venn Diagram by "ggplot2"* (Version 0.1.10) [Computer software]. https://cran.r-project.org/web/packages/ggvenn/index.html

Zhang, E., Thibaut, L. M., Terauds, A., Raven, M., Tanaka, M. M., van Dorst, J., Wong, S. Y., Crane, S., & Ferrari, B. C. (2020). Lifting the veil on arid-to-hyperarid Antarctic soil microbiomes: A tale of two oases. *Microbiome*, *8*(1), 37. https://doi.org/10.1186/s40168-020-00809-w

Zhang, Y., Lu, L., Chang, X., Jiang, F., Gao, X., Yao, Y., Li, C., Cao, S., Zhou, Q., & Peng, F. (2018). Small-Scale Soil Microbial Community Heterogeneity Linked to Landform Historical Events on King George Island, Maritime Antarctica. *Frontiers in Microbiology*, *9*. https://doi.org/10.3389/fmicb.2018.03065

Zhou, J., He, Z., Yang, Y., Deng, Y., Tringe, S. G., & Alvarez-Cohen, L. (2015). High-Throughput Metagenomic Technologies for Complex Microbial Community Analysis: Open and Closed Formats. *mBio*, *6*(1). https://doi.org/10.1128/mBio.02288-14

Zimmermann, J., Jahn, R., & Gemeinholzer, B. (2011). Barcoding diatoms: Evaluation of the V4 subregion on the 18S rRNA gene, including new primers and protocols. *Organisms Diversity & Evolution*, *11*(3), 173–192. https://doi.org/10.1007/s13127-011-0050-6

Appendix

Supplementary Information 1

Electrophoresis gels

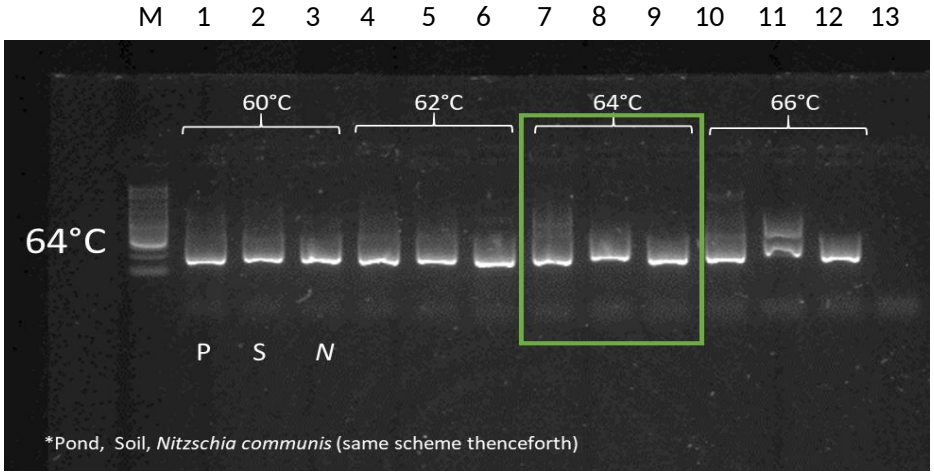

Figure S1. Annealing temperature optimization for the diatom analysis protocol. Gel electrophoresis results of the second semi-nested PCRs set at an annealing temperature of 64°C with first reaction PCR products (set at 60°C, 62°C, 64°C, and 66°C). Lane M, 100 bp marker. All temperatures were tested on the environmental samples (pond and soil) and the positive control (*Nitzschia communis)*. Lanes 7-9 correspond to the first PCR product set as 64°C, determined as the optimal temperature. Lane 13, negative control.

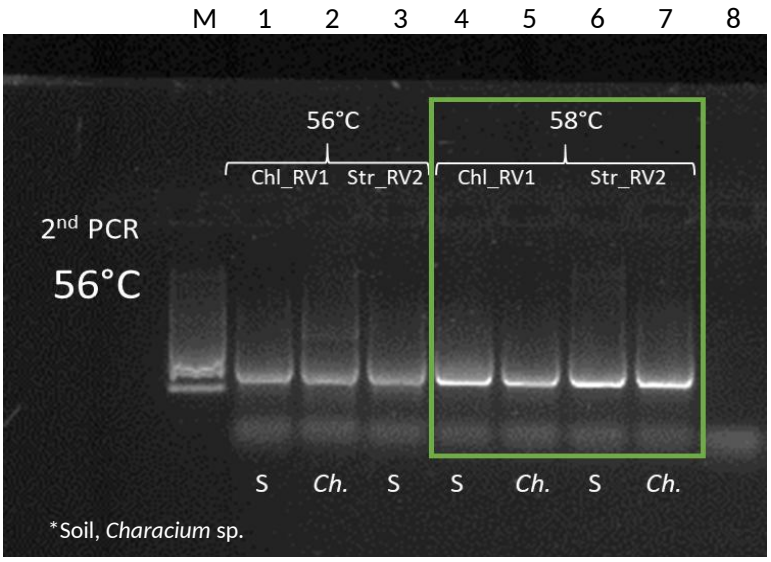

Figure S2. Annealing temperature optimization for the green algae analysis protocols. Gel electrophoresis results of the second semi-nested PCRs set at an annealing temperature of 56°C with first reaction PCR products (set at 56°C and 58°C with the Chlphy_RV1 and Strphy_RV2 reverse primers). All temperatures were tested on the environmental soil sample and the positive control (*Characium* sp.). Lane M, 100 bp marker. Lanes 4-7 correspond to the first PCR product set as 58°C, determined as the optimal temperature. Lane 8, negative control.

Supplementary Information 2

Table S1. Sampling sites

Code	Date	Place	Long (°)	Lat (°)	Observations
Svalbard, Arctic Ocean					
S1	24.07.2021	Cole mine 200 m	15.4514	78.2364	Rocky substrate. Crust dominated by cyanobacteria. Presence of lichens, moss, and small vascular plants.
S2	24.07.2021	Seed vault 200 m	15.4809	78.2361	Meadow. Humid soil. Crust dominated by cyanobacteria. Vascular plants and grass in the periphery.
S3	25.07.2021	Small glacier	15.5206	78.1964	Moraine edge next to a mountain with numerous bird nests. Crust dominated by moss; presence of lichens.
S4	25.07.2021	Glacier, bird nests	15.5089	78.1883	Moraine. Humid soil. Nests from different bird species. Patches of cyanobacteria, moss, and lichens.
S5	25.07.2021	Plateou	15.5344	78.1936	Rocky substrate. Humid soil, very early crust. Patches of moss and plants.
S6	25.07.2021	Edge of Longyearbyen	15.5680	78.1976	Streambank. Very humid soil. Crust dominated by moss.
S7	28.07.2021	West valley	15.3366	78.2203	Morain edge. Humid soil. Ptardigans nests. Moss and lichen dominated crust. Presence of vascular plants.
S8	29.07.2021	Foxfonna I	16.0601	78.1565	Morain. Humid soil. Crust rich in lichens. Scattered grass and vascular plants.
S9	29.07.2021	Foxfonna II	16.0923	78.1514	Morain. Crust rich in lichens. Scattered grass and vascular plants.
King George Island, Antarctic Peninsula					
K5	29.01.2022	Kristianka	-58.9407	-62.1971	Rocky substrate. Wet soil. Crust dominated by cyanobacteria. Presence of moss.
K6	29.02.2022	Suffield Point	-58.9269	-62.1907	Morain. Developed crusts, patches of moss and lichens.
K7	06.02.2022	Meseta Cruz	-58.9562	-62.2071	Rocky substrate. Developed crusts, patches of moss and lichens.
K9	12.02.2022	Strand Bellingshausen	-58.9565	-62.1981	Clayey soil. Crust dominated by moss in patches.
C2	26.02.2022	Collins 2	-58.8563	-62.1694	Developed crusts with moss and lichens.
C3	26.02.2022	Collins 3	-58.8528	-62.1698	Developed crusts with moss and lichens.
C4	26.02.2022	Collins 4	-58.8514	-62.1697	Developed crusts with moss and lichens.
Me1	07.03.2022	Meseta 1	-58.9266	-62.1769	Sandy and rocky substrate. Crust dominated by lichens. Presence of moss.
Me2	07.03.2022	Meseta 2	-58.9240	-62.1741	Presence of lichens and scattered moss.
Me3	07.03.2022	Meseta 3	-58.9307	-62.1788	Crust dominated by moss.
Thala Hills, Continental Antarctica					
BIO1	07.02.2022	Molodezhnaya	45.8607	-67.6676	Rocky and sandy soil. Young biocrust with presence of lichens.
BIO2	07.02.2022	Ovalnoye-Glubokoye	45.8684	-67.6687	Rocky and sandy soil. Crust dominated by lichens.
BIO3	08.02.2022	Sandiger See	45.8536	-67.6575	Sandy soil. Scattered areas with thowing snow. Moss dominated crust. Colorful lichens.
BIO4	10.02.2022	Blisnetzow	45.9194	-67.6629	Rocky and sandy soil. Scattered moss.

Supplementary Information 3

Rarefaction curves

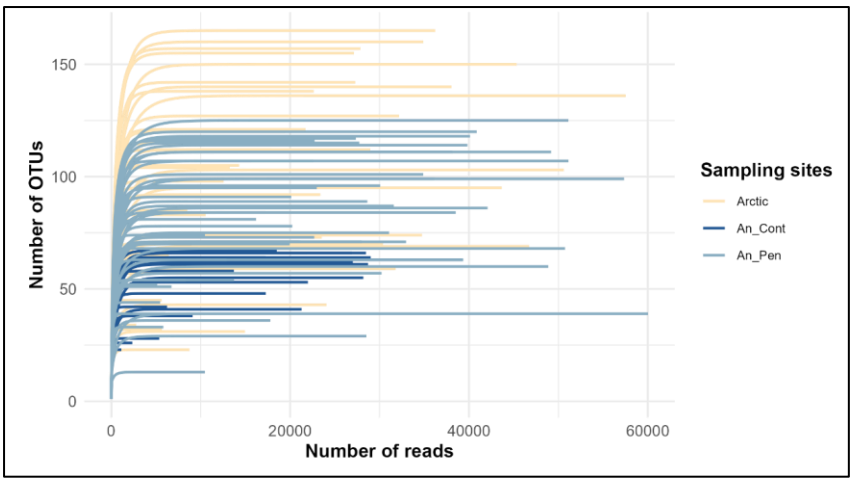

Figure S3. Rarefaction curves per sampling sites, Cercozoa

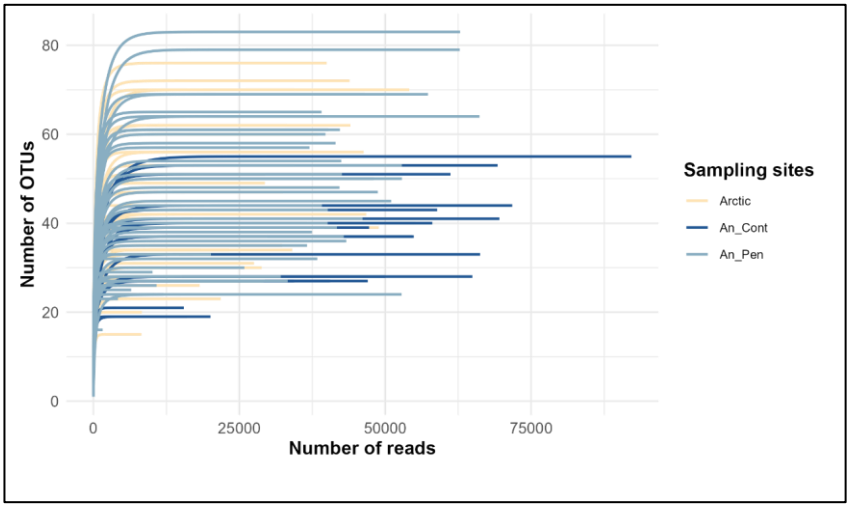

Figure S4. Rarefaction curves per sampling sites, green algae

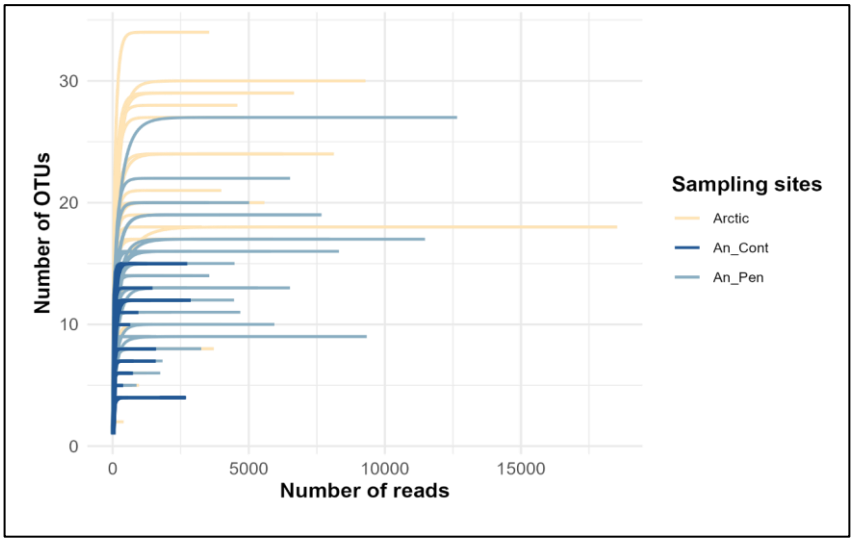

Figure S5. Rarefaction curves per sampling sites, ochrophytes

Supplementary Information 4

Chord diagrams with genera names

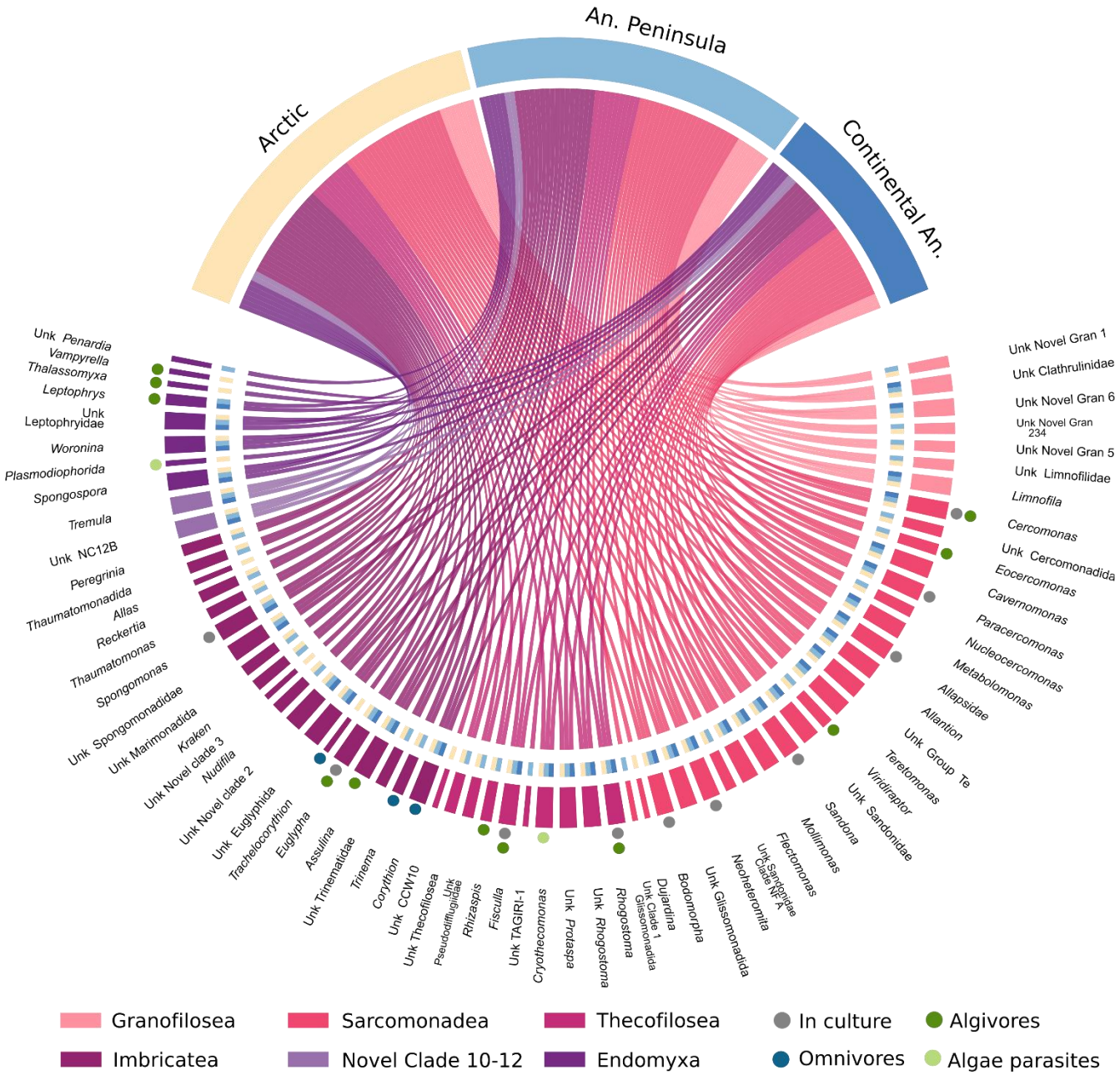

Figure S6. Cercozoan genera by sampling regions

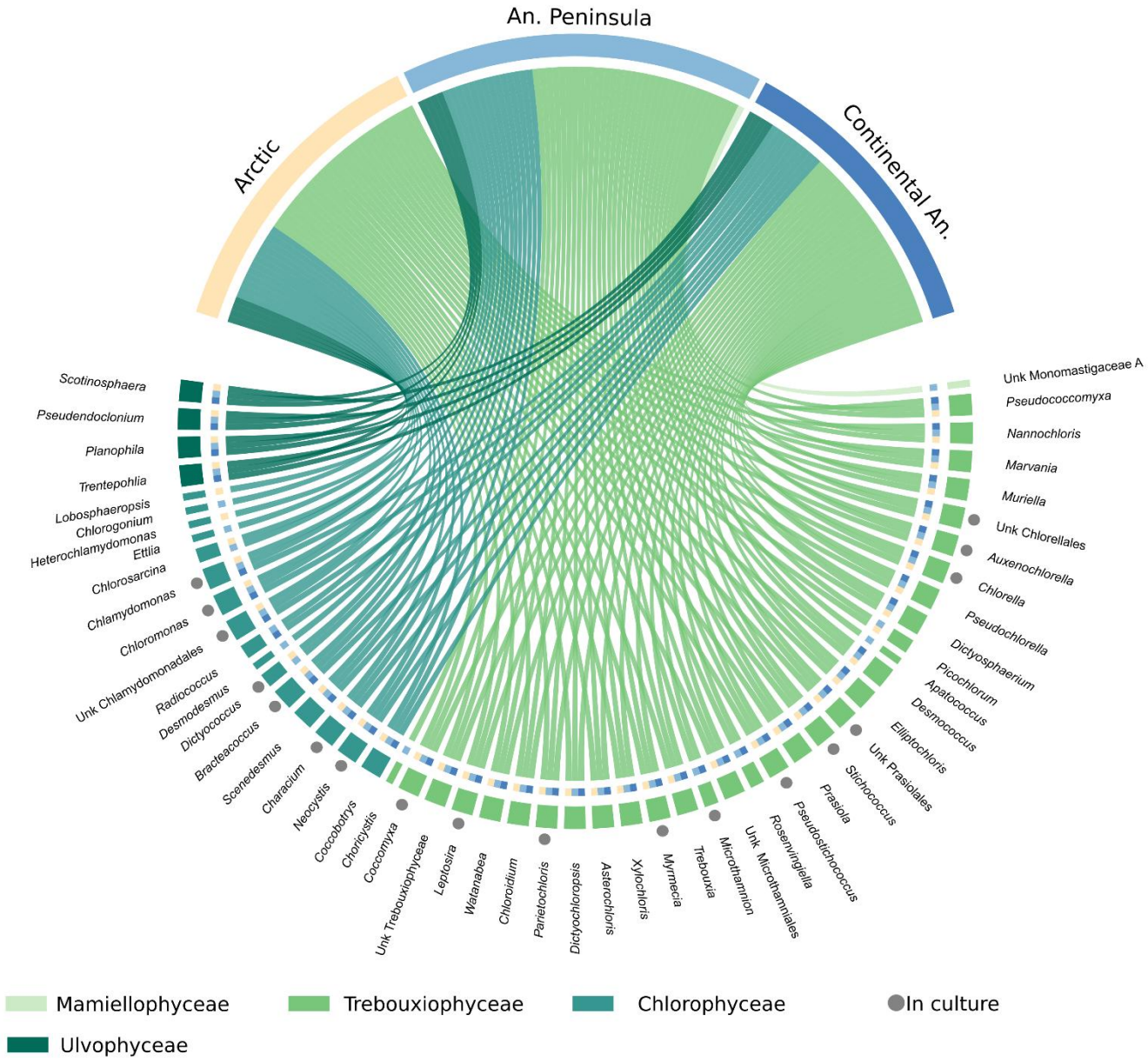

Figure S7. Green algal genera by sampling regionsvis

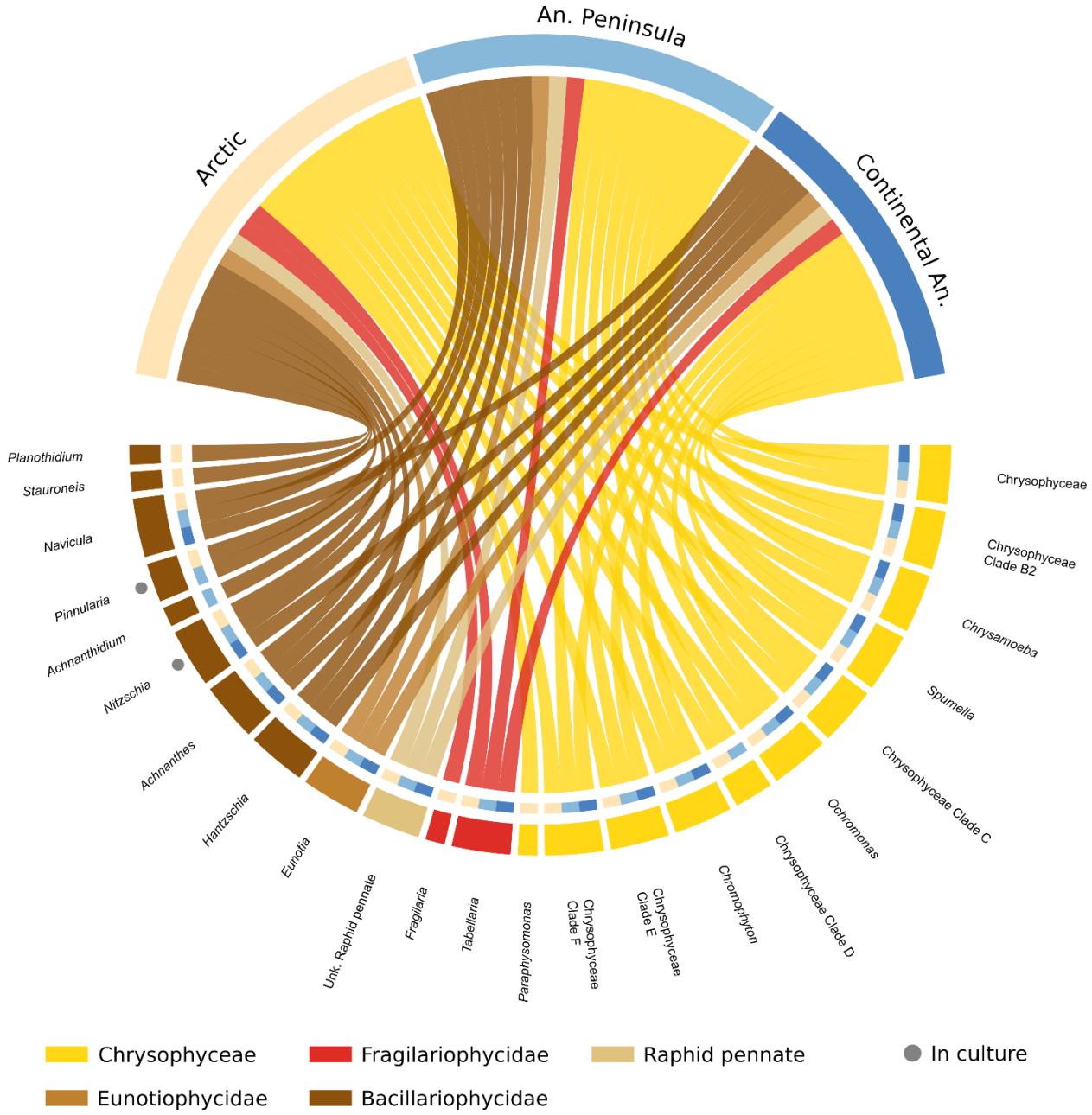

Figure S8. Ochrophyte genera by sampling regions

Supplementary Information 5

Alpha and Beta diversity statistics

Table S2. One-way ANOVA comparisons of alpha diversity indices — OTU richness, exponential Shannon, and inverse Simpson— across polar biocrusts samples (N=116) from Svalbard, the Antarctic Peninsula, and Continental Antarctica. Results presented separately for Cercozoa, green algae, and ochrophytes. The table displays F-values with degrees of freedom (df) for the nominator and denominator, along with associated p-values derived from one-way ANOVA comparisons.

ANOVA				
Taxon		*df*	*F*	*p*
Cercozoa	OTU richness	2, 113	10.368	**7.34e-5**
	Exp(Shannon)	2, 113	8.809	**0.000278**
	Inverse Simpson	2, 113	4.955	**0.009**
Green algae	OTU richness	2, 113	1.853	0.162
	Exp(Shannon)	2, 113	6.278	**0.003**
	Inverse Simpson	2, 113	3.888	**0.023**
Ochrophytes	OTU richness	2, 113	4.407	**0.014**
	Exp(Shannon)	2, 113	3.801	**0.025**
	Inverse Simpson	2, 113	3.217	**0.044**

Values marked in bold indicate statistical significance ($p < 0.05$).

Table S3. PERMANOVA results for taxonomic groups across environmental factors. Analysis of polar biocrusts samples (N=116) from Svalbard, the Antarctic Peninsula, and Continental Antarctica.

PERMANOVA				
Taxon	*Factor*	R^2	*F*	*p*
Cercozoa	Region	0.1208	10.246	**<0.001**
	pH	0.1061	18.009	**<0.001**
	Green algae	0.0348	5.903	**<0.001**
	P (g/kg)	0.0298	5.063	**<0.001**
	%C	0.0297	5.046	**<0.001**
	%N	0.0229	3.881	**<0.001**
	Ochrophytes	0.0206	3.493	**<0.001**
	CN ratio	0.0106	1.799	**0.040**
	Residuals	0.6247		
Green algae	Region	0.1429	12.695	**<0.001**
	pH	0.0817	14.511	**<0.001**
	Cercozoa	0.0537	9.540	**<0.001**
	%C	0.0377	6.702	**<0.001**
	Ochrophytes	0.0307	5.457	**<0.001**
	P (g/kg)	0.0281	5.002	**<0.001**
	CN ratio	0.0165	2.929	**0.006**
	%N	0.0123	2.192	**0.027**
	Residuals	0.6402		
Ochrophytes	Region	0.0571	3.777	**<0.001**

PERMANOVA				
Taxon	*Factor*	R^2	*F*	*p*
Ochrophytes	pH	0.0468	6.194	**<0.001**
	Cercozoa	0.0224	2.961	**0.004**
	%N	0.0192	2.540	**0.008**
	Green algae	0.0169	2.240	**0.016**
	P (g/kg)	0.0139	1.836	**0.047**
	%C	0.0123	1.636	0.077
	CN ratio	0.0099	1.321	0.197
	Residuals	0.8013		

Values marked in bold indicate statistical significance ($p < 0.05$).

Supplementary Information 6

FlashWeave: Network topology indices

Table S4. Network topological features, including inter- and intra-domain co-occurrences for Cercozoa, green algae, and ochrophytes. N=116.

	Features	*Svalbard*	*An. Peninsula*	*Continental An.*
Network OTU level	Total node number	306	303	135
	Total edge number	407	422	140
	Inter-domain edges	89	138	51
	Intra-domain edges	318	284	89
	Cercozoa/Endomyxa-algae edges	72/17.7%	86/20.4%	46/32.9%
	Potential predator-prey edges (according to Dumack et al, 2017)	26/6.4%	20/4.7%	13/9.3%
	Average degree	2.660	2.785	2.074
	Average clustering coefficient	0.013	0.001	0.018
	Average shortest path length	6.698	6.047	8.075
	Network density	0.009	0.010	0.021
Network aggregated to order level	Total node number	30	28	23
	Total edge number	157	153	71
	Average degree	10.47	10.93	6.17
	Average clustering coefficient	0.641	0.658	0.343
	Average shortest path length	1.848	1.817	2.182
	Network density	0.257	0.286	0.194

HMSC metrics

Table S5. Summary of co-occurrence and correlation interactions identified in Cercozoan-algae HMSC networks across models[a]

Model	Cercozoa trait	Type of association	Positive	Negative	Total (sub-network)	Total (model)	Potential predatory
modpa_null	Eukaryvores	Total	3895	2338	6233	21689	6.78%
	Eukaryvores	Potential predatory	836	634	1470		
	Bacterivores	Total	9158	6298	15456		
	Bacterivores	Cercozoa-algae	2013	1486	3499		
modpa_full	Eukaryvores	Total	2125	1686	3811	10515	**7.52%**
	Eukaryvores	Potential predatory	326	465	791		
	Bacterivores	Total	3654	3050	6704		
	Bacterivores	Cercozoa-algae	746	872	1618		
modabu_null	Eukaryvores	Total	699	512	1211	4215	3.53%
	Eukaryvores	Potential predatory	73	76	149		
	Bacterivores	Total	1694	1310	3004		
	Bacterivores	Cercozoa-algae	339	356	695		
modabu_full	Eukaryvores	Total	905	788	1693	5573	**4.79%**
	Eukaryvores	Potential predatory	135	132	267		
	Bacterivores	Total	2068	1812	3880		
	Bacterivores	Cercozoa-algae	460	446	906		

[a]Overview of interactions inferred between Cercozoa and microalgae using Hierarchical Modeling of Species Communities (HMSC) with null and full models for both presence-absence (modpa) and abundance (modabu) data. Interactions are categorized by Cercozoa traits (eukaryvores or bacterivores) and type of association (total, Cercozoa-algae subnetwork, and potential predatory interactions).

Table S6: HMSC diagnostics, explanatory and predictive powers of the models[a]

Category	Model	Explanatory power	Predictive power
Abundance			
	Null	0.5457634	0.1258039
	Full	0.6306775	0.1930154
Occurrence (presence-absence)			
	Null	0.9154173	0.7360737
	Full	0.9240136	0.7581433

[a]Explanatory and predictive powers of the HMSC models for species occurrences (measured as the AUC of the binomial model) and abundances (measured as R^2 of the normal model). Null models included only sequencing depth as the sole explanatory variable, while full models incorporated environmental predictors. Explanatory power was calculated based on the model fit to the entire dataset, while predictive power was assessed through 2-fold cross-validation. The AUC index ranges between 0.5 (random prediction) and 1 (perfect prediction), whereas R^2 ranges between 0 and 1.

Supplementary Information 7

1. *Feeding rate experiments*

Table S7. Summary of the ANCOVA models for predator counts.

Factor	*df*	SS	MS	*F*	*p*-value
Cercomonas grazing on *Auxenochlorella*					
Day	6	58855281605	9809213601	20.10161335	5.79E-09
Control	1	60712284112	60712284112	124.4151581	8.19E-12
Control:Day	6	14451082669	2408513778	4.935667087	**0.001473557**
Residuals	28	13663479445	487981408.7		
Cercomonas grazing on *Parietochloris*					
Day	6	9835765566	1639294261	114.3236789	2.27E-18
Control	1	4544600426	4544600426	316.9384852	8.38E-17
Control:Day	6	1411229706	235204950.9	16.40309243	**5.16E-08**
Residuals	28	401493721.5	14339061.48		
Euglypha grazing on *Parietochloris*					
Day	6	5255968285	875994714.2	54.5253969	3.69E-14
Control	1	148582160.7	148582160.7	9.248344942	0.005072897
Control:Day	6	237514957.7	39585826.28	2.463979353	**0.048586813**
Residuals	28	449842704.3	16065810.87		
Euglypha grazing on *Bracteacoccus*					
Day	6	1479888151	246648025.2	2.775651985	0.030254767
Control	1	4473059148	4473059148	50.33754271	1.02E-07
Control:Day	6	1607550323	267925053.9	3.015092892	**0.02114046**
Residuals	28	2488116213	88861293.32		
Euglypha grazing on *Auxenochlorella*					
Day	6	50498264697	8416377450	15.77906056	7.74E-08
Control	1	1.29524E+11	1.29524E+11	242.8326834	**2.51E-15**
Control:Day	6	1258543297	209757216.1	0.393253729	0.877040559
Residuals	28	14934892210	533389007.5		
Euglypha grazing on *Stichococcus*					
Day	6	2264766454	377461075.6	2.754748757	0.031223994
Control	1	1274220897	1274220897	9.299391802	0.00496823
Control:Day	6	936673396.3	156112232.7	1.139322719	0.365925722
Residuals	28	3836614896	137021960.6		
Euglypha grazing on *Pinnularia*					
Day	6	28443957.89	4740659.649	9.06382308	1.54E-05
Control	1	1411467.232	1411467.232	2.698630617	0.111619357
Control:Day	6	1154428.445	192404.7408	0.367864951	0.893068667
Residuals	28	14644865.53	523030.9116		
Fisculla grazing on *Auxenochlorella*					
Day	6	30474542577	5079090429	7.222679678	9.94E-05
Control	1	2.03121E+11	2.03121E+11	288.8465246	2.76E-16
Control:Day	6	10445655926	1740942654	2.475693494	**0.047723428**
Residuals	28	19689995731	703214133.3		
Rhogostoma grazing on *Leptosira*					
Day	6	19697244.03	3282874.005	1.119509938	0.376415631
Control	1	9361925.188	9361925.188	3.192558797	0.08480666
Control:Day	6	12325637.61	2054272.934	0.700538297	0.651469953
Residuals	28	82107776.84	2932420.601		

Table S8. Summary of the ANCOVA models for algae counts.

Factor	*df*	SS	MS	*F*	*p*-value
Cercomonas grazing on *Auxenochlorella*					
Day	3	154277550.5	51425850.15	54.60122053	1.26E-08
Control	1	313080937	313080937	332.4126142	3.97E-12
Control:Day	3	153040539.8	51013513.26	54.16342325	**1.34E-08**
Residuals	16	15069509.33	941844.3333		
Cercomonas grazing on *Parietochloris*					
Day	3	24870393	8290131	9.088187	0.001363
Control	1	42559538	42559538	46.65657	8.19E-06
Control:Day	2	18622961	9311481	10.20786	**0.001843**
Residuals	14	12770625	912187.5		
Euglypha grazing on *Parietochloris*					
Day	5	13995.58333	2799.116667	34.39187713	3.45E-10
Control	1	18000.69444	18000.69444	221.168942	1.31E-13
Control:Day	5	16437.13889	3287.427778	40.3916041	**6.40E-11**
Residuals	24	1953.333333	81.38888889		
Euglypha grazing on *Bracteacoccus*					
Day	5	235.5833333	47.11666667	4.167567568	0.007232903
Control	1	448.0277778	448.0277778	39.62899263	1.66E-06
Control:Day	5	731.8055556	146.3611111	12.94594595	**3.62E-06**
Residuals	24	271.3333333	11.30555556		
Euglypha grazing on *Auxenochlorella*					
Day	5	244.9166667	48.98333333	4.343349754	0.005891103
Control	1	684.6944444	684.6944444	60.71182266	5.02E-08
Control:Day	5	706.4722222	141.2944444	12.52857143	**4.75E-06**
Residuals	24	270.6666667	11.27777778		
Euglypha grazing on *Stichococcus*					
Day	5	69.13888889	13.82777778	1.575316456	0.204956781
Control	1	250.6944444	250.6944444	28.56012658	1.74E-05
Control:Day	5	93.13888889	18.62777778	2.122151899	0.097444559
Residuals	24	210.6666667	8.777777778		
Euglypha grazing on *Pinnularia*					
Day	5	207.1388889	41.42777778	4.131301939	0.007548441
Control	1	318.0277778	318.0277778	31.71468144	8.49E-06
Control:Day	5	659.1388889	131.8277778	13.14626039	**3.18E-06**
Residuals	24	240.6666667	10.02777778		
Fisculla grazing on *Auxenochlorella*					
Day	3	23802.45833	7934.152778	4.960654058	0.012716939
Control	1	107334.375	107334.375	67.108451	4.07E-07
Control:Day	3	25331.45833	8443.819444	5.279311902	**0.010092686**
Residuals	16	25590.66667	1599.416667		
Rhogostoma grazing on *Leptosira*					
Day	3	7617714	2539238	8.55482	0.001281
Control	1	9538204	9538204	32.13469	3.49E-05
Control:Day	3	7709935	2569978	8.658386	**0.001209**
Residuals	16	4749113	296819.5		

Acknowledgments

My sincere gratitude to Prof. Dr. Michael Bonkowski for hosting me in his research group and for fostering an environment of scientific curiosity and collaboration. To Kenny**,** my supervisor—thank you for your unwavering guidance, patience, and support throughout this journey. And to the team Dumack and AG Bonkowksi, being part of them has been a privilege, and I am grateful for the camaraderie and knowledge shared.

A big thank you to the members of my TAC meeting, Enrique Lara and Karin Glaser, for their valuable insights and constructive feedback throughout this process. I am also grateful to Burkhard Becker, my second reviewer, for his time and thoughtful evaluation.

I am deeply grateful to Jule Freudenthal for her assistance in the network analyses. Beyond her expertise, her kindness and willingness to help at any moment made all the difference—muchísimas gracias. The primer tags were designed after Franck Lejzerowicz's script. We thank Anna Maria Fiore-Donno for her assistance in the initial stage of the project and Marcel Dominik Solbach for providing the cercozoan DNA for the mock community.

A very special mention to my four extraordinary B.Sc. students—Olivia Piaseki, Natalie Kamischke, Stefan Rein, and Pablo Navarro—for their dedication and enthusiasm in protist isolation and culturing. Also, thank you for the wonderful moments in the lab; you brightened my days at the university.

Mi más profundo agradecimiento a la Campaña Antártica Española, al Comité Polar Español y a la Unidad de Tecnología Marina por incluirnos a Kenny y a mí en la expedición a bordo del Buque de Investigación Oceanográfica "Hespérides" y en el campamento Byers. Fue una experiencia única y transformadora, de esas que marcan no solo una carrera, sino también la manera en que uno ve el mundo.

Gracias a Michelle, cuyo apoyo fue fundamental para que este proyecto llegara a buen puerto. A mi familia y amigos, por su paciencia infinita, por recordarme que creían en mí cuando yo no lo hacía, y por esperarme en cada pausa que impuso este viaje académico. El camino fue largo y absorbente, pero el resultado hizo que cada sacrificio valiera la pena.

Aber vor allem, danke Henning, für deine Liebe und deine Gesellschaft in den Monaten, in denen ich diese Arbeit geschrieben habe. I went beyond because you showed me the way.

Declaration

Erklärung zur Dissertation

gemäß der Promotionsordnung vom 12. März 2020

„Hiermit versichere ich an Eides statt, dass ich die vorliegende Dissertation selbstständig und ohne die Benutzung anderer als der angegebenen Hilfsmittel und Literatur angefertigt habe. Alle Stellen, die wörtlich oder sinngemäß aus veröffentlichten und nicht veröffentlichten Werken dem Wortlaut oder dem Sinn nach entnommen wurden, sind als solche kenntlich gemacht. Ich versichere an Eides statt, dass diese Dissertation noch keiner anderen Fakultät oder Universität zur Prüfung vorgelegen hat; dass sie - abgesehen von unten angegebenen Teilpublikationen und eingebundenen Artikeln und Manuskripten - noch nicht veröffentlicht worden ist sowie, dass ich eine Veröffentlichung der Dissertation vor Abschluss der Promotion nicht ohne Genehmigung des Promotionsausschusses vornehmen werde. Die Bestimmungen dieser Ordnung sind mir bekannt. Darüber hinaus erkläre ich hiermit, dass ich die Ordnung zur Sicherung guter wissenschaftlicher Praxis und zum Umgang mit wissenschaftlichem Fehlverhalten der Universität zu Köln gelesen und sie bei der Durchführung der Dissertation zugrundeliegenden Arbeiten und der schriftlich verfassten Dissertation beachtet habe und verpflichte mich hiermit, die dort genannten Vorgaben bei allen wissenschaftlichen Tätigkeiten zu beachten und umzusetzen. Ich versichere, dass die eingereichte elektronische Fassung der eingereichten Druckfassung vollständig entspricht."

Teilpublikationen:

Martínez Rendón C, Braun C, Kappelsberger M, Boy J, Casanova-Katny A, Glaser K, Dumack K. Enhancing microbial predator-prey detection with network and trait-based analyses. *Microbiome*. 2025 Feb 4;13(1):37. doi: 10.1186/s40168-025-02035-8. PMID: 39905550; PMCID: PMC11792678.

Datum: 22.02.2025

Name und Unterschrift: Ana Cristina Martínez Rendón

Contributions to the publication

Martínez Rendón C, Braun C, Kappelsberger M, Boy J, Casanova-Katny A, Glaser K, Dumack K. Enhancing microbial predator-prey detection with network and trait-based analyses. *Microbiome*. 2025 Feb 4;13(1):37. doi: 10.1186/s40168-025-02035-8. PMID: 39905550; PMCID: PMC11792678.

Keneth Dumack and Karin Glaser conceived and designed the study. I conducted the molecular laboratory work and was responsible for the bioinformatics processing, the data analysis, and finally generated all figures. Karin Glaser was responsible for the analyses of the chemical properties of biocrusts. Kenneth Dumack and I jointly interpreted the results, and while I was primarily responsible for writing the manuscript, he provided critical revisions and contributed to specific sections. Maria Kappelsberger collected samples in the Thala Hills Oasis, Enderby Land during the expedition PS128 of 2022 of the R/V Polarstern. Christina Braun collected samples in King George Island in 2022. Angelica Casanova-Katny collected samples on the Fildes Peninsula during the 56th Antarctic Scientific Expedition (ECA). All authors read, commented on, and approved the final manuscript.

Curriculum Vitae

A n a C r i s t i n a M a r t í n e z R e n d ó n

M.Sc. in Biological Sciences

Email: c.martinezrendon@uni-koeln.de

Address: Cologne, Germany

https://orcid.org/0009-0006-8886-5448

EDUCATION

06/2021 – To date | Doctoral Candidate – Terrestrial Ecology, Institute of Zoology, University of Cologne

04/2019 – 05/2021 | M.Sc. in Biology – University of Cologne
Scholarship from the Guatefuturo Foundation, guatefuturo.org

01/2008 – 11/2014 | B.Sc. in Chemical Biology – San Carlos University, Guatemala

CONFERENCE PRESENTATIONS

2024 | Annual Meeting of the German Protistology Society

2022 | Annual Meeting of the Phycology section, German Botanic Society

2016 | Continental Waters of the Americas Symposium: Present and Future

POSTER PRESENTATIONS

2022 | Annual Meeting of the German Protistology Society

2021-2023 I Annual Meetings of the DFG Priority Program "Antarctic Research with comparative investigations in Arctic ice areas"

2015 I Water Symposium – National Council of Science and Technology (CONCYT), Guatemala

2014 I Symposium on Scientific and Technological Research in the Atitlán Lake Basin

TEACHING EXPERIENCE

2021-2023 | AG Bonkowski–Terrestrial Ecology, Institute of Zoology, University of Cologne

1:1 Teaching of Four Bachelor students during their Bachelor's theses.

2016-2017 | Panamerican University, Sololá, Guatemala

Teacher of Microbiology (4 hours per week), Biology (4 hours per week), and Biochemistry (2 hours per week), BSc. Level, in the School of Nursing

EMPLOYMENTS

01/2025 – To date | Environmental Expert

Müller BBM Cert Umweltgutachter GmbH

06/2021 – 08/2024 | Research Associate

Doctoral Candidate at the Chair of Terrestrial Ecology, Institute of Zoology, University of Cologne

11/2013 – 05/2018 | Water Quality Technician

Authority for the Sustainable Management of Atitlan's Basin - Panajachel, Guatemala -AMSCLAE- Department of Research and Environmental Quality

01/2013 – 07/2013 | Head of Clinical Laboratory and Blood Bank

National Hospital of Sololá, Guatemala*

*In hospitals in rural regions of Guatemala, trained medical staff is rare. These positions are often filled by motivated B.Sc. students.

LINGUISTIC PROFICIENCY

Spanish – Native

English – Fluent

German – Conversational (B2)